HIDRAULICA

HYDRAULICS-PNEUMATICS-TRIBOLOGY-ECOLOGY-SENSORICS-MECHATRONICS

2022

December

No. 4

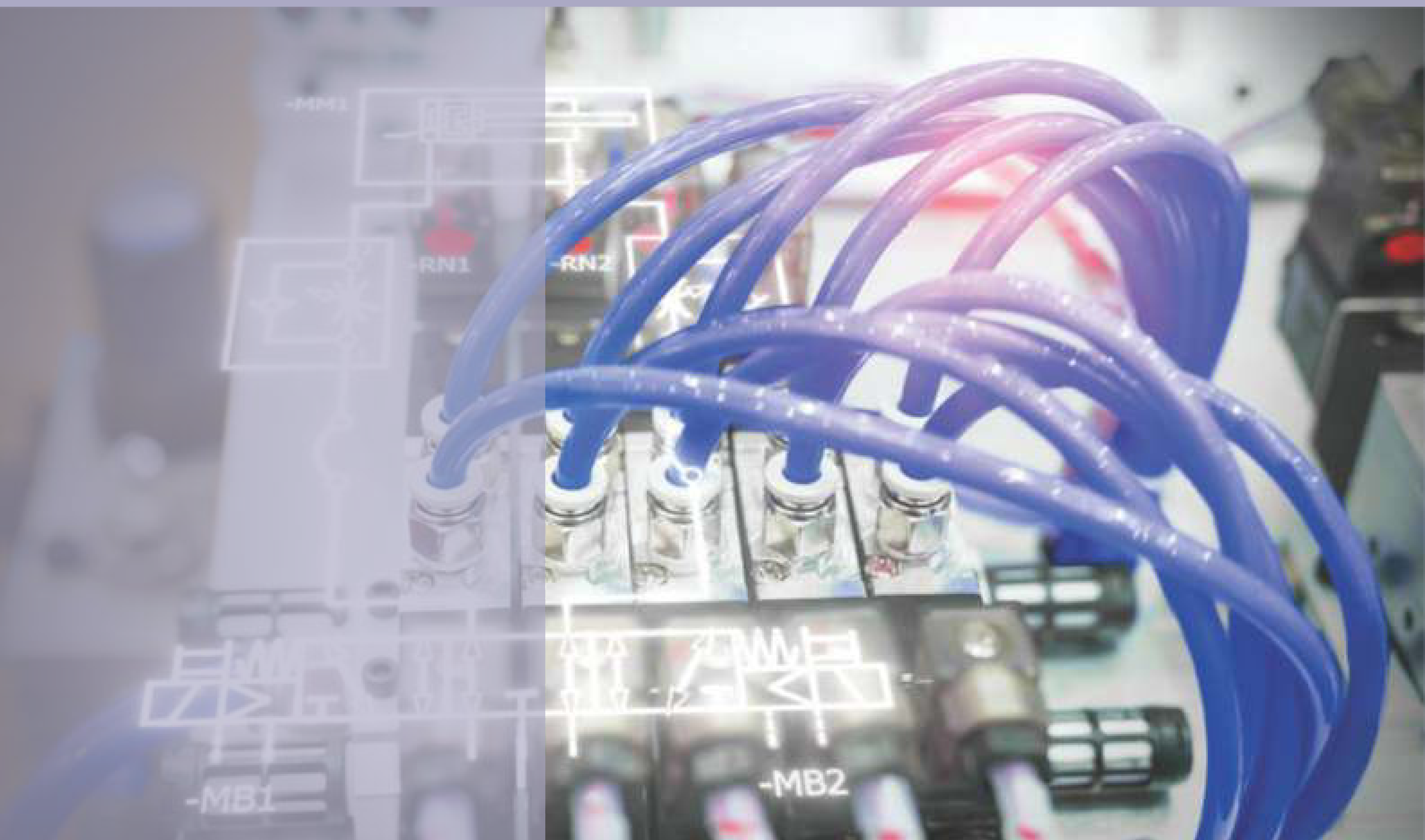

ISSN 1453 - 7303
ISSN-L 1453 - 7303

https://hidraulica.fluidas.ro

CONTENTS

Published by:
Hydraulics and Pneumatics Research Institute, Bucharest-Romania
Address: 14 Cuţitul de Argint, district 4, Bucharest, 040558, Romania
Phone: +40 21 336 39 91; Fax: +40 21 337 30 40; e-Mail: ihp@fluidas.ro; Web: www.ihp.ro
with support from:
National Professional Association of Hydraulics and Pneumatics in Romania - FLUIDAS
e-Mail: fluidas@fluidas.ro; Web: www.fluidas.ro

HIDRAULICA Magazine is indexed by international databases

ISSN 1453 – 7303; ISSN – L 1453 – 7303

EDITORIAL

Rezultate așteptate

Dr. Ing. Gabriela Matache
REDACTOR ȘEF

Strategia Națională de Cercetare, Inovare și Specializare Inteligentă 2022-2027 prezintă obiective mărețe, cu accent pe recunoașterea performanței cercetătorilor individuali și a organizațiilor de cercetare pe baza unor evaluări obiective, cu indicatori și criterii transparente, așa cum subliniază ministrul Sebastian Burduja. În 2022, Legea bugetului de stat miza pe un PIB de 1.317,2 miliarde de lei, iar bugetul alocat Ministerului Cercetării și Inovării era de 1,78 miliarde de lei. În aceste condiții, cercetarea primea doar 0,12 din PIB, cea mai mică alocare de după 2016. Chiar dacă a înregistrat o majorare de 0,67% față de anul 2021, creșterea bugetului alocat cercetării a fost cea mai mică comparativ cu cele înregistrate de celelalte ministere. Ne-am fi asteptat ca, având în vedere țintele prioritare propuse în Strategia mai sus menționată, cercetarea să primească ceva mai mult, pentru a nu mai fi la coada clasamentului UE în ceea ce privește alocarea resurselor pentru cercetare. Dar ce să vezi! … s-a decis că cercetarea nu merită 1% din PIB nici anul viitor, deoarece guvernul are alte priorități pentru cheltuirea banilor publici.

Ajung să mă întreb încotro se îndreaptă cercetarea românească, ajung să-mi pară rău că am ales această cale foarte anevoioasă, urmată doar de persoane ce cred cu adevărat în idealurile lor. Am crezut întotdeauna în faptul că, având coerență și respect față de aceste idealuri, voi obține și succes. Cred că succesul construiește success, iar calitate aduce calitate. Însă ceea ce se întâmplă astăzi cu cercetarea românească, punctul în care a ajuns recunoașterea cercetătorului român, mă face să nu-mi mai doresc să fac parte din această categorie ajunsă la pragul susbzistenței.

Dicţionarele nu ne ajută foarte mult când vine vorba despre definirea conceptului de cercetare, limitându-se, normal, la definirea lingvistică a termenului şi uzanţelor sale. Astfel, (DEX) activitatea de cercetare ar fi "producerea de noi cunoștințe, care pot fi noi numai dacă sunt recunoscute ca atare pe plan internațional. În caz contrar, nu poate fi vorba de o activitate de cercetare, ci de documentare". Sunt însă definiţii empirice, perfect adevărate, dar, din păcate, reprezintă doar descrieri ale fenomentului, nu şi explicaţii ale sale.

Îmi doresc să ajung în acele timpuri în care oamenii de valoare să fie apreciați și lăsați să-și ducă la bun sfârșit munca, în condiții decente și fără grija zilei de mâine; timpuri în care să iasă din cercetarea românească produse ce vor putea fi apreciate și introduse în fabricație în industria autohtonă. Dar de unde fabricație, de unde industrie? Am văzut cum, pe parcursul celor aproape 30 de ani petrecuți în cercetare, au dispărut rând pe rând toate fabricile, am văzut cum rând pe rând cercetătorii devin ... vânzătorii „cercetărilor" aduse din afară, am văzut cum tinerii care promiteau o carieră strălucitoare sunt „îndrumați" cu succes către centrele de cercetare din afara țării să creeze astfel produsele ce se întorc în țară sub forma produselor cu eticheta UE și, nu în ultimul rând, am văzut cum am devenit doar o piață de desfacere pentru tot ce produc marile puteri ale lumii cu „creiere românești".

EDITORIAL

Expected results


Ph.D.Eng. Gabriela Matache
EDITOR-IN-CHIEF

The National Strategy for Research, Innovation and Smart Specialization 2022-2027 presents great objectives, with emphasis on recognizing the performance of individual researchers and research organizations based on objective evaluations, with transparent indicators and criteria, as emphasized by Minister Sebastian Burduja. In 2022, the State Budget Law bet on a GDP of 1,317.2 billion lei, and the budget allocated to the Ministry of Research and Innovation was 1.78 billion lei. Under these circumstances, research received only 0.12 of GDP, the lowest allocation since 2016. Even though it registered an increase of 0.67% compared to 2021, the increase in the budget allocated to research was the smallest compared to those recorded by the other ministries. We would have expected, given the priority targets proposed in the aforementioned Strategy, that the research would receive somewhat more, in order not to be at the bottom of the EU ranking in terms of allocating resources for research. Lo and behold! … it was decided that research does not deserve 1% of GDP next year either, because the government has other priorities for spending public money.

I get to wonder where the Romanian research is going, I get to feel sorry that I chose this very difficult path, followed only by people who really believe in their ideals. I have always believed in the fact that by having coherence and respect for these ideals I will also achieve success. I believe that success builds success and quality brings quality. But what is happening today with the Romanian research, the point at which the recognition of the Romanian researcher has reached, makes me no longer want to be part of this category that has reached the threshold of subsistence.

Dictionaries do not help us much when it comes to defining the concept of research, limiting themselves, of course, to the linguistic definition of its term and usages. Thus, (DEX) the research activity would be 'the production of new knowledge, which can only be new if it is recognised as such internationally. Otherwise, it cannot be a research activity, but a documentation". These are empirical definitions, perfectly true, but, unfortunately, they are only descriptions of the phenomenon, not explanations of it.

I want to reach those times when valuable people are appreciated and allowed to carry out their work, in decent conditions and without worrying about tomorrow; times when products that would be appreciated and introduced into manufacturing in the local industry would arise from the Romanian research. But which manufacturing, which industry can we talk about? I have seen during the almost 30 years spent in research how all the factories disappeared one by one, I have seen how one by one the researchers become ... sellers of "research" brought from abroad, I have seen how young people who promised a brilliant career are successfully "guided" to research centers located abroad to create thus the products that return to the country in the form of products with the EU label, and last but not least I have seen how we have become just an outlet for everything that the great powers of the world produce with "Romanian brains".

Mathematical Modeling, Laboratory Testing and Numerical Simulation of a Servo-Pump as Part of a Closed Circuit Primary Control Hydrostatic Transmission for Multi-Purpose Trucks

PhD. Stud. Eng. **Alexandru-Polifron CHIRIȚĂ**[1,2,*], Prof. PhD. Eng. **Cristian PAVEL**[1]

[1] Technical University of Civil Engineering of Bucharest (UTCB), Faculty of Technological Equipment, Bucharest, Romania

[2] National Institute of Research & Development for Optoelectronics / INOE 2000 – Subsidiary Hydraulics and Pneumatics Research Institute / IHP, Bucharest, Romania

* chirita.ihp@fluidas.ro

Abstract: *The current paper presents the dynamic mathematical models of the components of a hydrostatic transmission, the results of physical tests performed in the laboratory on a servo-pump that is part of a closed circuit primary control hydrostatic transmission, and its numerical simulation results. The acquisition of the experimental data as well as the control of the experimental stand have been carried out with the LabVIEW application, while the numerical simulation has been carried out by using the AMESim software; in order for the results of the numerical simulation to be as close as possible to those obtained in the laboratory, the library of hydraulic components that take into account the influence of temperature on the hydraulic fluid and on the hydraulic components of the transmission has been used.*

Keywords: *Mathematical modeling, laboratory testing, numerical simulation, closed circuit, primary control, hydrostatic transmission, servo-pump*

1. Introduction

In hydraulic transmissions, power is transmitted through a fluid; it connects the pump to the hydrostatic motor [1]. The hydraulic pump receives mechanical energy from the internal combustion engine or the electric one and transfers it to the fluid in the form of flow and pressure (hydraulic energy) [2]. The fluid carries the hydraulic energy to the hydraulic motor where it is converted back into mechanical energy [1, 3].

The basic elements of a hydraulic transmission are: the pump, the fluid and the motor. They have the following roles [4, 5]:

• The pump transforms mechanical energy into hydraulic energy;
• The fluid carries the hydraulic energy from the pump to the motor;
• The motor converts hydraulic energy into mechanical energy.

Hydrostatic transmissions involve connecting a positive displacement pump to a positive displacement motor [3]. In this case, the pump produces the flow that turns the motor shaft, and the pressure in the circuit is produced by the torque resisting the motor shaft [1, 4].

Closed loop transmissions have both pump and motor ports connected together. The discharge port of the pump is connected to the "A" port of the motor and the "B" port of the motor is connected to the suction of the pump [6].

In a closed circuit hydrostatic transmission there are three ways of controlling the speed of the hydraulic motor shaft [3]:

• Primary control – when the pump displacement is variable.
• Secondary control – when the hydrostatic motor displacement is variable;
• Mixed control – when both pump and motor displacement are variable.

In the first of the cases listed above, that is, primary control, when the pump flow rate is variable and depends on the variation of the pump displacement, and the motor displacement is fixed, the motor speed is directly proportional to the flow rate delivered by the pump to the hydraulic motor port [6, 7]. In this particular case, the torque produced at the motor shaft is constant over the entire motor speed range [8] - from minimum speed rate to maximum speed rate - and the pressure created in the system is proportional to the torque. This is the most popular configuration [4, 6] and

is used because the transmission ratio is infinitely variable. Moreover, the reversal of the direction of rotation of the motor is achieved without shocks and continuously [9, 10, 11].
The mathematical models related to the main components of a hydrostatic transmission are presented below as follows:
The dynamic mathematical model and an illustration of a pump are presented in Fig. 1; Fig. 2 shows the dynamic mathematical model of a high-speed hydrostatic motor; Fig. 3 - the dynamic mathematical model of a low-speed hydrostatic motor; and finally, Fig. 4 shows an illustration of a hydraulic cylinder as well as its dynamic mathematical model.

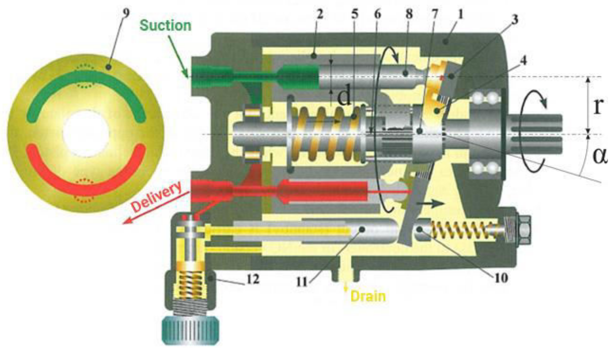

from the control and adjustment system

χ_p

known characteristics:
constructive: $V_{0p}; J_r; \alpha_p; \beta_p; \gamma_p; \delta_f; \varepsilon_f$
of hydraulic environment: $\nu; \rho; E$

from the power source (directly or indirectly): ω_I, M_I

$$Q_p = \chi_p \cdot \frac{V_{0p}}{2\pi} \cdot \omega_I - \alpha_p \cdot p - \chi_p \cdot \beta_p \cdot \frac{dp}{dt}; \ [m^3/sec]$$

$$J_{rp} \cdot \frac{d\omega_I}{dt} + \left(\gamma_p + \chi_p \cdot \frac{V_{0p}}{2\pi} \cdot \delta_f\right) \cdot \omega_I + \chi_p \cdot \frac{V_{0p}}{2\pi} \cdot (1 + \varepsilon_f) \cdot p = M_I; \ [N \cdot m]$$

to the H.D.S.: Q_p, p

Fig. 1. Swash plate hydraulic pump and the dynamic mathematical model of the pump – adapted from [1] and [12]

known characteristics:
constructive: $V_{0p}; J_r; \alpha_M; \beta_M; \gamma_M; \delta_f; \varepsilon_f$
of hydraulic environment: $\nu; \rho; E$

from the H.D.S.: Q_M, p, p_0

$$Q_M = \frac{V_{0M}}{2\pi} \cdot \omega_E \cdot \alpha_M \cdot (p - p_0) + \beta_M \cdot \frac{dp}{dt}$$

$$J_{rM} \cdot \frac{d\omega_E}{dt} + \left(\gamma_M + \frac{V_{0M}}{2\pi} \cdot \delta_M\right) \cdot \omega_E + sgn(\omega_E) \cdot \frac{V_{0M}}{2\pi} \cdot \varepsilon_f \cdot (p - p_0) + M_E = \frac{V_{0M}}{2\pi} \cdot (p - p_0)$$

from the driven working body: ω_E, M_E

Fig. 2. Dynamic mathematical model of a high-speed fixed-displacement motor - adapted from [12]

$$Q_M = \left(\frac{V_{0M}}{2\pi} - k^*\right) \cdot \omega_e + \alpha_M^* \cdot p^2 + \beta_M \cdot \frac{dp}{dt};$$

$$J_{SM} \cdot \frac{d\omega_e}{dt} + \left(\frac{V_{0M}}{2\pi} - k^*\right) \cdot \delta_M^* (\omega_e - \omega_S)^2 + M_E = \left(\frac{V_{0M}}{2\pi} - k^*\right) \cdot p;$$

$$\alpha_M^* = (\pi \cdot d \cdot z \cdot k \cdot j^3 / 96 \cdot b \cdot \eta) \cdot 2\pi \cdot d \cdot z \cdot k / \rho \cdot g \cdot V_{0M}$$

Fig. 3. Dynamic mathematical model of a low-speed radial piston motor - adapted from [12]

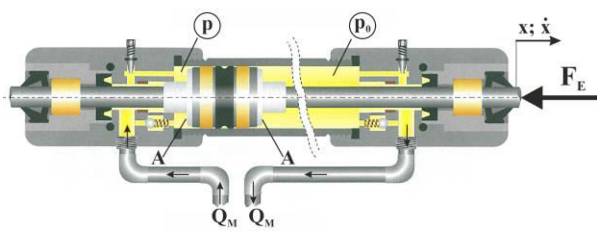

known characteristics:
constructive: $A; M_r; \alpha_C; \alpha; \beta_{ML}; \gamma_{ML}; \varepsilon_f$
of hydraulic environment: $\nu; \rho; E$

from the H.D.S.: Q_M, p, p_0

$$Q_M = A \cdot \frac{dx}{dt} + \alpha_C \cdot (p - p_0) + \beta_{ML} \cdot \frac{dp}{dt}; \ [m^3/sec]$$

$$M_r \cdot \frac{d^2x}{dt^2} + \gamma_{ML} \cdot \frac{dx}{dt} + sgn(\dot{x}) \cdot \varepsilon_f \cdot A \cdot (p - \alpha \cdot p_0) + F_E = A \cdot (p - \alpha \cdot p_0); \quad [N]$$

from the driven working body: $\dot{x}$, F_E

Fig. 4. Hydraulic cylinder and the dynamic mathematical model of a hydraulic cylinder – adapted from [1] and [12]

2. Material and method

This chapter is divided into two subchapters, the first of which deals with the methodology of physical experimentation, in the laboratory, and the second deals with the methodology of virtual experimentation with the help of numerical simulation.

2.1 Methodology of physical experimentation in the laboratory

The figures below show the experimental bench and its components. Experiments related to the adjustment characteristic and the response of the servo-pump to the step signal have been carried out on this bench.

Fig. 5. The experimental test bench - front view

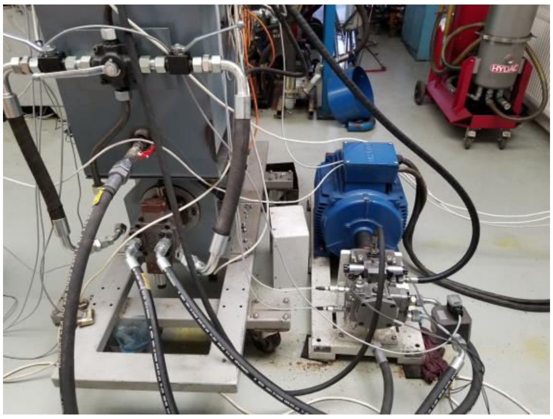

Fig. 6. The experimental test bench - side view

Fig. 7. The electric cabinet for the bench and electric motor control

As one can see in **Error! Reference source not found.**, **Error! Reference source not found.** and **Error! Reference source not found.**, the test bench consists of four distinct components:

- The first of these components is the **electric pump**, which has an asynchronous electric motor - with the power of 30 kW and the synchronism speed of 1500 rev/min – as one of its parts and the A10VG28 servo-pump;
- **Load simulation unit**, comprising: the hydraulic oil tank, the panel with digital displays for speed, temperature and torque, the A6VM servo-motor and the F112A fixed displacement pump;
- **Experimental data acquisition system**, consisting of a laptop equipped with LabVIEW experimental data acquisition software, NI 6211 experimental data acquisition board, various transducers and a programmable voltage source;
- **Electric cabinet for the bench and electric motor control**, shown in Fig. 7, with the following parts: 30-kW circuit breaker, star delta starter, 24 V power supply, 12 V power supply, 1P – 10 A automatic fuse, 3P – 1 A automatic fuse, IEM3255 three-phase meter with Modbus RTU communication and ±10 V proportional controller.

The hydraulic schematic diagram of the experimental test bench on which the research on the closed-circuit primary control hydrostatic transmission has been carried out is shown below, in Fig. 8.

Operation of the experimental test bench: one supplies the test bench with electricity and opens the LabVIEW application related to the experiment to be performed.

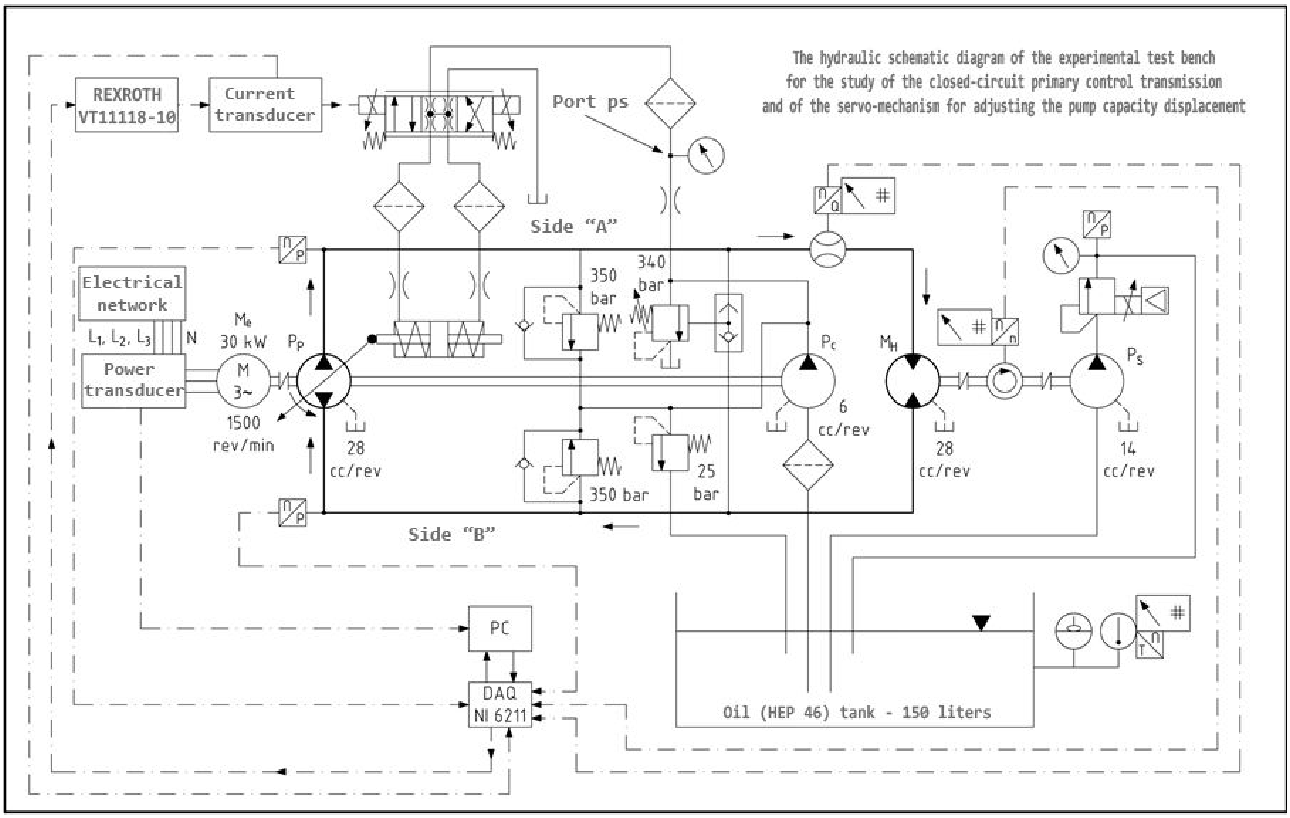

Fig. 8. Hydraulic schematic diagram of the experimental test bench for the study of the closed-circuit primary control transmission and the pump displacement control servo-mechanism
Notations in the hydraulic diagram: M_e – electric motor, P_P – main pump, P_c – compensation pump, M_H – hydrostatic motor, P_s – pressure gauge port, DAQ – experimental data acquisition board, PC – laptop and REXROTH VT11118-10 – signal conditioner for driving the pump servo-mechanism

From the electrical cabinet, the electric motor is turned on; one waits for it to switch from star to delta, and then presses the "start" button of the LabVIEW application. The control signal is transmitted from the PC to the experimental data acquisition board, which converts it to voltage (0 - 10 V); this voltage reaches the VT11118-10 proportional controller which conditions the signal and transforms it into the control current (0 – 600 mA) of the electromagnets of the proportional directional valve that is part of the pump displacement control servo-mechanism. The proportional directional valve controls the displacement of the hydraulic cylinder with bilateral rods; this displacement is directly proportional to the control signal, the swash plate angle, the main pump displacement, and its flow rate. After the swash plate angle exceeds the value of + 3º, the main pump discharges, on side "A", a flow of hydraulic fluid that passes through the flow transducer and reaches the hydrostatic motor; the flow rate determines the speed rate of the hydrostatic motor, which is measured by the speed transducer; this speed rate drives the load pump, whose flow is forced through the proportional pressure control valve, which creates a resisting torque on the motor shaft; this torque is proportional to the pressure reached at the pressure control valve. Given the ratio of the displacement of the hydrostatic motor to that of the load pump, when on the high-pressure side of the closed circuit the pressure is 70 bar, a pressure of 140 bar is installed at the proportional pressure control valve. The flow rate of the compensation pump, with a value of approximately 9 l/min at a pressure of 25 bar, provides the required flow rate to the servo-mechanism at a pressure of 20 bar, measured at port *ps*, compensates the volumetric losses of the pump with the help of check valves, and the rest of the flow drains to the tank through the pressure control valve set at 25 bar. The throttle between the compensation pump and the proportional directional control valve is meant to limit the pressure pulsations of the compensation pump that would reach the directional control valve. The throttles on the ports of the hydraulic cylinder have the role of equalizing its displacement speed and slowing the response of the servo-mechanism to the control signal. The pressure control valves set at 350 bar act as safety valves, and the pressure control valve (set at 340 bar) which is controlled by the pressure in the closed circuit branches via the selector valve has the role of reducing the pump capacity if the pressure in the closed circuit exceeds the set value. The power transducer directly communicates to the PC the time-variation of the power absorbed by the electric motor, and the rest of the transducers transmit to the PC, by means of the experimental data acquisition board, signals proportional to the parameter values measured by them. After the data acquisition completion condition has been reached, the acquisition stops automatically; then the electric motor and the power supply to the bench are switched on; after performing these operations, the results of the experiment can be saved.

2.2 Methodology of virtual experimentation with numerical simulation

The initial data of the experimentation and those of the numerical simulation of the servo-pump are identical, including the control signal. In this subsection, the initial parameters of the components will be presented briefly.

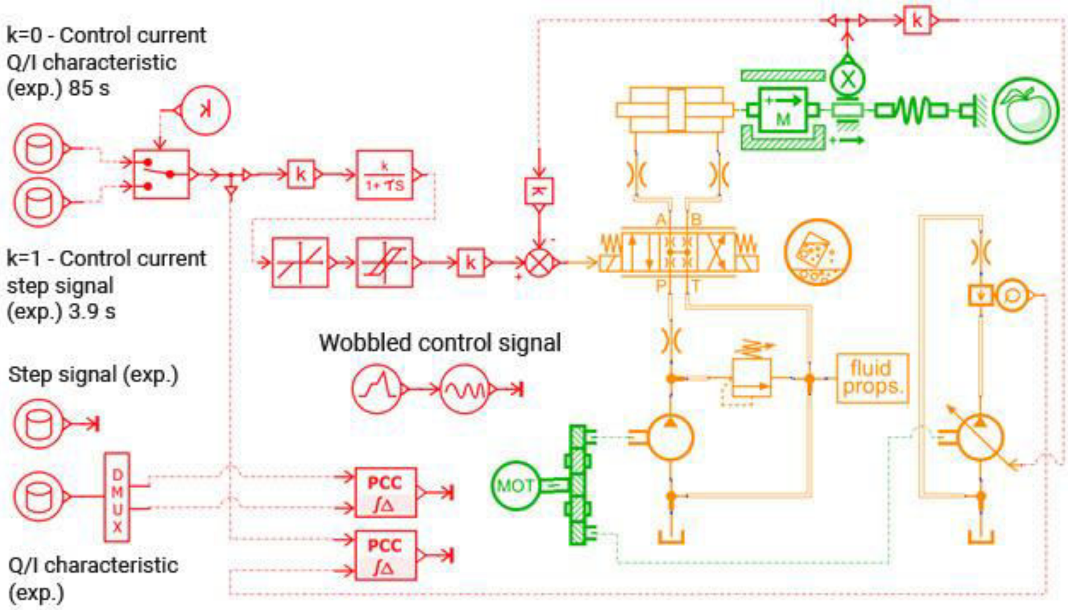

Fig. 9. Servo-pump simulation network

The servo-pump simulation network is presented in Fig. 9; on it, one can identify: in green colour - mechanical components, in red - electronic components or those carrying various signals, and in orange - hydraulic components, which also take thermal phenomena into account; without them, the results of the numerical simulation could not have been compared with the results of the laboratory experiments. The current control signal is the one determined experimentally; it passes through the electronic blocks, which condition it and send it to the servo-mechanism that controls the pump displacement volume (flow rate) proportional to the value of the control current. The main pump has a displacement of 28 cm^3/rev, and the compensation pump - a displacement of 6 cm^3/rev; the hydraulic fluid is ISO VG 46, and the pressure control valve is set at 20 bar.

3. Results

Just like the previous chapter, this chapter is divided into two subchapters, the first of which presents the results of physical experimentation and the second presents the results of virtual experimentation.

3.1 Results of physical experimentation in the laboratory

To be able to have an overview of the experiments in this section of the chapter and for an easier interpretation of the results of the experiments carried out, the experimental data related to the servo-pump flow rate, measured with the flowmeter placed in the closed circuit, have been imported into MS. Excel. There, the four curves have been superimposed so that the lag shown in Figure 10 can be read on the "X" axis of the graph.

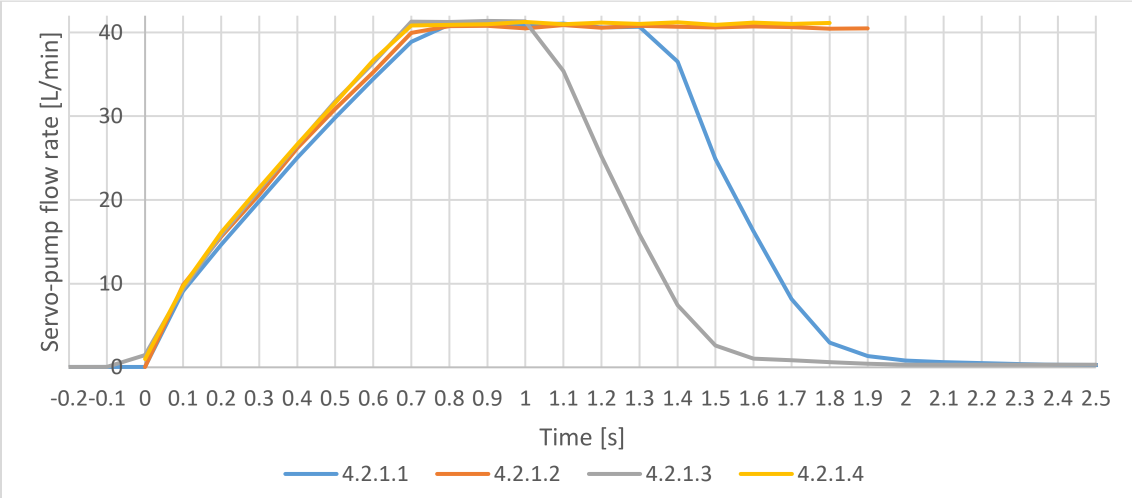

Fig. 10. Response to step signal – centralized results

On the panel of the application made in LabVIEW for the response to the step signal of the servo-pump - shown in Fig. 11, one can see the graphs for the following parameters that vary over time: the control current, the flow rate of the servo-pump, the control voltage, as well as the pressure on the two sides of the transmission.

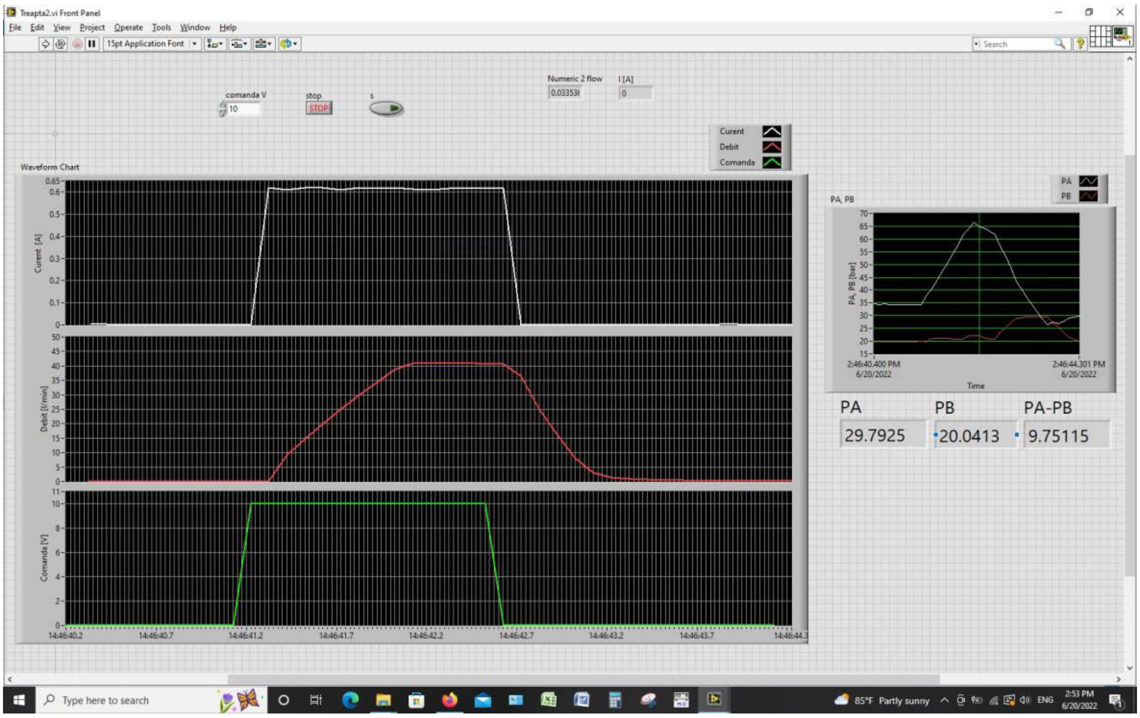

Fig. 11. Application panel – A10VG28EP4 servo-pump response to step signal

A10VG28EP4 servo-pump flow rate/control characteristic and transmission characteristic

The application panel related to the experimentation with load created by the hydrostatic motor and the maximum control signal is shown in Fig. 12, while for the minimum control signal the application panel is shown in Fig. 13. These panels contain pump and transmission characteristics on the first row, and on the second row, as a function of time, there are shown variation of power absorbed by the electric motor, variation of the control current of the proportional directional valve in the servo-pump structure, and pressure variation on the sides of the closed circuit.

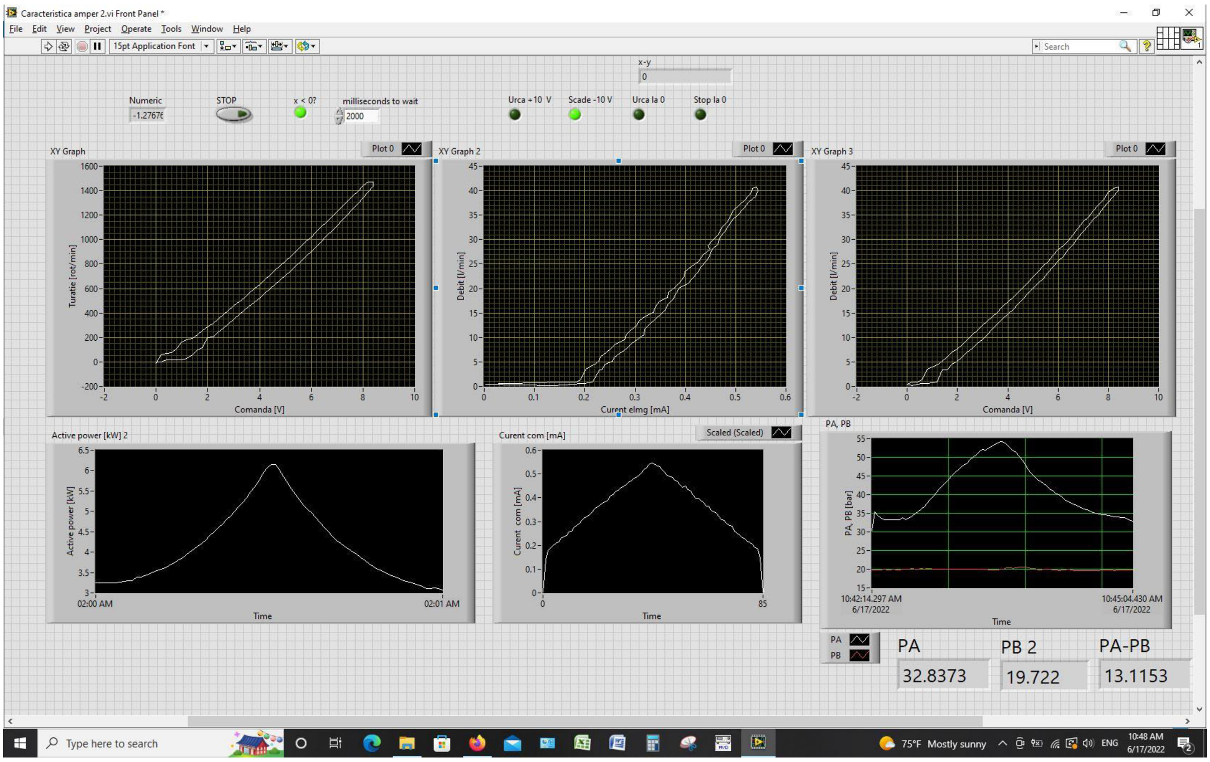

Fig. 12. Application panel related to the experimentation with load created by the hydrostatic motor and the maximum control signal

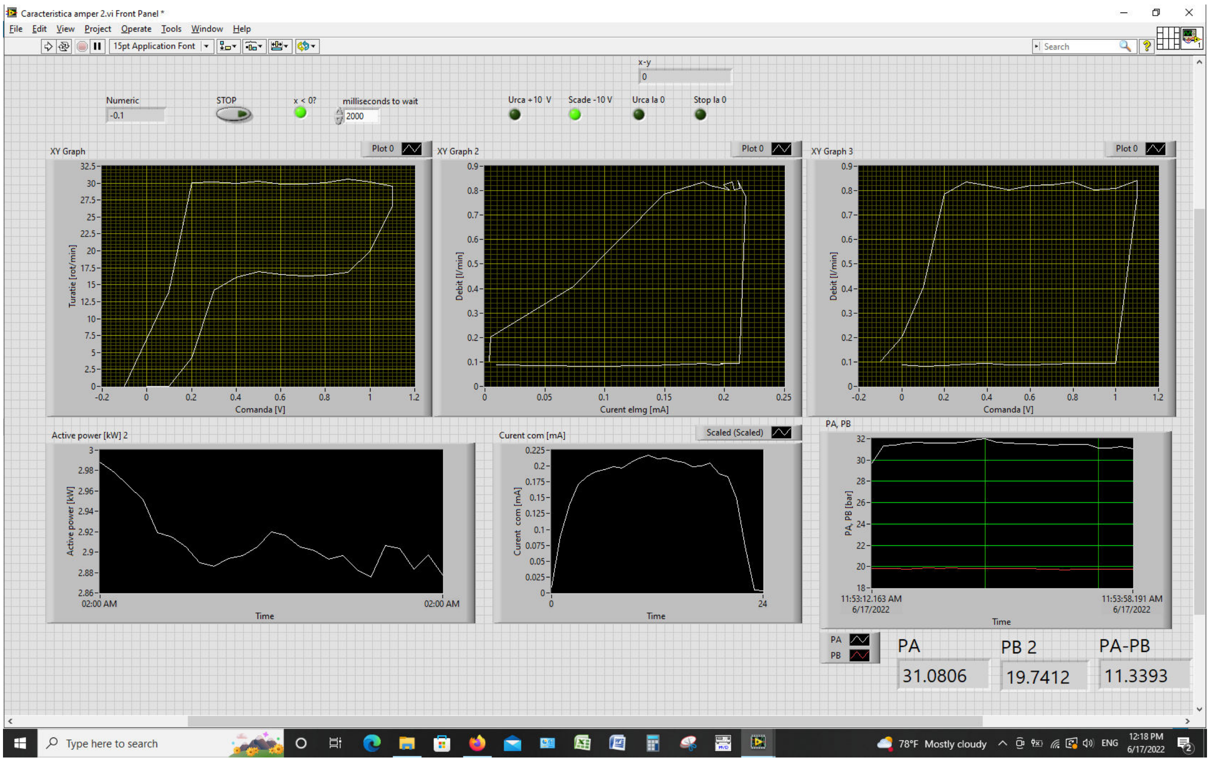

Fig. 13. Application panel related to the experimentation with load created by the hydrostatic motor and the minimum control signal

3.2 Results of virtual experimentation with numerical simulation

Servo-pump response to step signal

In Fig. 14 one can see that the time-variation of the simulated servo-pump flow rate is almost identical to the experimental one; the control current is common.

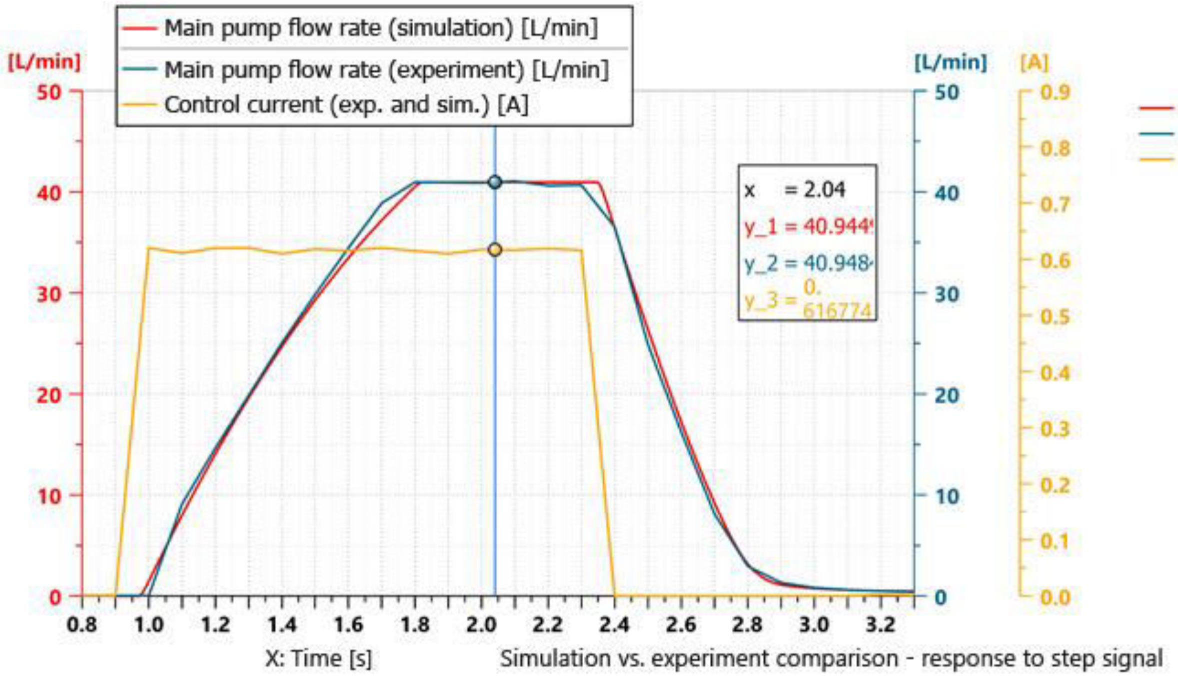

Fig. 14. Main pump flow rate and its control current – validation of numerical simulation

Flow rate/control characteristic of the servo-pump

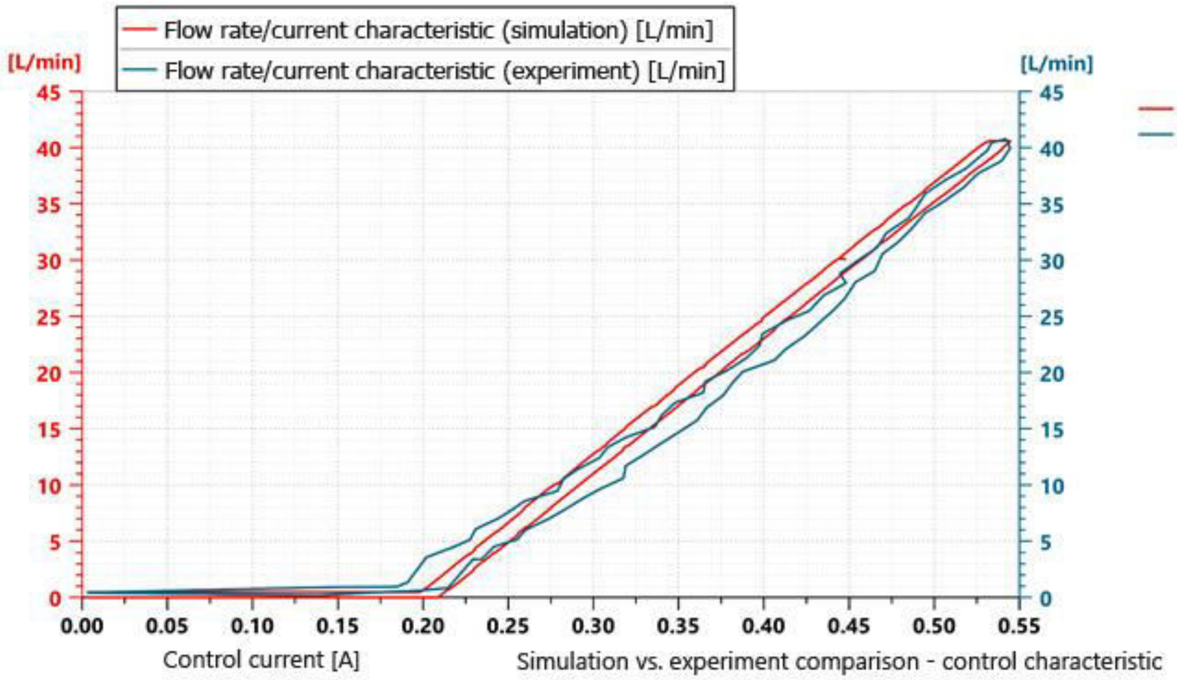

Fig. 15. Flow rate/control current characteristic – validation of numerical simulation results

In Fig. 15 one can see that the simulation results coincide with those of physical experimentation; the maximum flow rate is identical, and the current value from which the control of the pump displacement starts is similar; in this case, too, the control current is common.

The linear correlation coefficient

Fig. 16 estimates - as the name suggests - the linear correlation of two signals (physical parameters), in the present case, the linear correlation of the pump displacement control current, measured in amperes, and the servo-pump flow rate. A value of 0 or close to 0 of this coefficient indicates no linear correlation of the two signals, while a value close to 1, whether positive or negative, indicates a good linear correlation of the two signals.

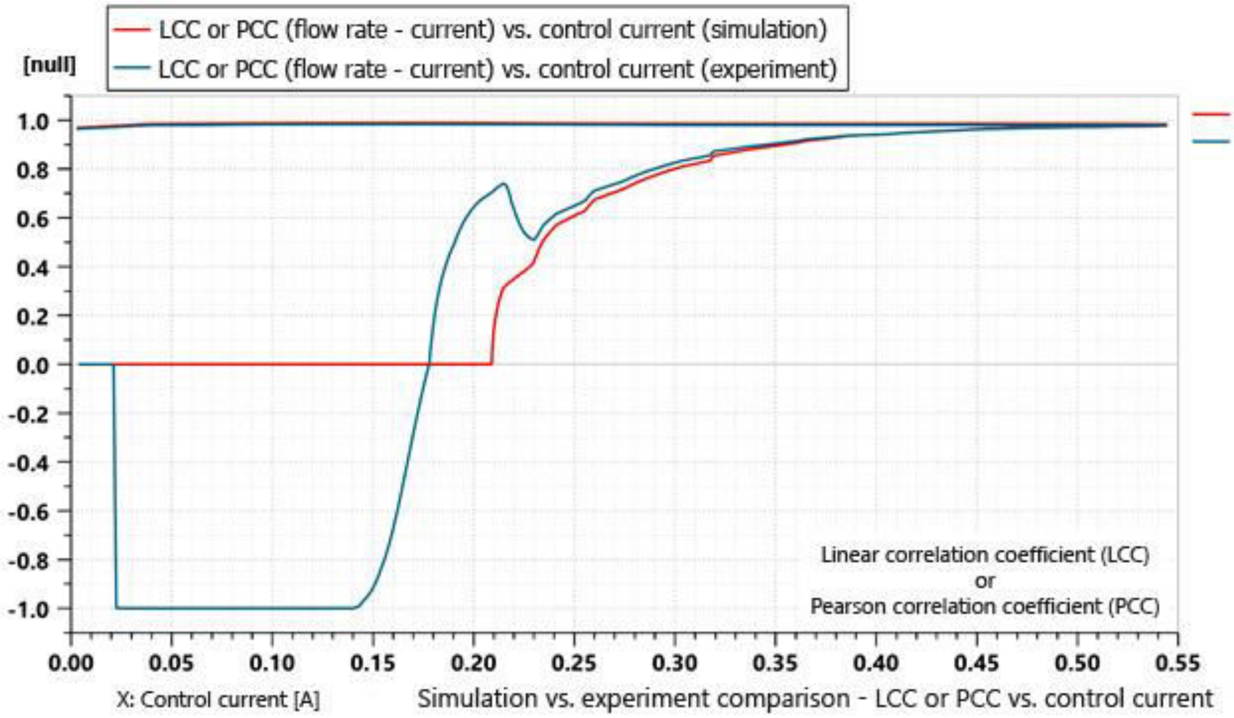

Fig. 16. Linear correlation coefficient - simulation vs. experimentation

The control current with which the displacement of servo-pumps for mobile applications is controlled has an insensitive "dead zone", in which the pump rate flow does not respond to the control signal, to avoid the alternate rectilinear movement of the motor truck when the swash plate of the servo-pump is in the neutral position and oscillates around it. In this case, the numerical simulation shows a superior linear correlation of the control current and the pump flow rate, because in simulation the conditions can be better controlled.

Frequency response of the servo-pump to the wobble control signal

The wobble control signal - constant amplitude and variable frequency control signal – is shown in Fig. 17 below.

Fig. 18 shows the time-variation of the servo-pump flow rate in response to the wobble control signal. This analysis is necessary for the correct tuning of the PID controller in the structure of the hydrostatic transmission of the motor truck.

Frequency response of the servo-pump flow rate is shown in Fig. 19 (Bode plot). On this graph, one can see what percentage of the flow rate amplitude is still available for a certain frequency, and also the phase shift. Comparing the results in this figure with the characteristics of the pump P7, one can see that the pump P7 achieves small amplitude flow rates at a maximum frequency of

17 Hz and a pressure of 70 bar, and the simulation reveals that the simulated servo-pump achieves small amplitude flow rates at 12 Hz, at a pressure of 20 bar.

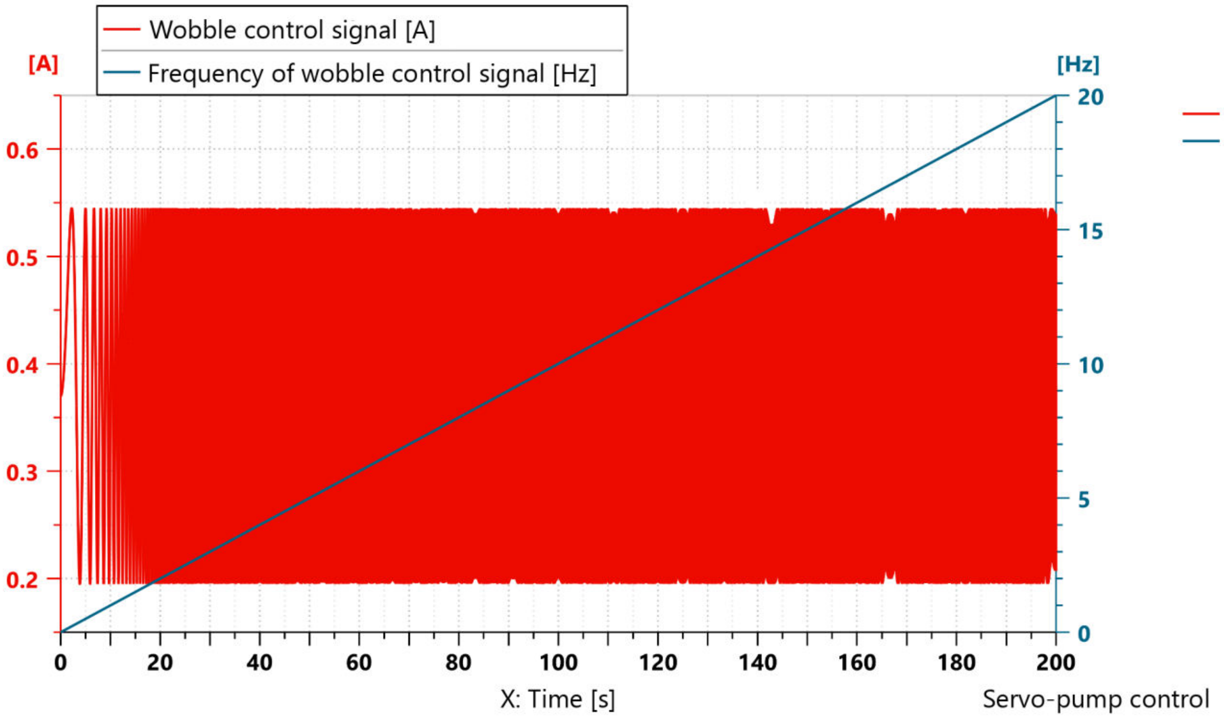

Fig. 17. Amplitude and frequency of wobble control signal

The influence of the wobble control signal on the flow rate of the servo-pump is shown in Fig. 18. On this figure one can see how, due to the increase in the frequency of the control signal, the amplitude of the servo-pump flow rate decreases. This attenuation of the flow rate amplitude can be counteracted by increasing the control pressure or by decreasing the mass of the components of the servo-control mechanism.

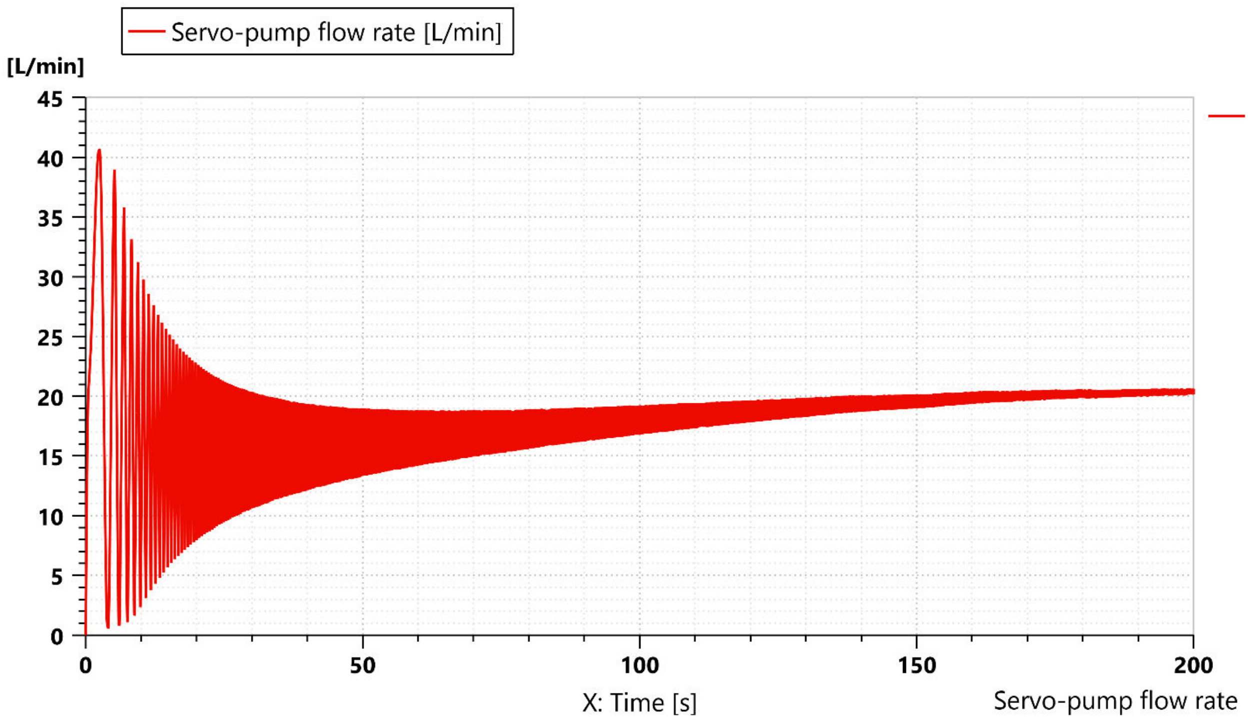

Fig. 18. Servo pump flow rate in response to wobble control signal

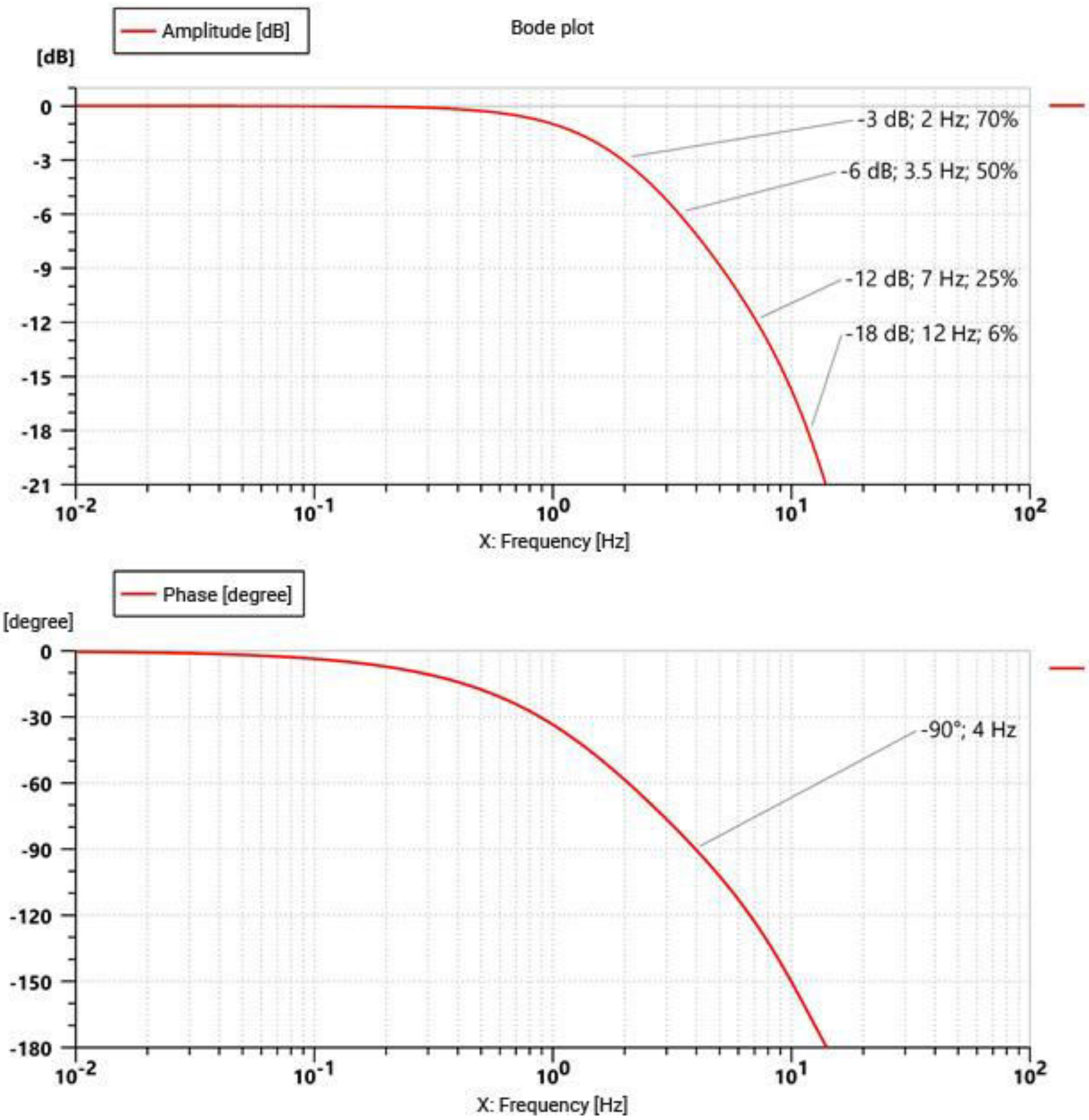

Fig. 19. Bode plot for frequency response of the servo-pump flow rate

4. Conclusions

- The time required for the servo-pump to reach maximum flow rate varies between 0.83 seconds and one second; it is measured between the time when the voltage control signal has been given and the time when the pump has reached maximum flow rate. If we exclude the time for processing the electrical signals from the calculation, one can see that the servo-pump reaches the maximum flow rate in 0.7 – 0.8 seconds. Regardless of the angle of the pump swash plate (0° or 33°) from which the voltage control is given, or of the load in the closed circuit, the servo-pump reaches maximum flow rate or 0 flow rate in no more than one second.
- The maximum theoretical flow rate of the servo-pump if it were to be driven at the synchronism speed of the asynchronous electric motor, is 42 l/min; two values have been determined experimentally, 40.77 l/min (with load) and 41.17 l/min (no load). The maximum flow rate of the servo-pump is load dependent: in proportion to the increase in pressure,

volumetric losses also increase. The flow rate of the servo-pump is also influenced by the variation of the speed rate of the asynchronous motor; this variation occurs as a result of the slippage between the stator and the rotor of the electric motor; this slippage is influenced by the resistive torque on its shaft; the torque is directly proportional to the pressure in the closed circuit.

- The minimum flow rate of the servo-pump is 0.116 l/min; it depends on the load since volumetric losses are proportional to pressure. The minimum flow rate is 0.2762% of the maximum theoretical flow rate of the servo-pump at a speed of 1500 rev/min, ($0.116/42 * 100 = 0.2762\,\%$).
- The pump flow rate becomes proportional to the control signals from the value of about 0.8 l/min, proportional adjustment starting from the voltage value of 1.1 volts and the control current value of 215 mA. The proportional relationship between the servo-pump flow rate and the control current is not significantly influenced by the load (pressure) in the closed circuit as long as the pump is operated at the nominal conditions specified by the manufacturer; the increase in pressure causes the increase in volumetric losses, and the latter reduce the flow rate for the same control current.
- Comparing the results of the numerical simulation with those determined experimentally, namely the response to the step signal and the control characteristic, it can be confidently stated that the numerical simulation model of the servo-mechanism controlling the displacement of the servo-pump is very similar to the one in the laboratory and can be used for further research.
- The previously mentioned conclusion is also strengthened by the strong linear correlation between the control signal and the flow rate of the servo-pump, both in the case of experimentation and in the case of numerical simulation.

Acknowledgments

The research presented in this article has been financed under a project funded by the Ministry of Research, Innovation and Digitalization through Programme 1- Development of the national research & development system, Sub-programme 1.2 - Institutional performance - Projects financing the R&D&I excellence, Financial Agreement no. 18PFE/30.12.2021.

References

[1] ASSOFLUID. *Hydraulics in Industrial and Mobile Applications*. Brugherio (Milano), Grafiche Parole Nuove s.r.l., 2007.
[2] Chapple, P. J. *Principles of Hydraulic System Design*. Oxford, Coxworth Publishing Company, 2003.
[3] Vasiliu, N., and I. Catană. *Hydraulic and electrohydraulic transmissions. Vol. I – Positive displacement hydraulic machines / Transmisii hidraulice şi electrohidraulice. Vol. I - Maşini hidraulice volumice*. Bucharest, Technical Publishing House, 1988.
[4] Merritt, H. E. *Hydraulic control systems*. New York, John Wiley & Sons, 1967.
[5] Stringer, J. *Hydraulic system analysis: an introduction*. Hoboken, John Wiley & Sons, 1976.
[6] Blackburn, J.F., G. Reethof, and J.L. Shearer. *Fluid power control*. Vols. 1, 2, and 3. New York & London, Technology press of M.I.T. and John Wiley & Sons, 1960.
[7] Manring, N. D., and G. R. Luecke. "Modeling and designing a hydrostatic transmission with a fixed-displacement motor." *Journal of Dynamic Systems, Measurement, and Control* 120 (1998): 45-49.
[8] Gies, H. M. S. *Fluid technology for mobile applications / Fluidtechnik für mobile anwendungen*. Aachen, Shaker Verlag, 2008.
[9] Costa, G. K., and N. Sepehri. *Hydrostatic transmissions and actuators: operation, modelling and applications*. West Sussex, John Wiley & Sons Inc., 2015.
[10] Zarotti, L. G., and R. Paoluzzi. "In quest of the transmission size." Paper presented at the Third JHPS International Symposium on Fluid Power, Yokohama, Japan, November 4 - 6, 1996.
[11] Wei, X., L. Wang, X. Ni, S. Han, X. Zhao, and S. Li. "Speed control strategy for pump-motor hydraulic transmission subsystem in hydro-mechanical continuously variable transmission." *Journal of Mechanical Science and Technology* 35, no. 12 (2021): 5665-5679.
[12] Axinti, G., and A. S. Axinti. *Hydraulic and pneumatic drives. Vol. 2. Dynamics of equipment and systems / Acționări hidraulice și pneumatice. Vol. 2. Dinamica echipamentelor şi sistemelor*. Chișinău, "Tehnica-Info" Publishing House, 2008.

About Computer Tools Available for Dynamic Analysis of Mechanic and Hydraulic Systems of the Loader Bucket

Prof. Dr. Eng. **Carmen Nicoleta DEBELEAC**[1,*]

[1]"Dunarea de Jos" University of Galati, Engineering and Agronomy Faculty in Braila,

Research Center for Mechanics of Machines and Technological Equipments

* carmen.debeleac@ugal.ro

Abstract: *The paper focuses on modelling and simulation a feedlot bucket (0.7 m^3 capacity) from skid steer loader, with hydraulic acting, using specialized engineering computer-based environments. It was highlighted the capabilities of these design tools by exemplifying some case analyzes (drawing 2D and 3D shape of component elements, testing the mechanical resistance, evaluating the kinematic parameters, building the hydraulic circuit in order to simulate the system behavior).*

Keywords: *Feedlot bucket, hydraulic cylinder, dynamics, simulation, Matlab*

1. Introduction

Modeling and simulation constitute powerful tools which permit designers to test the complex systems and processes using virtual environments instead of real experiments. Moreover, numerical simulation becomes indispensable when the designers coupled multi-disciplinary systems, where different components (mechanical, hydraulic, pneumatic etc.) work together to obtain optimal responses in exploitation. Thus, computer-aided systems for industrial area of product development have been widely developed during the last two decades. Specialized CAD applications, like Catia, Nastran, Solid Edge, Solid Work, Inventor etc., improving quality of the work environment, allowing engineers to quickly manufacture prototypes [1-3]. Basically, the product form (as 3D technical design) is imported from the CAD environments and transferred to the CAE environments in order to analyze it's for static or/and dynamic behavior.
In this paper, it is provided a brief overview of some computer applications that allow testing of driving mechanism of the feedlot bucket usually mounted as attachment on the wheel loader. In Figure 1 representative examples of these kind of buckets are shown.

Fig. 1. Examples of feedlot buckets for hydraulic loader [4-6]

These feedlot buckets feature clamps, actioned by one or two hydraulic cylinders, to allow large capacities of irregular shaped of materials (e.g., logs, construction materials resulting from demolitions, round bales etc.), to be handled efficiently and accurately for gripping, loading, sorting and transport. The drive mechanism for clamp motion (hydraulic cylinder / actuator) will be involve for better understanding of possibilities to analyze it using computer-aided methods [7,8].

2. Conceptual design for feedlot bucket

Equipment design focuses on the basic conceptual principles taking into account the actual desideratum: to be able to perform working specific requirements with maximum economy and efficiency. Starting from these aspects, a basic constructive solution of a virtual prototype of feedlot bucket (with 0.7 m^3 capacity) it was drawn in Figure 2.

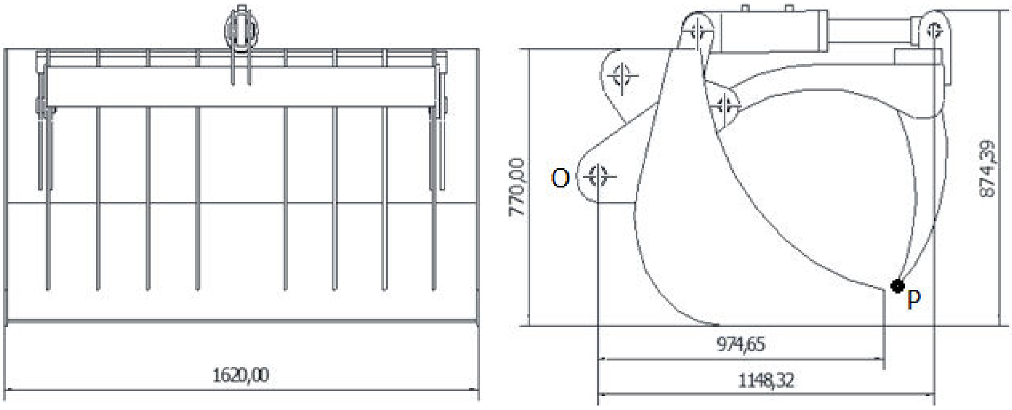

Fig. 2. 2D technical drawing of feedlot bucket

To operate the feedlot bucket, it is required a skid steer loader (as base machine) with power P_m = 45 HP and angular speed n_m = 2400 rpm, able to provide a minimum flow of 2 m^3/h for attachment driving. The model of pump with constant parameters will be assumed, functioning at 200 bar pressure. The discharge valve acts as a protection of the circuit when the maximum value of the working pressure is exceeded (preset to 115 bar).

2. Dynamic simulation of the feedlot bucket

The components of the bucket were three-dimensional designed and assembled in the Autodesk Inventor software, for analysis of model motion containing constraints between bodies, contacts, forces, and actuator [9]. In order to simulate the functionality of the bucket ensemble, a group of main parameters (Table 1 and 2) are required to be set within the dialog box through the values entered by the users.

Table 1: Operational parameters of feedlot bucket

Parameter	Value
Overall load bucket	9000 N
Bucket capacity	0.4 m^3
Bucket width	1.6 m

Table 2: Cylinder feedlot bucket properties

Parameter	Value
Diameter	50/32 mm
Stroke cylinder	0.156 m
Pressure	115 bar
Piston velocity	0.052 m/s

Testing the functionality of clamp mechanism before it will be physically achieved is a very simple process with help of computer simulation. Thus, 3D CAD model will be transferred to the *Dynamic Simulation* module of Inventor environment, the loads that acting on bucket will be setup with the help of specific tools, and the responses will be gained as evolutive diagrams, by sets of specific values or directly in graphic representation forms, as it can be seen in Figure 3.
Design revisions are easier to perform if motion problems are identified before practical achievement of the physical assembly of feedlot bucket. In addition, with help of *Dynamic*

Simulation module capabilities it can be easily solve a lot of problems regarding the kinetics of structural elements of analyzed mechanical system.

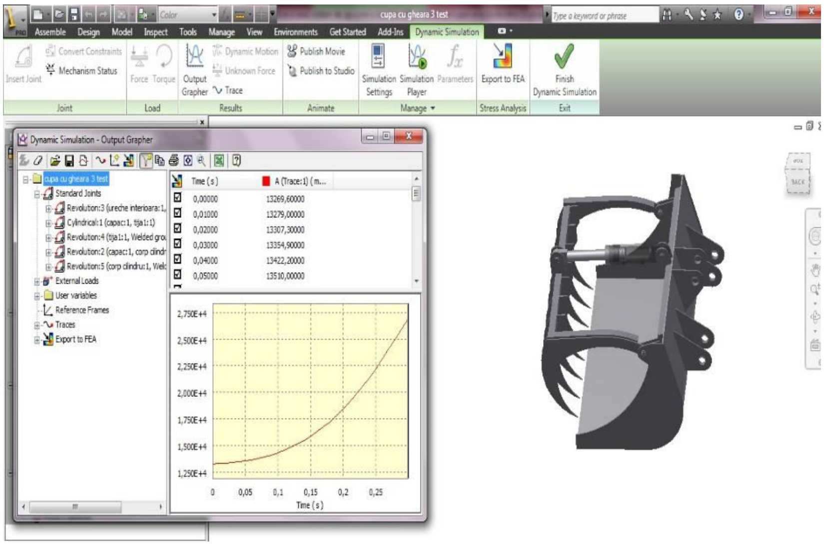

Fig. 3. Feedlot bucket model implemented in Inventor environment

Therefore, using the module dedicated to kinematic analysis, in *Dynamic Simulation* module within Inventor, it is possible to evaluate the values of specific parameters (e. g. speed, acceleration etc.) for the elements in motion, as parts of the assembly. As example, it was considered an extreme point on the clamp (see point P in fig. 3) for which it was evaluated the speed and, respectively, the acceleration. The graphic representation of time variation of these parameters is given in Figure 4.

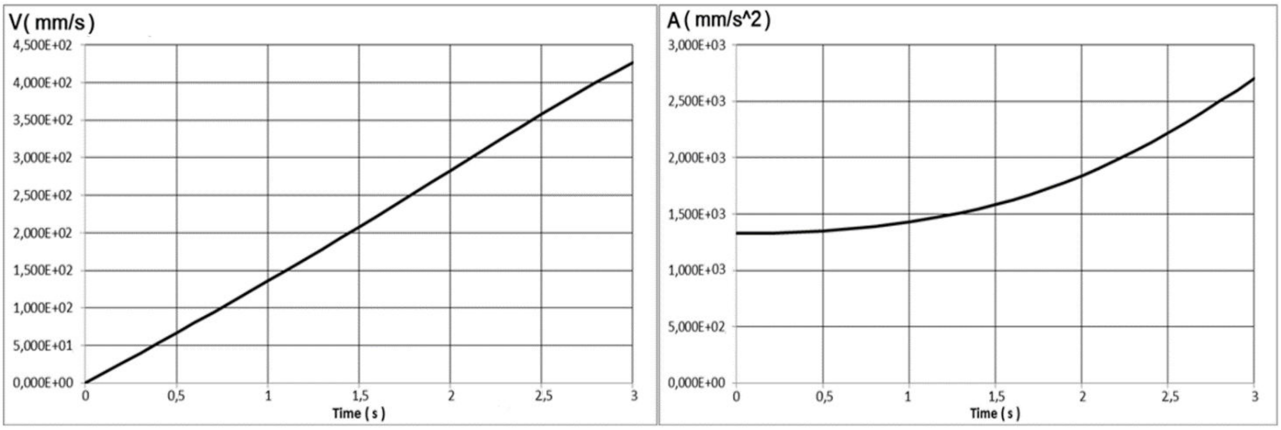

a) b)

Fig. 4. Kinematical parameters of end of clamp (in terms of timed evolution):
a) velocity; b) acceleration.

The results give the numerical information that is necessary to fully understand the dynamic evolution and the operational performances of the clamp design. As you make the initial design results that, through systematically step-by-step model changes, you can compare initial with actual datum, in order to verify design improvement. If we change the velocity of the piston movement in extension stroke, the clamping elements will acquire different kinematical parameters and, respectively, the cycle time for operational tasks with the feedlot bucket will be adjusted.
The next step, after the dynamic simulation of the motion bucket, supposes that the previously created model will be exported to the FEA module, using the *Export to FEA option* from the *Dynamic Simulation module*. The aim is to analyze the acting element consist on hydraulic cylinder (linear actuator), in order to verify its mechanical stress (see Figures 5 and 6).
By discretizing the model, using the *INVENTOR / FEA* specific option, a total of 1284 elements and

2536 nodes were result. Mechanical properties of material ASTM A572used for FEM analysis are: density: 785 kg/m^3; Young’s modulus: 199947.96 N/mm^2; Poisson’s ratio: 0.29; yield point: 290 MPa; tensile strength: 415 MPa. After the boundary conditions were established (revolute joints for both ends of cylinder and cylindrical joints for piston), the individual parts of the cylinder (rod and barrel) were analyzed.

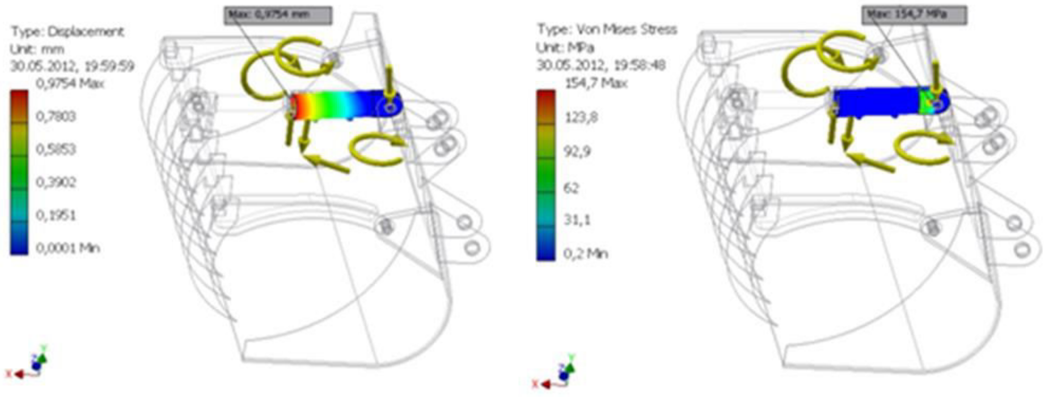

a) b)

Fig. 5. FEM analysis results from actuator’s barrel:
a) displacement; b) Von Mises Stress.

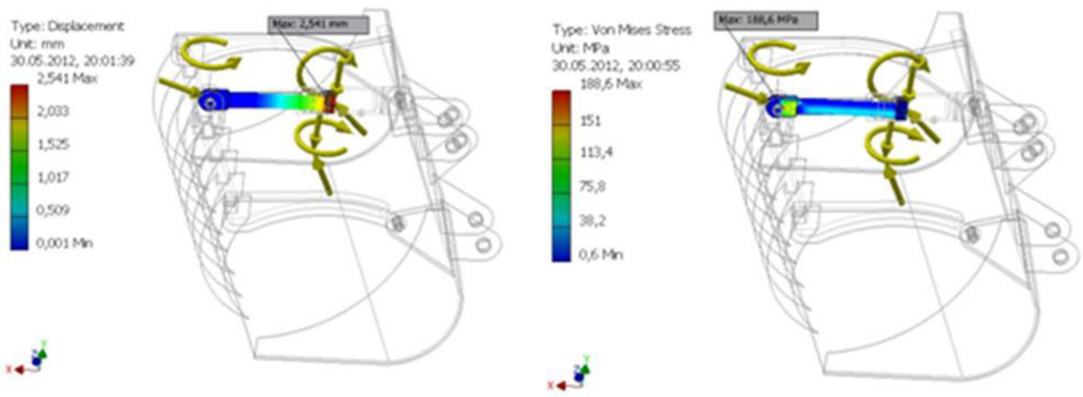

a) b)

Fig. 6. FEM analysis results from actuator’s piston rod:
a) displacement; b) Von Mises Stress.

The finite element analysis was conducted in order to estimate the behavior of clamp cylinder when loads were applied, along with boundary conditions [10]. Results obtained from the simulation, for both main parts of the clamp actuator, were centralized in Table 3.

Table 3: FEM simulation results

	Displacement [mm]		Von Mises Stress [Pa]	
	Barrel	Piston rod	Barrel	Piston rod
Min.	0	0	0.2	0.6
Max.	0.9754	2.541	154.7	188.6

The verification of the clamp actuator model (both FEA and dynamic simulation) is a necessary process to assure that this model is correctly designed and implemented [11,12]. As can be seen, the obtained results conduct to model validation at this stage, but its optimization according to the imposed criteria is not excluded in the future.

3. Simulation of the hydraulic system behavior for clamp bucket acting

A simple configuration of a hydraulic system mainly comprises a few basic groups of components, interconnected to perform a specific function, as: hydraulic power supply, control elements, actuators and other auxiliary elements. Matlab is one of the most popular and recognizable program for constructing simulation models with different types of power transmissions (e. g. hydraulic, pneumatic, mechanic, electric, electronic etc.). Starting from this idea, the cylinder actuation system in Matlab/Simscape environment can be performed through the step-by-step model building. If we want to connect the hydraulic system to mechanical system, then we can build a simple scheme (see Figure 7), by dragging the predefined blocks from the Matlab libraries.

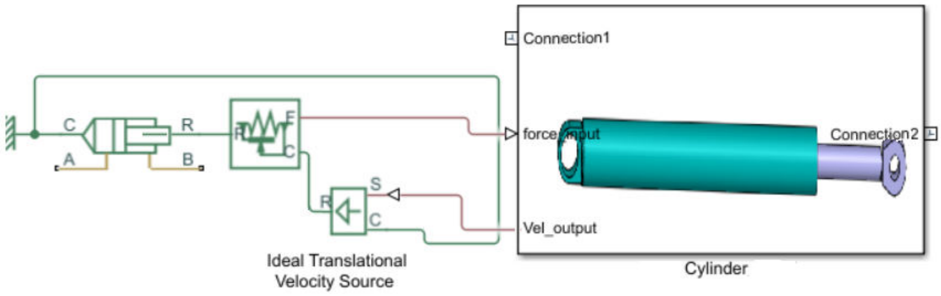

Fig. 7. Connection of the cylinder in mechanical system

An example of an actuation scheme, for the clamp driving cylinder and considering that this is a part of the front loader attachment [13], is presented in Figure 8.
The model contains the basic components required by the hydraulic drive system of these type of heavy machine (e. g. motor, pump, directional valve with 6 ways and 3 positions, actuator, control device, fluid, pipelines). The pump is driven by a diesel engine simulated with a model that takes into account the change in speed caused by the load on the output shaft. All blocks are controlled by the same position signal, provided through the physical signal port *S*. The clamp actuator is controlled by an open center directional valve.

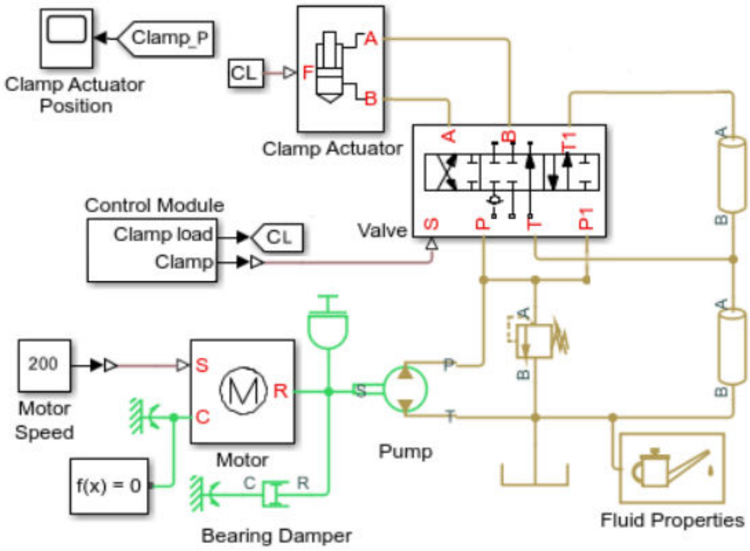

Fig. 8. Actuation system of clamp cylinder simulated in MATLAB/Simscape environment

The actuation system is simulated with the motion and load commands generated as a function of time (see *Clamp load* and *Clamp* as input signals in *Control Module*, fig. 8) that have particular laws depending on the characteristics of the base machine (loader, excavator, tractor etc.), on the inertial forces of working equipment being in motion (tilt / lift), on the operational load etc.
Thus, the hydraulic actuator draws oil flows (denoted Q_A and Q_B in fig. 8) and provides mechanical displacement to the clamp of bucket. By changing the parameters in above scheme (such as

pressure, pipe diameters, piston area, stroke, different fluid types etc.) we can find the optimum parameters values of the hydraulic system in order to be fulfilled the operational requirements at high performance [3,10]. The dynamics of the mechanical system is affected by the mass variation of the moving elements (e. g. clamp) and the external forces acting at working tool. Therefore, these parameters must be estimated carefully if dynamics of the system has the highest priority. In addition, the valve response time can be crucial for fast dynamics and longtime of the valve response must be avoided (only for particular cases when a certain rotation speed is required for feedlot bucket). Furthermore, another important parameter that alters the system dynamics is represented by the bulk modulus and this must be carefully evaluated during the modeling and simulation processes.

4. Conclusions

A feedlot bucket acting the clamp by a single hydraulic cylinder was successfully designed and analyzed using dedicated software that is able to provide necessary information in order to manufacture this attachment on the hydraulic loader instead of basic bucket. Thus, *Dynamic Simulation module* and *Export to FEA* was two powerful instruments useful for hydraulic cylinder analysis, providing results in order to validate the proposed solution, both from the point of view of functionality and operational safety. Testing of the hydraulic system can be performed in the specific programming environment (Matlab, in the present case). Having predefined the main hydraulic elements, the model of hydraulic scheme become easily to build only by taking over the symbols in libraries and drawing the connections between added elements within the diagram. This software application allows deeply investigation of the characteristics of the hydraulic system that are acting the working tool (e. g. feedlot bucket) and gives useful information about operational efficiency, system stability, time response to the commands etc.
The aspects presented in this paper highlight computational tools for 3D generating of geometric forms, intended for evaluation of its dynamic behavior and for comparing to the objective functions usually used in optimization process (such as: mass minimization, easy execution technology, short manufacturing time, high reliability, short time response etc.).

References

[1] Rix, Joachim, Stefan Haas, and Jose Teixeira (eds.). *Virtual Prototyping: Virtual environments and the product design process*. London, Springer, Kluwer Academic Publishers, 1995.
[2] Debeleac, Carmen. "Design and analysis of side dump bucket for wheel loader using CAD/CAE/CAM technologies." *IOP Conference Series: Materials Science and Engineering* 564 (2019): 012061.
[3] Pascu, Marius. "Optimizing the hydraulic systems using the Simhydraulics programming environment." *Journal of Engineering Studies and Research* 16, no. 4 (2010): 25-32.
[4] Emily Ets. https://www.emily-equipment.co.uk/our-products/multi-purpose-bucket-with-rear-rams/. Accessed Sept. 17, 2022.
[5] RocksFair. https://rocksfair.com/product-category/hydraulic-grapple-bucket/. Accessed Sept. 17, 2022.
[6] Craig Manufacturing. https://www.craigattachments.com/products/loader/loader-buckets/feedlot-bucket/. Accessed Sept.17, 2022.
[7] Debeleac, Carmen, and Silviu Nastac. "Conceptual product design in virtual prototyping." *Journal of Industrial Design and Engineering Graphics – JIDEG*, no. 5 (June 2009): 17-20.
[8] Baroiu, Nicuşor, Virgil Gabriel Teodor, and Georgiana-Alexandra Costin. "Constructive-functional analysis of single-rod double-acting hydraulic cylinders." *TEHNOMUS JOURNAL - New Technologies and Products in Machine Manufacturing Technologies* (2017): 126-131.
[9] Tucki, K., A. Bączyk, R. Mruk, I. Wielewska, and P. Radziszewski. "The simulation model of the grapple loader operation." *MATEC Web of Conferences* 252 (2019): 05021.
[10] Mickoski, Hristijan, and Marjan Djidrov. "Modeling of mechanism with linear hydraulic drive system." *Mathematical Models in Engineering* 5, no. 3 (2019): 73-78.
[11] Lealin, Stanislav. "Stress Analysis, Frame Analysis and Calculation of Metal Structures in Inventor Software." *Applied Mechanics and Materials* 809–810 (2015): 871–877.
[12] Debeleac, Carmen. "Integrated technologies for CAD/CAM/CAE analysis of a cylinder piston rod." *TEHNOMUS JOURNAL - New Technologies and Products in Machine Manufacturing Technologies* 28, (2021): 101-106.
[13] https://www.mathworks.com/. Accessed Sept. 22, 2022.

Effective Solutions to Reduce Energy Consumption in the Turbo-Blowers of a Sewage Treatment Plant

Prof.PhD.Eng. **Mariana PANAITESCU**[1,*], Prof.PhD.Eng. **Fănel-Viorel PANAITESCU**[1], Lect. PhD. Eng. **Alexandru-Andrei SCUPI**[1]

[1] Constanta Maritime University, Romania

* panaitescumariana1@gmail.com

Abstract: *Since the energy consumption of the turbo blowers represents 68% of the energy consumption of the station, it was sought to reduce this consumption by installing oxygen sensors in the bioreactors; these sensors detect the reaching of the optimal (maximum) oxygen threshold of 2.0% and at this moment they partially close the butterfly valves from the discharge of the turbo blowers, which leads to the reduction of the flow rate and implicitly the energy consumption of the turbo blowers. Through the SEAU's SCADA system for the oxygen volume, the necessary data were obtained to calculate the percentage opening of the butterfly valves from the discharge of the turbo blowers in order to monitor the efficiency of the regulation system, and implicitly, the reduction of energy consumption. The following were calculated: the initial annual consumption established by design, the three-day consumption, the value of the optimized energy, the value of the energy saved, obtaining the economic efficiency of the proposed solution. The regulation system tests the oxygen concentration in the aerobic bioreactor and maintains its value at around 1.5%. The rapid control valve system is set to operate in the 15%-65% opening range. When the oxygen detector detects reaching the 1.5% threshold, the valves open and the air flow increases; at the same time, the power consumed by the turbo blower obviously increases. The diagram of the variation of the oxygen regime and the response of the opening of the turbocharger discharge valve are represented in parallel.*

Keywords: *Energy, consumption, sewage, plant, solution, optimization*

1. Introduction

In the operational flow of a sewage treatment plant, under anoxic conditions, the denitrification process takes place, and under aerobic conditions, the nitrification process takes place in the four lines of the bioreactors. Therefore, four blowers are installed in operating mode, assistance 1 and 2 and stand-by to cover the oxygen requirement in the bioreactors. The electricity consumption of the turbo blowers has an important share in the general energy consumption of the station. Thus, each of the four THOLANDER turbochargers has a nominal power of 355 [kW], while the FLYGT C 3400 intake pumps have a nominal power of 125 [kW] each (five pumps) and the FLOTTWEG centrifuges have a nominal power of 55 [kW] each (4 centrifuges) [1]. The energy share of turbo blowers is over 68% in the general annual consumption [2, 3].
Control of ventilation systems mainly comprises a concentration of two separate control cycles:
- the air regulating valves controlled by the concentration of dissolved oxygen which influences the pressure in the air line and
- air blowers that are controlled by the pressure inside the air pipe; in this way, the blowers operate in a variable speed regime and implicitly in electricity consumption.

The ventilation system has the following characteristics (Figure 1) [4]:

- Typical conditions for oxygen demand: 85639 [kg O_2/day]
- Maximum oxygen absorption per hour: 3586 [kg O_2/h] at 27[°C]
- Air requirement: 37,820 [m3/h]

The turbo blowers work in 3+1 stand-by mode with a suction flow of 13,000 [Nm^3/h], total 39,000 [Nm^3/h].

Fig. 1. Air flow through a screw blower [4]

Where 1- the admitted air is trapped; 2- the volume is reduced; 3- exhaust under pressure; 4- room completely evacuated.

2. Materials and methods

2.1 Materials

Under these conditions, the Constanta North Wastewater Treatment Plant, where oxygen detectors were placed on the bioreactors, was chosen as the study location. The biological needs of aerobic bacteria were taken into account. Diaphragm diffusers with small bubbles absorb air under pressure. The air supply lines to the bioreactors are equipped with air control valves, with each tank having an air control valve. Two oxygen flowmeters (a main probe and a reference probe) will be installed at each bioreactor to regulate the air intake volume in the bioreactor in question. Air flow to each bioreactor line separately is measured and recorded by flowmeters.[5]
At the Constanta-North treatment plant, chambers five and six are non-variable aerobic zones, where nitrification takes place. These furnaces are equipped with aeration systems to provide the necessary dissolved oxygen (included in the pressurized air).

2.2 Methods and researches

Next, the efficiency of the regulation system is calculated from the point of view of energy consumption, given that the turbo blowers have a significant weight in the station's consumption (over 68%).

The estimated consumption value by design is taken as the basis of calculation, i.e.:

$$E = 9125.68 \text{ [MWh/an]}. \tag{1}$$

This value is obtained from the sum of the electricity consumption of the turbo blowers, intake pumps and centrifuges. These consumptions are specific to the sewage treatment plant depending on the flows, so on the number of equivalent inhabitants.
The regulation system tests the oxygen concentration in the aerobic bioreactor and maintains its value at around 1.5%.
The rapid control valve system is set to operate in the 15%-65% opening range. When the oxygen detector detects reaching the 1.5% threshold, the valves open and the air flow increases; at the same time, the power consumed by the turbo blower obviously increases.
Next, the consumption and concentration of oxygen in the bioreactor is taken from the station's SCADA system. The data from the period: 01-31 July 2022, 01-31 October 2022, 01-15 November 2022 were available. The diagram of the variation of the oxygen regime and the response of the opening of the turbocharger discharge valve are represented in parallel (e.g. Fig. 2, Fig. 3) [1].

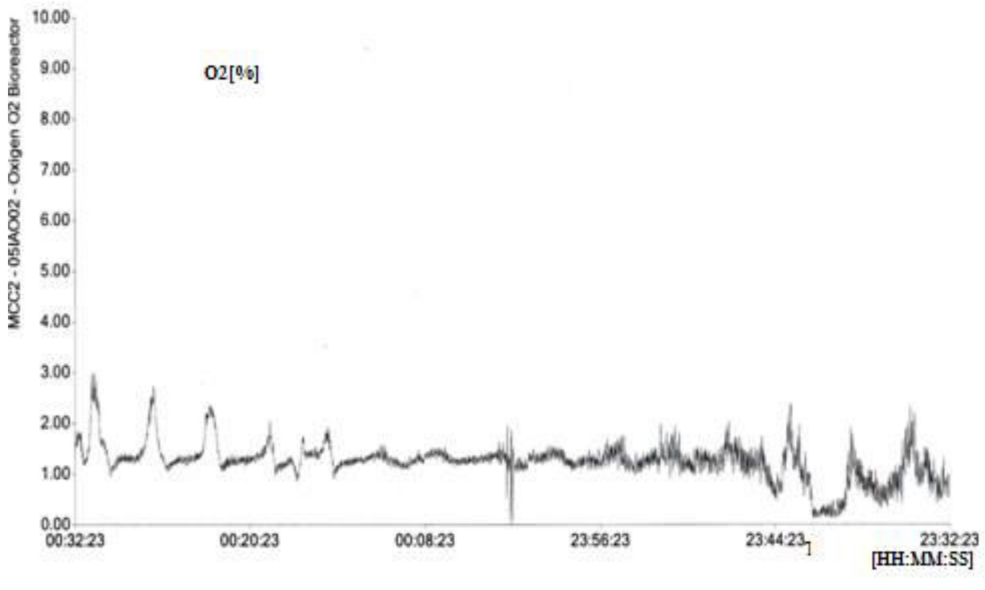

Fig. 2. Variation of oxygen during July 1-15, 2022

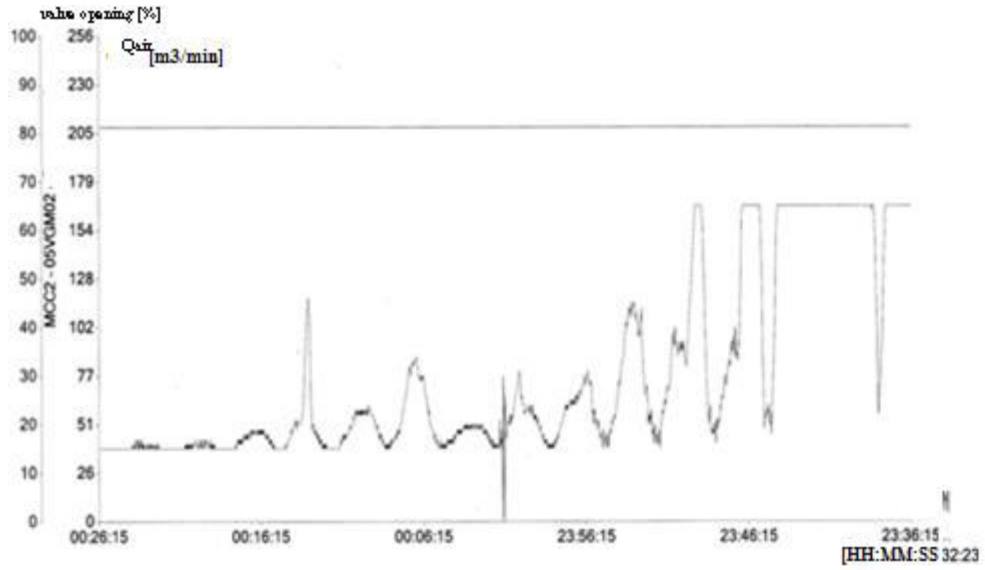

Fig. 3. The variation of the opening of the air butterfly valve between July 1-15, 2022

The same is done for all periods.

3. Results and interpretations

In the period 16.07-31.07 2022 it is observed that the variation of the oxygen concentration required in the bioreactor varies between the limits of 0-10 [%].In the period 1.10-15.11.2022 It is observed that the variation of the concentration of oxygen required in the bioreactor varies between the limits of 0-10 [%] (Fig. 4).

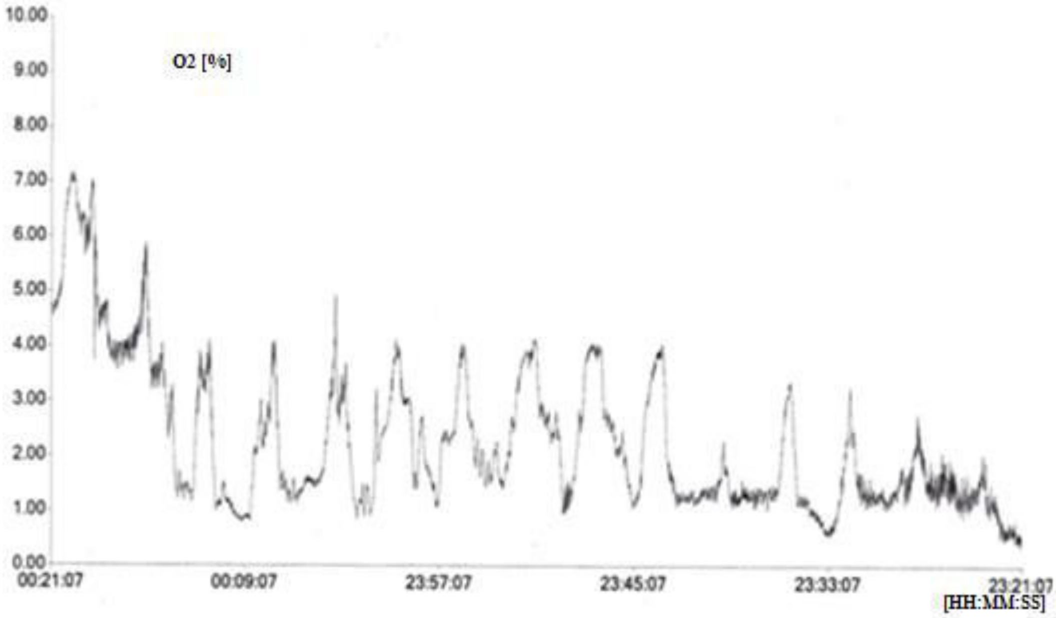

Fig. 4. Oxygen variation in the period October 1-November 15, 2022

The variation of the opening of the air butterfly valve during the period October 1-November 15, 2022 is presented in Fig. 5.

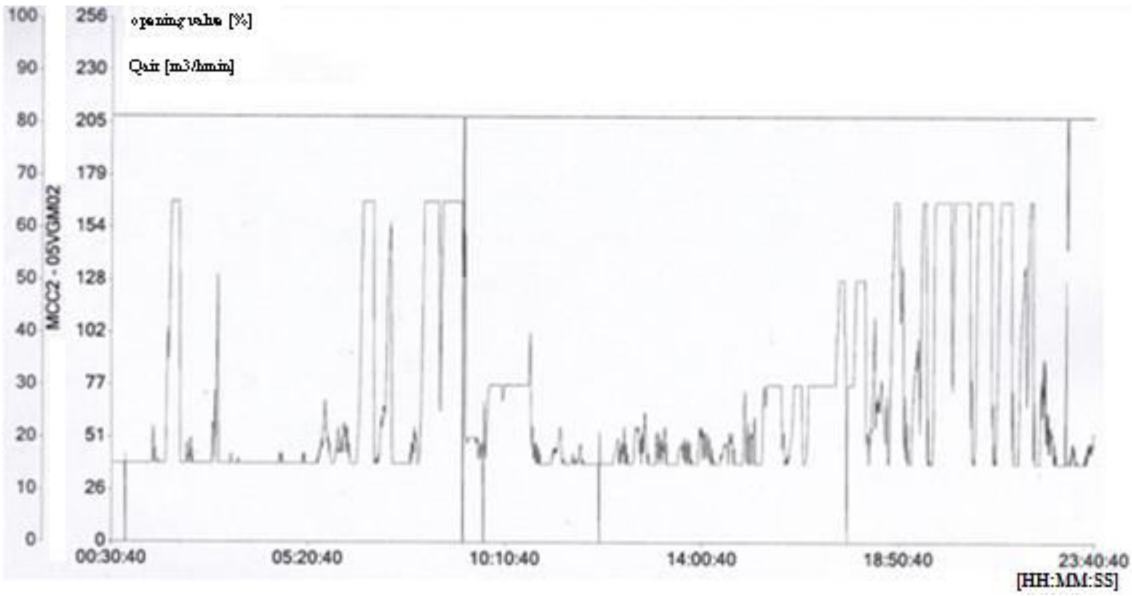

Fig. 5. The variation of the opening of the air butterfly valve

In the period 16.10-31.10.2022 for MCC2 group it is observed that the variation of the valve opening varies between the limits of 15-65 [%], frequently 15 [%], but there are also jumps (42%). The air flow variation is between 40 [m3/min] and 170 [m3/min] (Fig. 6).

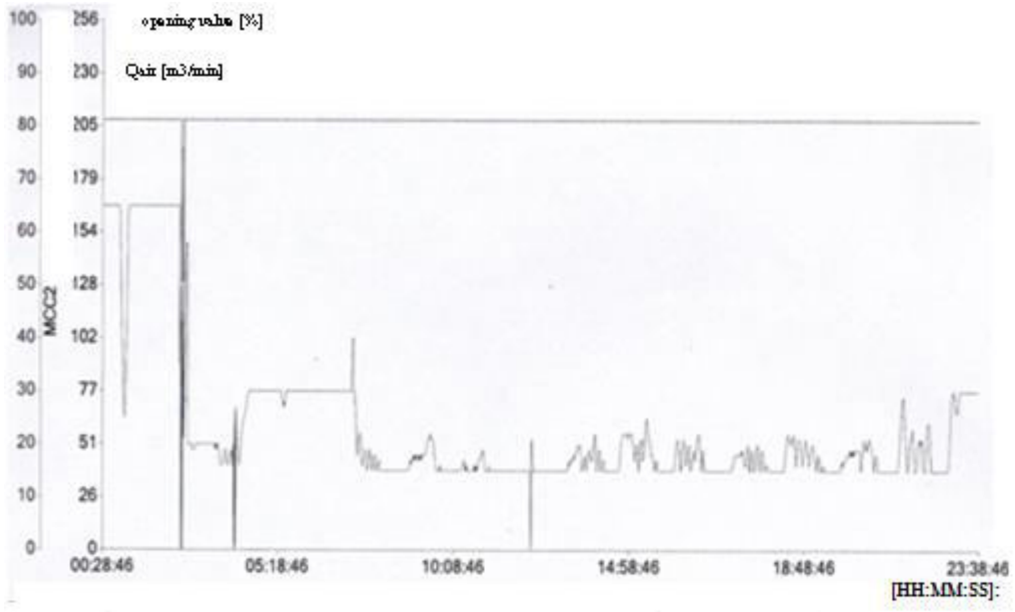

Fig. 6. The variation of the opening of the air butterfly valve between October 16-31, 2022

During the period 01.11-15.11.2022 it is observed that the variation of the oxygen concentration required in the bioreactor varies between the limits of 0-10 [%] (Fig. 7).

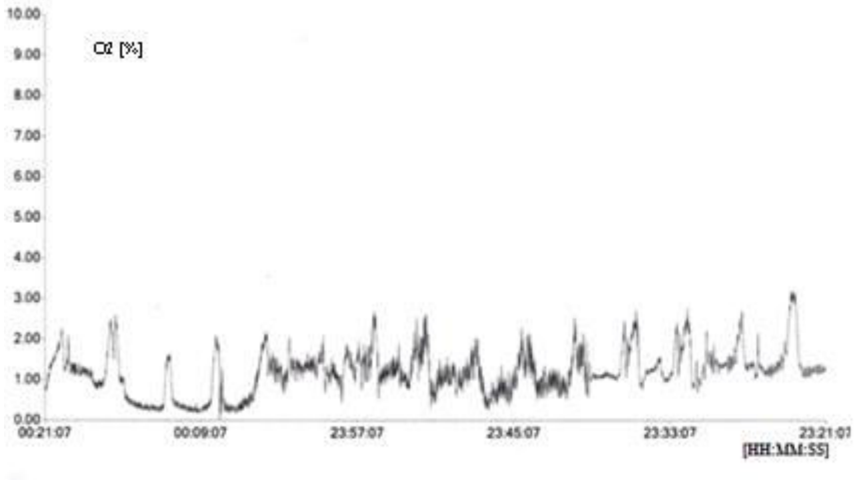

Fig. 7. The variation of the oxygen concentration in the bioreactor

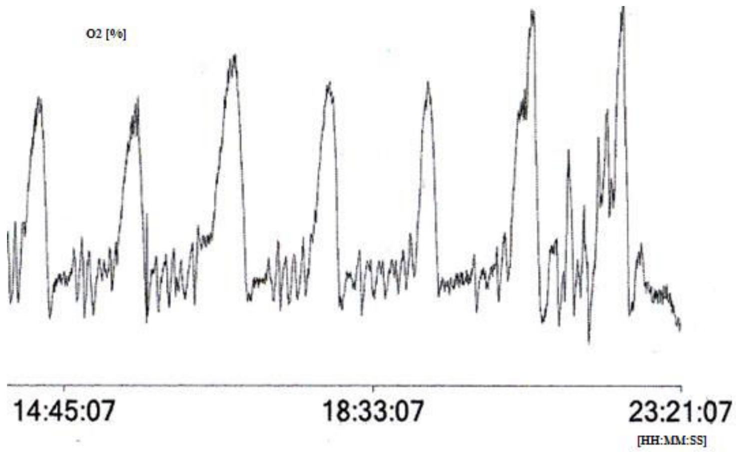

Fig. 8. Oxygen variation - period 26 October H14:45:07 - 31 October H32:21:07

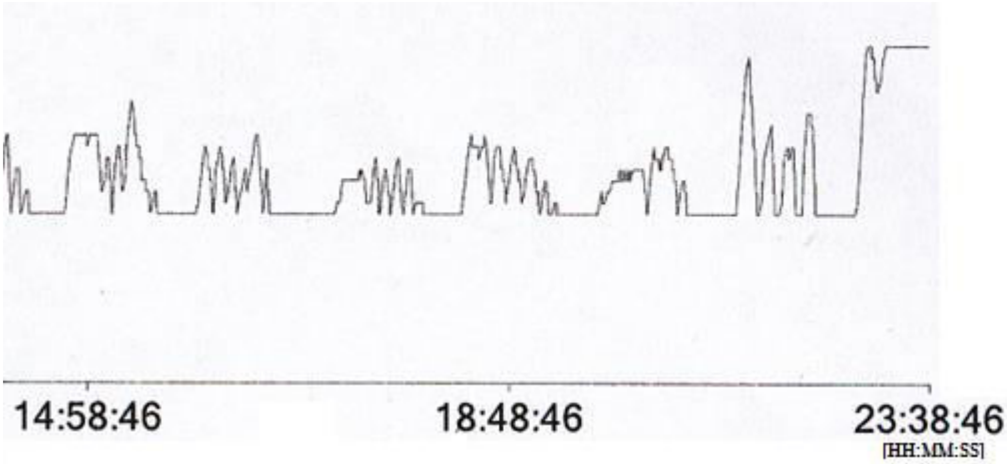

Fig. 9. The variation of the opening of the air butterfly valve - the period October 26 H14:45:07 - October 31 H32:21:07

It is observed that the variation of the valve opening varies between the limits of 15[%] and 65 [%], and the air flow varies between the limits of 30-170 [m^3/min] (Fig. 8, Fig. 9).
Following the superimposition of the two graphs, proceed by drawing the vertical line for the moment of starting the opening of the air butterfly valve (with a black line) marked A, respectively the moment of finishing the opening of the air butterfly valve and returning to the minimum opening value of 15 % (with green line) marked B (Fig. 10).

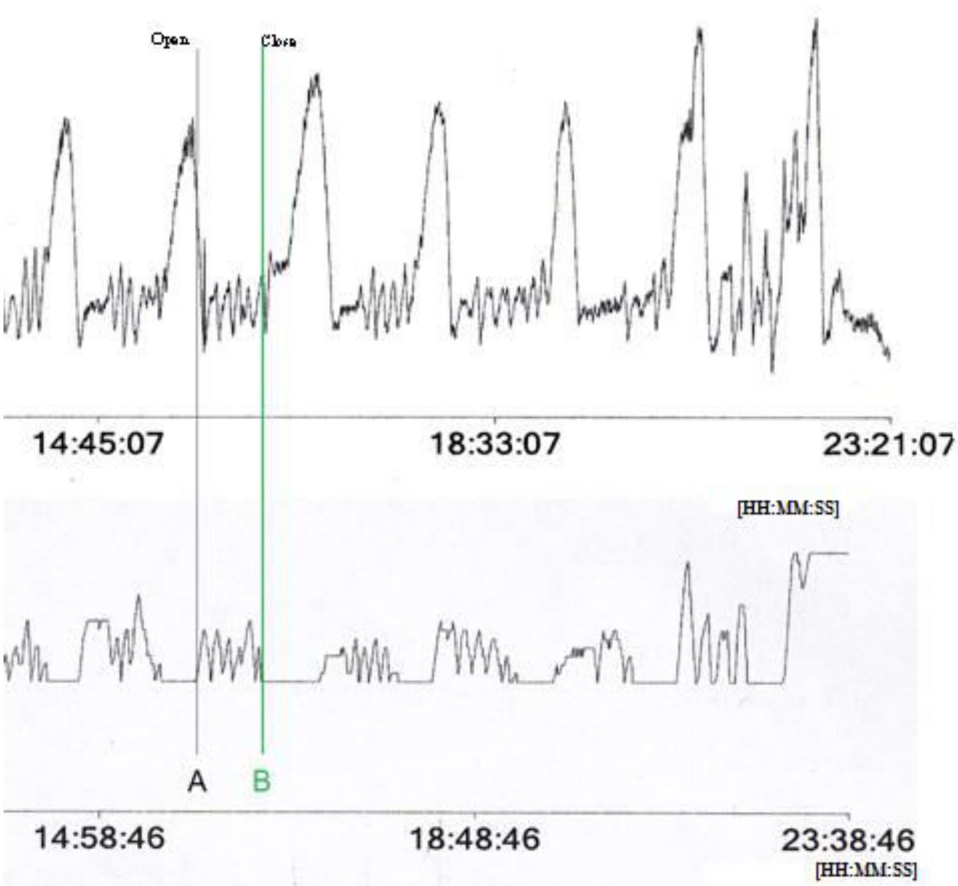

Fig. 10. Overlap of the variation of oxygen and the opening of the air butterfly valve - period 26 October H14:45:07 - 31 October H32:21:07

The variation of the consumed power is calculated depending on the opening of the valve on discharge (Fig. 11).

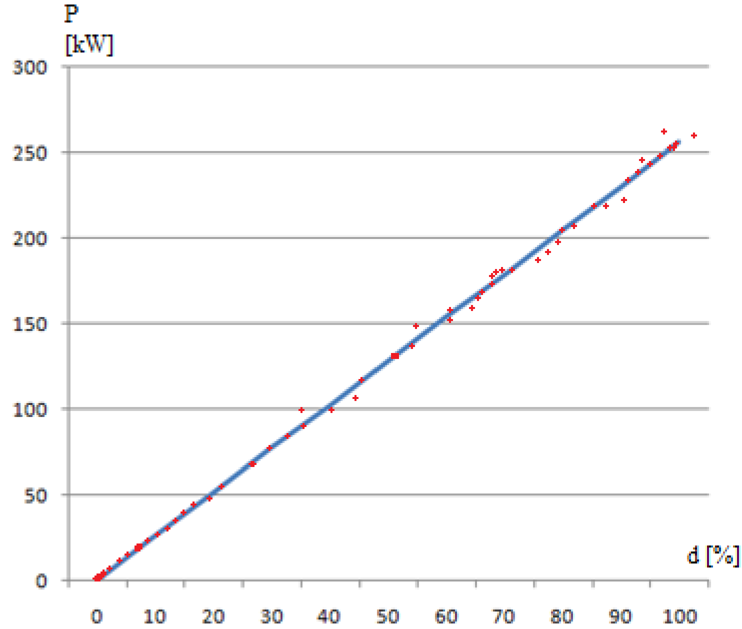

Fig. 11. The variation of the power of the turbo blower depending on the opening of the butterfly valve on discharge

The actual energy consumed after the introduction of the regulation system is E_{real}=51354 [kWh] (for 3 days) and was obtained from the station's SCADA system [2, 5, 6, 7, 8].

4. Conclusions

Since the energy consumption of the turbo blowers represents 68% of the energy consumption of the station, it was sought to reduce this consumption by installing oxygen sensors in the bioreactors [9]; these sensors detect the reaching of the optimal (maximum) oxygen threshold of 2.0% and at this moment they partially close the butterfly valves from the discharge of the turbo blowers, which leads to the reduction of the flow rate and implicitly the energy consumption of the turbo blowers. The initial annual consumption established by design is:

$$E = 9125.68 \text{ [MWh/an]}. \tag{2}$$

So the consumption for three days is:

$$E_{initial} = E/365 *3 = 75005.5 \text{ \{kWh]} \tag{3}$$

The value of the optimized energy was obtained from the data acquisition system of the station and is:

$$E_{optimized} = 51354 \text{ [kWh]}. \tag{4}$$

In order to quantify the energy savings obtained, $E_{economised}$ was calculated by the difference between the energy consumed when operating with nominal flow of the turbo blower (during 3 days) $E_{initial}$, and the optimized $E_{optimized}$:

$$E_{economised} = E_{initial} - E_{optimized} \tag{5}$$

So $E_{economised}$ = 23.651 [kWh].

Considering the unit price of energy P_e=350 [lei/MWh], the economic efficiency of the solution was obtained:

$$C = P_e *E_{economised} *1/3 \tag{6}$$

So: C= 2759 [lei/day].

In conclusion, through the wastewater treatment plant SCADA system for the volume of oxygen, the necessary data were obtained to calculate the percentage opening of the butterfly valves from the discharge of the turbo blowers in order to monitor the efficiency of the regulation system, and implicitly, the reduction of energy consumption.

Acknowledgments

Acknowledgments of Polytechnic University of Bucharest, Doctoral School of Energy Engineering, Prof.PhD. Robescu Niculaie, dr. Vintila Ileana-Irina.

References

[1] Panaitescu Ileana-Irina, Dan Robescu, and Diana Robescu. "Analysis on energy efficiency in a wastewater treatment plant." Paper presented at the International Energy-Environment Conference (CIEM), Bucharest, Romania, November 7-8, 2013.

[2] Mocanu, C.R., L. Stan, I.I. Panaitescu, and L. Balanescu. "Optimum placement for the split-type air-conditioners in order to improve the houses indoor air quality." Paper presented at the 4th International Conference on Development, Energy, Environment, Economics (DEEE13), WSEAS, Paris, France, October 29-31, 2013.

[3] Panaitescu, Ileana-Irina, A. A. Scupi, and D. N. Robescu. "Flow modeling and simulation in a sand and fat tank from a wastewater treatment station." *The Scientific Bulletin of the Politehnica University of Bucharest, Series D* 76, no. 4 (2014): 185-194.

[4] Rajerdren, "R. Water treatment, Aeration." In: Kirk-Othmer (Ed.). *Kirk-Othmer Encyclopedia of Chemical Technology*. Index to Volumes 1 - 26, 5th Edition. Publishing House John Wiley & Sons Inc., Published Online, 2000.

[5] Gillot, S., B. De Clercq, D. Defour, F. Simoens, K. Gernaey, and P. A. Vanrolleghem. "Optimization design a wastewater treatment plant operation and management simulation and cost analysis method." Paper presented at the 72nd Annual WEF Conference and Exposition, New Orleans, USA, October 9 – 13, 1999.

[6] Gligor, E.T. *Contributions to the energy optimization of installations and equipment within wastewater treatment plants / Contribuţii la optimizarea energetică a instalaţiilor şi echipamentelor din cadrul staţiilor de epurare a apelor uzate.* Doctoral thesis. Oradea University Publ., 2011.

[7] Henze, M., M.C.M. van Loosdrecht, G.A. Ekama, and D. Brdjanovic. *Biological Wastewater Treatment: Principles, Modelling and Design*. London, IWA Publishing, 2008.

[8] Ianculescu, Ovidiu, Gheorghe Ionescu, and Raluca Racoviţeanu. *Wastewater treatment / Epurarea apelor uzate*. Bucharest, Matrix Rom Publishing House, 2001.

[9] Olsson, G., and B. Newell. *Control of Biological Wastewater Treatment Plants*. London, IWA Publishing, 2001.

Modification of Cavitation Erosion Resistance of Aluminum Alloy 7075 by Maintaining of Artificial Aging Heat Treatment at 180°C

Prof.PhD.Eng. **Ilare BORDEAȘU[1]**, Dipl. Eng. **Alexandru Nicolae LUCA[2,*]**,
PhD.Eng. **Iosif LAZĂR[3]**, Dipl. Eng. **Dragoș LAZĂR[4]**, Lecturer PhD.Eng. **Rodica BĂDĂRĂU[5]**,
Prof.PhD.Eng. **Brândușa GHIBAN[6]**, Dipl. Eng. **Andreea Daniela BUZATU[7]**,
Dipl. Eng. **Alin Mihai DEMIAN[8]**, Dipl. Eng. **Ovidiu Petrișor ODAGIU[9]**,
Assoc.Prof.PhD.Eng. **Lavinia Mădălina MICU[10]**

[1] Politehnica University of Timisoara, ilarica59@gmail.com

[2] Politehnica University of Timisoara, alexandru.luca2@student.upt.ro

[3] Politehnica University of Timisoara, office@ducodan.ro

[4] Politehnica University of Timisoara, dragoslazar.1997@yahoo.com

[5] Politehnica University of Timisoara, cghera2000@yahoo.com

[6] Politehnica University of Bucharest, ghibanbrandusa@yahoo.com

[7] Politehnica University of Bucharest, buzatuandreea@gmail.com

[8] Politehnica University of Bucharest, demianalin96@gmail.com

[9] Politehnica University of Bucharest, odagiuovidiu2017@gmail.com

[10] Banat University of Agricultural Sciences and Veterinary Medicine of Timisoara, lavimicu@yahoo.com

* Corresponding author: Alexandru Nicolae Luca, alexandru.luca2@student.upt.ro

Abstract: *The use of volume heat treatments aims to change the microstructure and the values of the mechanical properties, with homogeneous distribution in the volume of the part, so as to confer resistance to various stresses. From the point of view of the hydrodynamic stresses of the microjets generated by the cavitation mechanism, these treatments ensure an increase in the life of the required surface. In the case of aluminum-based alloys, volume thermal treatments do not produce important changes in the structural phase, but they cause important changes in the values of the mechanical properties. As these alloys have small specific masses and good mechanical properties, research is currently being resumed aimed at extending their use to parts that work in cavitation such as: propellers of motor boats and pleasure boats, pump rotors in the cooling system of thermal engines and aircraft wings. In this sense, the vibratory cavitation tests are carried out on aluminum alloy 7075 subjected to volumetric thermal treatment of artificial aging at 180^{0}C with a holding time of 24 hours. The comparison with the results previously obtained on the delivered state and the regime with the same temperature and duration of one hour shows that the effect of increasing the duration of the heat treatment leads to a significant increase compared to the state of delivery and slightly different from that obtained by the one with a duration of one hour.*

Keywords: *Aluminum alloy, microstructure, mechanical properties, cavitation, cavitation erosion, strength, average depth of erosion, erosion speed*

1. Introduction

Usually, aluminum alloys, developed in the form of laminated semi-finished products, such as alloy 7075 state T651, are used in the manufacture of parts without going through volumetric or surface heat treatments. Use in this form is dictated by ease of machining and high mechanical property values comparable to low alloy steels [1-5]. As a result, they are mainly used in the strength structures of aircraft and river and marine vessels (sailboats, motor boats). However, industrial development in naval, aeronautical and automotive systems aims to extend the use of this alloy to parts that operate in hydrodynamic conditions, such as pump rotors and boat propellers, dangerous through the effects of cavitational erosion and/or hydroabrasion [6, 7, 8, 9]. In order to increase their lifetime to the cyclical stresses of cavitational microjets, the effects of traditional technologies (volumetric and surface thermal treatments [10, 11]) and new technologies (use of laser [7, 12] are being researched to lead to the modification of the mechanical resistance characteristics of the required surface structure, which provides increased resistance to such demands. As volumetric heat treatment furnaces have become more and more efficient, through the rigorous control of regime parameters (temperature and duration), the paper studies the effect of the cavitation erosion behavior of the alloy 7075 state T651 structure obtained by thermal aging at 180^0C for a duration of 24 hours.

2. The material studied

Alloy 7075 state T651, in semi-finished state (laminated sheet), is characterized by the chemical composition and mechanical property values shown in table 1 and by the microstructure shown in fig.1.
Through the heat treatment of artificial aging at 180^0C, with a holding time of 24 hours, the values of the mechanical properties have been changed, as can be seen in table 1 (notation TT180/24). Through this treatment modification, the microstructure also suffered, fig.2, but not one of phase, but only of the size and degree of dispersion of the chemical/intermetallic compounds, which, along with the mechanical properties, change the behavior and resistance to the fatigue stresses of cavitation.

Table 1: Chemical composition and values of mechanical properties

State	Chemical composition, [%] Wt									
	Si	Fe	Cu	Mn	Mg	Cr	Zn	Ti	Zr	Al
Semi-finished (SF)*	0.68	0.107	1.58	0.076	2.05	0.19	5.76	0.2	0.23	rest

Mechanical properties				
Stare	R_m MPa	$R_{p0.2}$ MPa	HB daN/cm^2	KCU J
Semi-finished (SF)*	531.841	424.82	140	12.8
TT 180/1h*	549.549	410.55	157	14.1
TT180/24h*	570.921	417.51	140	12.7

* Values determined in the Laboratory of the Special Materials Research and Expertise Center - Polytechnic University of Bucharest.

From table 1 it can be seen that through the thermal treatment of artificial aging, the values of the mechanical properties, compared to the state of the semi-finished product, suffer increases (R_m), decreases (R_{p02}) or insignificant modification (KCU) and the identical hardness (HB). Compared to the one-hour treatment, it shows a decrease in hardness (HB) and resilience (KCU) and an increase in mechanical strength (R_m) and yield strength (R_{p02}).

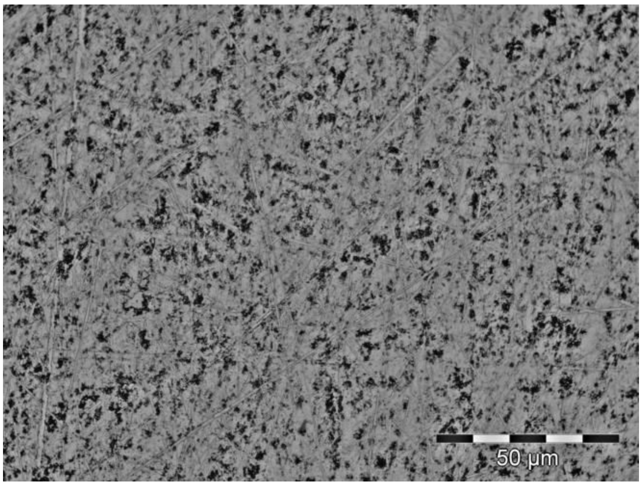

Fig. 1. Microstructure of aluminum alloy 7075 state T651
(semi-finished state)

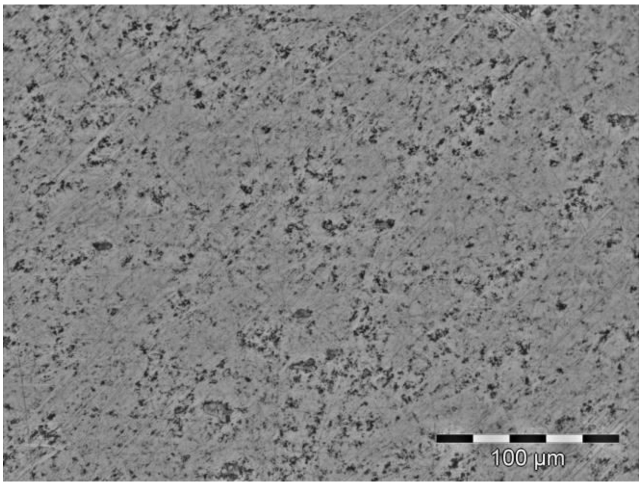

Fig. 2. Microstructure of aluminum alloy 7075 state T651
(after artificial aging at 180^0C, maintaining 24 hours)

Fig.1 and Fig. 2 show the effect of heat treatment, compared to the semi-finished state, by reducing the size and density of the intermetallic compounds.

3. Experimental research

a) Devices and method used for the cavitation test

The behavior and resistance tests of the heat-treated structure to cavitation erosion were carried out in potable water from the network, using the standard vibrating device of the Cavitation Erosion Research Laboratory, from the Politehnica University of Timișoara [6, 13]. The total request/test duration (165 minutes), divided into intermediate periods (of 5, 10 and 15 minutes), the water temperature during cavitation (22 ± 1^{0}C) as well as the way of processing and interpreting the results are in accordance with the laboratory's custom [6], which complies with the requirements of ASTM G32-2016 [14]. The stages completed in the experimental program can be seen in detail in [6].

b) Specific curves and parameters. Discussions

In fig. 3 shows the diagram showing the accuracy of the research, through the dispersion band of the experimental values, obtained on the three tested samples, against the analytical curve of MDE(t) mediation and the value of the standard deviation σ. The upper S96(t) and lower I96(t) limits of the dispersion band, corresponding to the tolerance interval (96 %) and the value of σ of 0.306 certify the accuracy of the experiment.
The diagrams of fig. 4 and fig. 5 contain the elements necessary to characterize the behavior and resistance to the vibratory cavitation stress of the structure obtained by thermal aging at 180^{0}C, with a holding time of 24 hours.

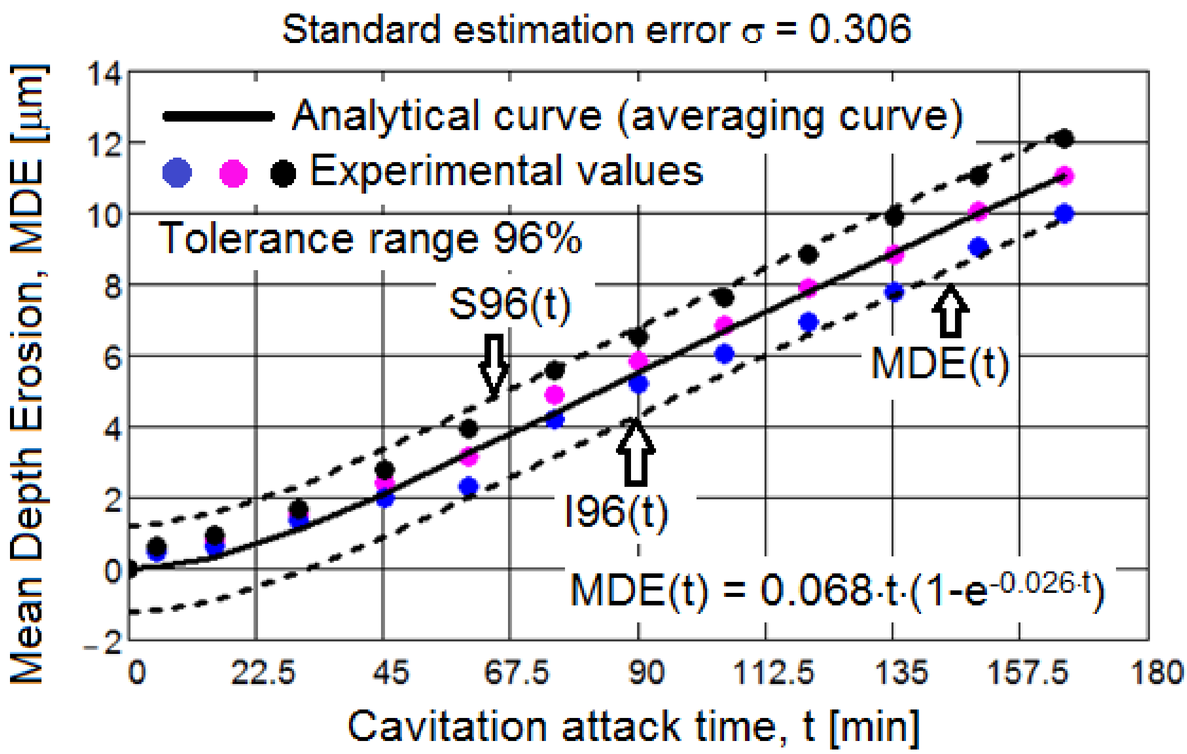

Fig. 3. The dispersion range of the experimental values.
Statistical reference parameters of the dispersion band

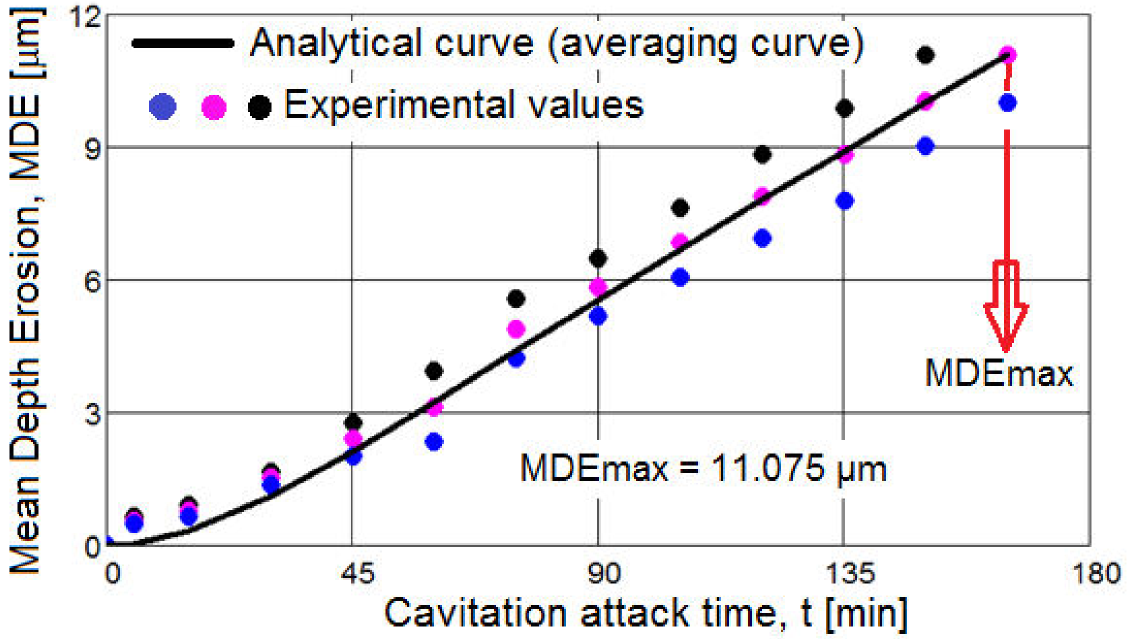

Fig. 4. Variation of cumulative mean depth of erosion with duration of cavitation stress

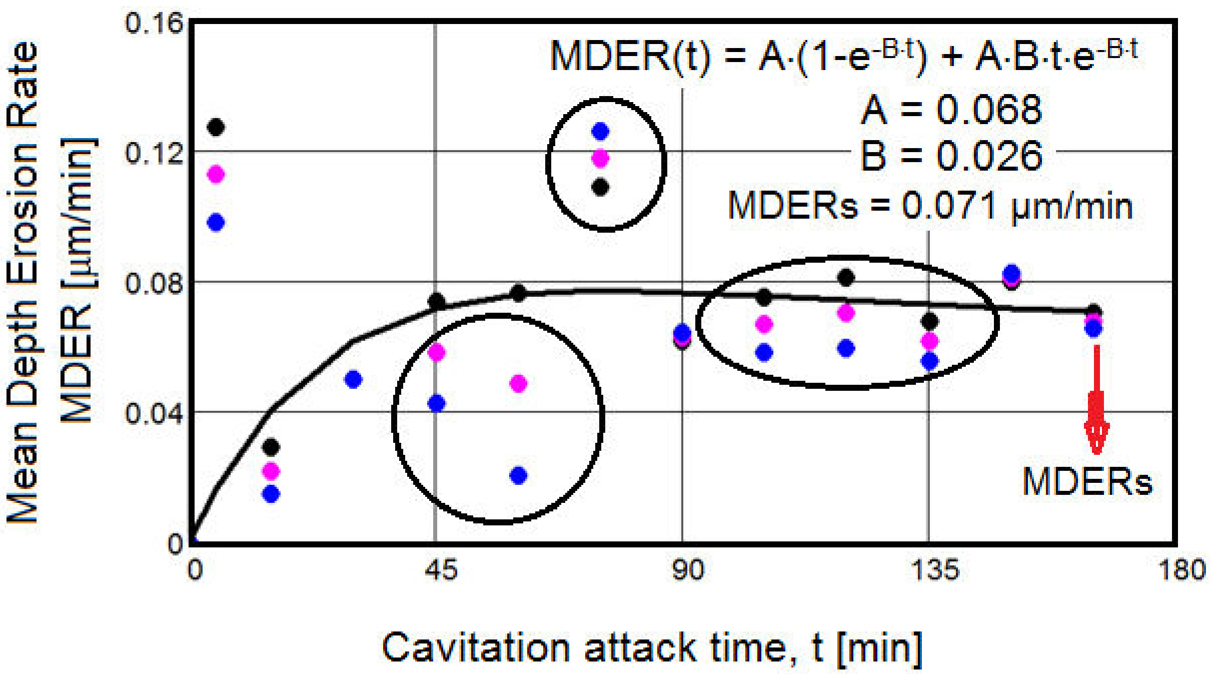

Fig. 5. Variation of average erosion penetration rate with duration of cavitation stress

Findings resulting from the data contained in the diagrams in fig. 4 and fig. 5:

1. the experimental values of the cumulative average depths of penetration, fig. 4, continuously increase, which shows that the mechanical properties, according to experience and data from the literature [9, 15, 16] are correlated and homogeneously distributed in the structure of the required surface;
2. according to the MDE value, during the first 30 minutes of cavitation, the three samples behave almost identically, the differences being insignificant. After the 30 minutes and until the end (165 minutes) the behavior is different, explained by the microstructures that cannot be perfectly identical. Even the hardness in table 1, which is the algebraic mean of at least 10 measured values, may show differences between the three samples;

3. the variation of the experimental values compared to the MDER(t) averaging curve - the intervals enclosed by the dark, colored, black curves - fig. 5, shows that at certain periods the stress of the microjets leads to large expulsions of grains, as a result of the type of microstructures;
4. fig. 5 shows that in the interval 60-90 minutes there is a jump in the penetration speed. It is characterized by an important expulsion of material, characterized by the base metal, but especially by the intermetallic compound. This plot also shows that the samples with red and blue have close and slightly different behaviors than the one with black. This observation confirms the accuracy of volumetric heat treatment of artificial aging;
5. the shape of the averaging curves of the experimental values, MDE(t) and MDER(t), according to the literature [6, 17, 18], is specific to surfaces with good mechanical properties and homogeneously distributed in the volume of the material (see table 1) which strengthen the bonding forces of the grains (see photo images in fig.6 and 7) and ensure good resistance to cavitation erosion.

c) The morphology of destruction by cavitation erosion

Fig. 6 shows 4 photographic images, taken with the Canon Power Shot A 480 camera, at the most significant durations of exposure to vibrating cavitation.

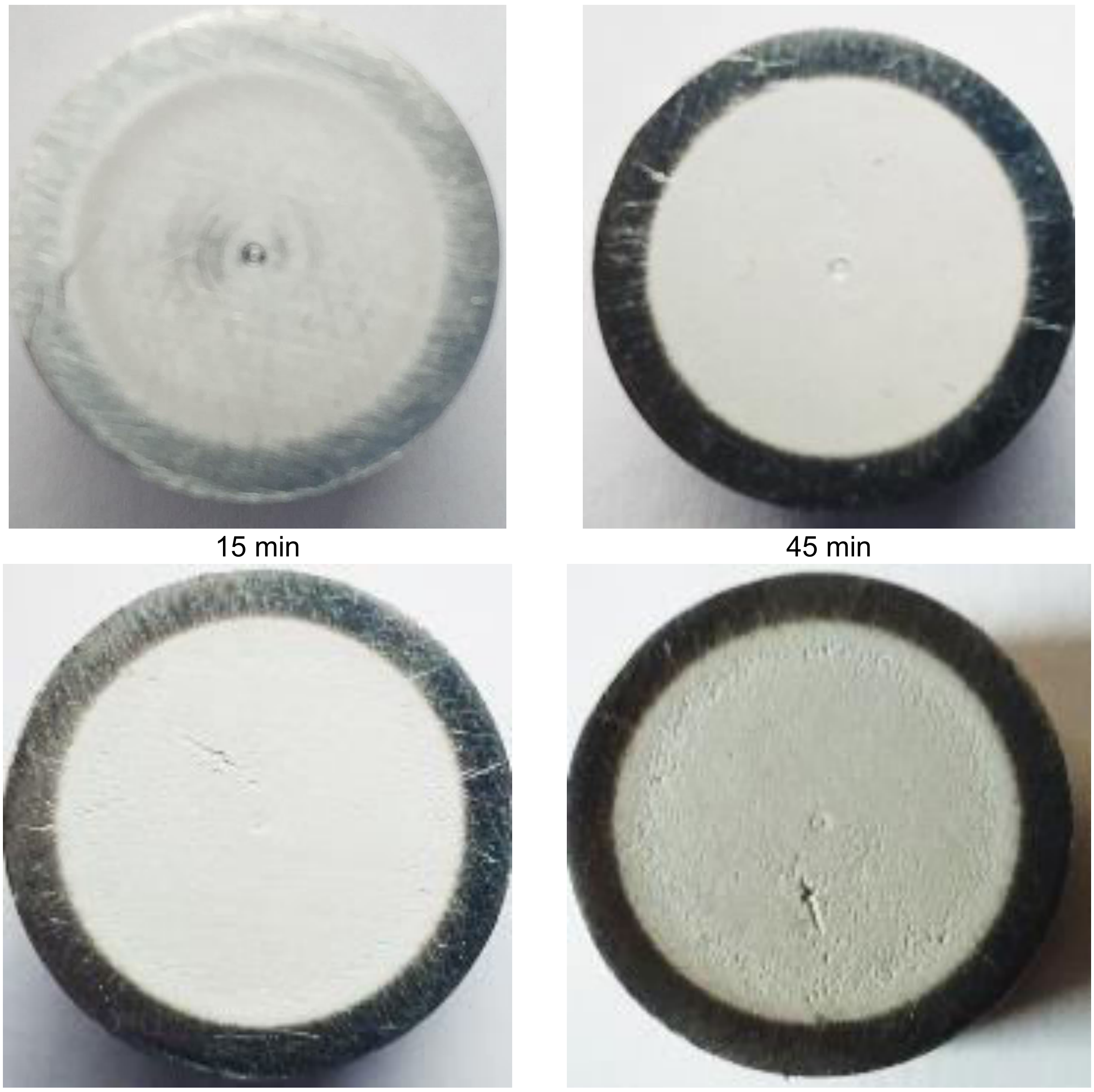

15 min 45 min

105 min 165 min

Fig. 6. The evolution of erosion in the area of the attacked surface

The 4 images justify the statements written in the analysis performed on the curves in fig.4 and fig. 5, related to the allure of the mediation cubes (MDE(t) and MDER(t)) and the dispersion of the three experimental values in relation to them. It can be seen that the erosion is continuous with small caverns, which multiply continuously with the duration of cavitation, and some deepen, confirming the expulsion of weak elements, such as intermetallic compounds.

Fig.7 shows microscopic images of the eroded surface. They show the caverns, in terms of surface area, but also in depth. It should be noted that the SEM images, regardless of the trapped area (at the periphery, fig. 7b, or inside the exposed surface, fig. 7a), as well as the depth one in fig. 7c, shows that the erosion is specific to surfaces with mechanical properties (R_m, R_{po2}, HB and KCU) with high values and well correlated with the microstructure of the surface [15, 16], determining a relatively constant behavior and with good resistance to impacts with cavitational microjets.

Note the significant difference of almost 5 times between the MDE_{max} value of 11,075 µm and the cavern caught in the section plane (53 µm). This difference confirms the importance of eliminating microstructural defects (through volumetric or surface heat treatments), such as these chemical compounds, which are unavoidable in the manufacturing phase of aluminum alloy semi-finished products.

a) Microscopic image measuring the depth of a cavern in the eroded area

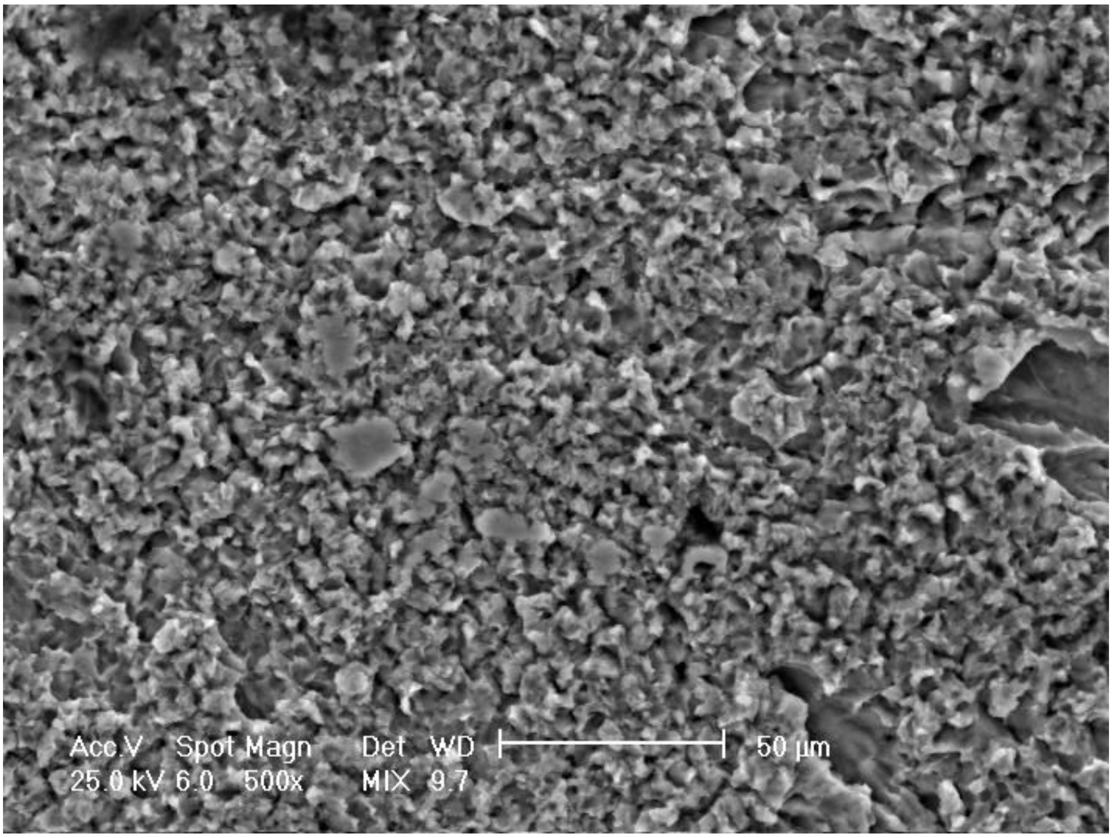

b) SEM image – on an interior area (500X)

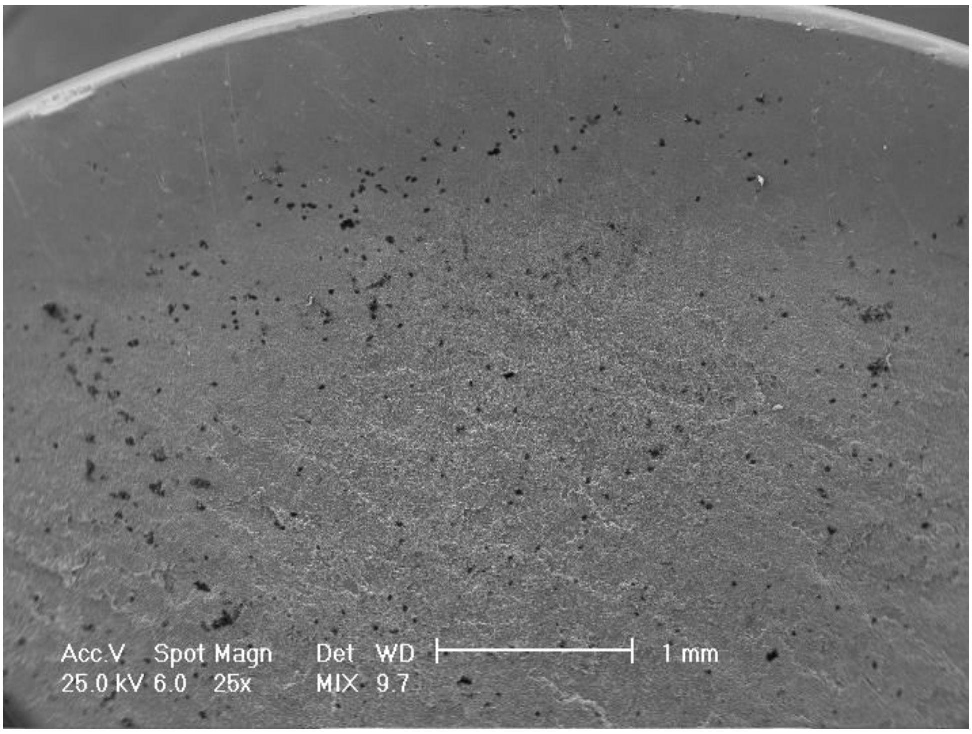

c) SEM image - at the periphery of the sample (25 x)

Fig. 7. Microscopic images (a,b) and macroscopic image (c) of the destruction produced in the surface of one of the samples

d) Comparison of results

To evaluate the resistance to the erosion of the vibrating cavitation, is made the histogram from fig. 8, in which the values of the parameters recommended by the ASTM G32-2016 norms are compared.

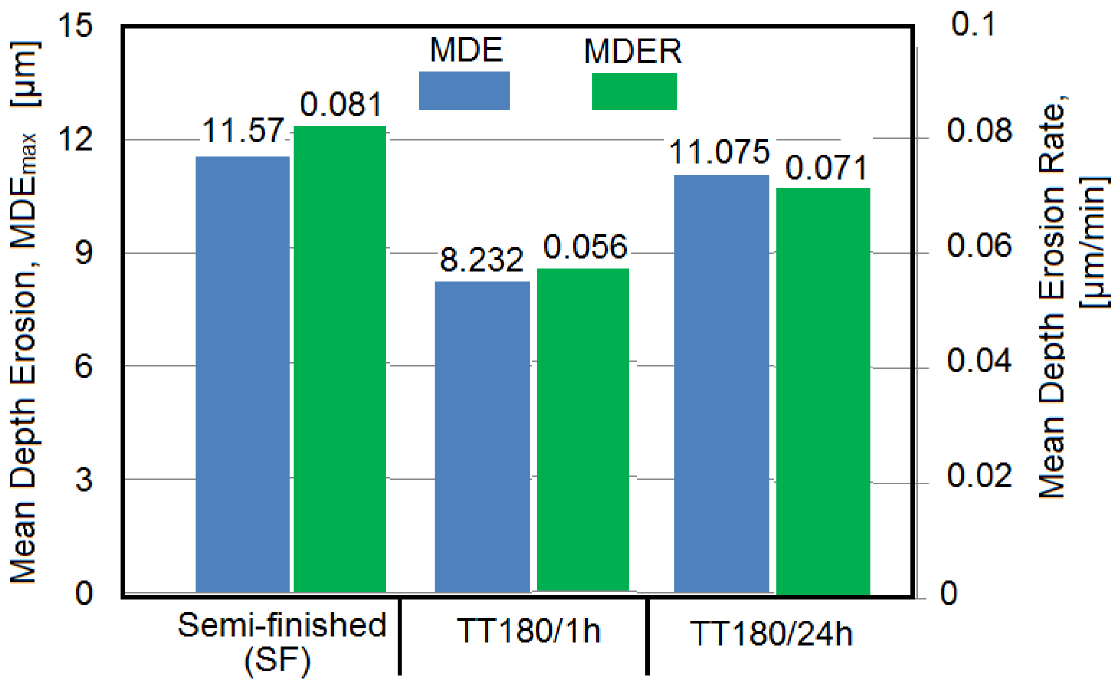

Fig. 8. Value comparison histogram

The data in the histogram shows:
1 - compared to the semi-finished state, the increase in cavitation resistance is reduced, by about 4% according to the value of MDE_{max} and by about 14% according to the value of the $MDER_s$ parameter;
2 - compared to artificial aging with a duration of one hour, is noted an important decrease in cavitation resistance; more than 34% after the value of MDE_{max} and more than 26% after the value of $MDER_s$;
3 - there is a correlation between the holding time and the aging temperature, so that through the values of the mechanical properties, especially hardness and resilience, and the resulting microstructural changes, in terms of the density and dimensions of the chemical/intermetallic compounds specific to aluminum alloys (in general), which can lead to significant increases in resistance to cyclic, destructive cavitation stresses.

4. Conclusions

1. Volumetric heat treatment, such as artificial aging at 180^0C, is a solution to increase the strength of aluminum alloy 7075 used for parts that work in cavitational currents, such as pump rotors and propeller blades of airplanes and ships.
2. The holding time at the aging temperature is a parameter with influence on the resistance of the 7075 aluminum alloy structure to the erosive stresses of cavitational microjets.
3. Not always the long holding time at a certain temperature, as is the case in this work, ensures the microstructure and the values of the mechanical properties that lead to the increase of resistance to cavitation erosion.
4. Correlating the holding time with the temperature of the aging heat treatment can lead to important increases in the resistance to cavitation through the values of the mechanical properties and the resulting microstructure.
5. The paper shows the need to study the influence of the same type of thermal treatment with other regime parameters (temperatures and holding times).

References

[1] Bordeasu, Ilare, Cristian Ghera, Dionisie Istrate, Laura Salcianu, Brandusa Ghiban, Dumitru Viorel Bazavan, Lavinia Madalina Micu, Daniel Catalin Stroita, Alexandra Suta, Ileana Tomoiagă, and Alexandru Nicolae Luca. "Resistance and Behavior to Cavitation Erosion of Semi-Finished Aluminum Alloy 5083." *Hidraulica Magazine*, no. 4 (December 2021): 17–24.
[2] Istrate, Dionisie, Beatrice-Gabriela Sbârcea, Alin Mihai Demian, Andreea Daniela Buzatu, Laura Salcianu, Ilare Bordeasu, Lavinia Madalina Micu, Cristian Ghera, Bogdan Florea, and Brândusa Ghiban. "Correlation between Mechanical Properties—Structural Characteristics and Cavitation Resistance of Cast Aluminum Alloy Type 5083." *Crystals* 12 (2022): 1538.
[3] Bordeașu, Dorin, Octavian Proștean, and Cornel Hatiegan. "Contributions to Modeling, Simulation and Controlling of a Pumping System Powered by a Wind Energy Conversion System." *Energies* 14, no. 22 (2021): 7696.
[4] Pereira, D., J. P. Oliveira, T. G. Santos, R. M. Miranda, F. Lourenço, J. Gumpinger, and R. Bellarosa. "Aluminium to Carbon Fibre Reinforced Polymer tubes joints produced by magnetic pulse welding." *Composite Structures* 230 (2019): 111512.
[5] Torzewski, J., K. Grzelak, M. Wachowski, and R. Kosturek. "Microstructure and Low Cycle Fatigue Properties of AA5083 H111 Friction Stir Welded Joint." *Materials* 13 (2020): 2381.
[6] Bordeasu, Ilare. *Monograph of the Cavitation Erosion Research Laboratory of the Polytechnic University of Timisoara (1960-2020) / Monografia Laboratorului de cercetare a eroziunii prin cavitaţie al Universităţii Politehnica Timişoara: (1960-2020)*. Timisoara, POLITEHNICA Publishing House, 2020.
[7] Mitelea, Ion, Ilare Bordeasu, Eduard Riemschneider, Dragos Utu, and Corneliu Marius Craciunescu. "Cavitation erosion improvement following TIG surface-remelting of gray cast iron." *Wear* 496 (2022): 204282.
[8] Micu, Lavinia Madalina, Dorin Bordeasu, Ilare Bordeasu, Mihaela Popescu, Octavian Victor Oanca, and Sebastian Titus Duma. "Influence of Nitriding Thermochemical Treatments upon Cavitation Erosion Resistance of Duplex X2CrNiMoN22-5-3 Stainless Steels." *Hidraulica Magazine* 4 (2017): 27-33.
[9] Milos, Teodor, Mircea Octavian Popoviciu, Ilare Bordeasu, Rodica Badarau, Adrian Bej, and Dorin Bordeasu. "The 3d blade surface generation for kaplan turbines using analytical methods and cad techniques." *Hidraulica Magazine* no. 2 (2013): 65-74.

[10] Bordeasu, Ilare, Ion Mitelea, Laura Salcianu, and Corneliu Marius Craciunescu. “Cavitation Erosion Mechanisms of Solution Treated X5CrNi18-10 Stainless Steels.” *Journal of Tribology-Transactions of the ASME* 138, no. 3 (2016): Article Number 031102.
[11] Bordeasu, Ilare, Mircea Octavian Popoviciu, Ion Mitelea, Cornelia Laura Salcianu, Dorin Bordeasu, and A. Iosif Duma. “Researches upon the cavitation erosion behaviour of austenite steels.” *IOP Conference Series: Materials Science and Engineering* 106, no. 1 (2016): 012001.
[12] Bordeasu, Ilare, Mircea Octavian Popoviciu, Lavinia Madalina Micu, Octavian Victor Oanca, Dorin Sebatian Titus Bordeasu, Adrian Pugna, and Constantin Bordeasu. “Laser beam treatment effect on AMPCO M4 bronze cavitation erosion resistance.” *IOP Conference Series: Materials Science and Engineering* 85, no. 1 (2015): 012005.
[13] Bordeasu, Ilare, Mircea Octavian Popoviciu, Ion Mitelea, Brandusa Ghiban, and Dumitru Tucu. “Chemical and mechanical aspects of the cavitation phenomena.” *Revista de Chimie* 58, no. 12 (2017): 1300-1394.
[14] ***. “Standard method of vibratory cavitation erosion test.” ASTM, Standard G32, 2016.
[15] Hammitt, Frederick G., and N.R. Bhatt. *Cavitation damage resistance of hardened steels*. Univ. of Michigan, 1970: 1-36.
[16] Franc, Jean-Pierre, Jean-Louis Kueny, Ayat Karimi, Daniel-H. Fruman, Didier Fréchou, Laurence Briançon-Marjollet, Jean-Yves Billard, Brahim Belahadji, François Avellan, and Jean-Marie Michel. *La cavitation. Physical mechanisms and industrial aspects*. Grenoble, Press Universitaires de Grenoble, France, 1995.
[17] Micu, Lavinia Madalina, Ilare Bordeasu, and Mircea Octavian Popoviciu. “A New Model for the Equation Describing the Cavitation Mean Depth Erosion Rate Curve.” *Revista de Chimie* 58, no. 4 (2017): 894–898.
[18] Bordeasu, Ilare, Constantin Patrascoiu, Rodica Badarau, Liliana Sucitu, Mircea Octavian Popoviciu, and Victor Balasoiu. “New contributions to cavitation erosion curves modeling.” *FME Transaction* 34 (2016): 39–43.

A State-of-the-art Review of Compaction Control Tests Methods

PhD. Student Eng. **Andrei BURAGA[1,*]**, Prof. Dr. Eng. **Carmen Nicoleta DEBELEAC[1]**

[1]"Dunarea de Jos" University of Galati, Engineering and Agronomy Faculty in Braila, Braila, Romania

* andrei.buraga@dmmc.utm.md; carmen.debeleac@ugal.ro

Abstract: *Quality control methods have been used by construction civile industry and road for many years to control the compaction process carried out, either of the soil or of the asphalt mixtures. These control procedures are based upon experimental and/or statistical concepts and their goal are to be an instrument to assist the contractor to carry out the execution checks in insuring that impose degree compaction was achieved in accordance with technical project of the works. These concepts are built around the idea according to which it is possible to randomly select a small sample of a soil or asphalt mixture and then to predict from this sample an average value of compaction quality to be assigned to the entire area of the layer tested. For the most part, these aspects are valid in our country, but the technical regulations of developed countries provide for a variety of methods based on the in-situ measurement of specific compaction parameters in order to predict the quality of the area under control. The paper will describe the methods used in Romania (laboratory and in-situ tests) along with those implemented in the world and used with remarkable results.*

Keywords: *Compaction, soil, laboratory and in-situ tests, control, quality*

1. Introduction

Soil compaction testing is the process by which the density property of a material (which can be soil or mixture asphalt) soil mass is increased in the field using the various technologies, and monitored by quality control delegates from the local building department. Thus, during the compaction of backfill material, density testing is impetuously necessary in order to evaluate whether the final terrain compaction levels are adequate to support building foundations, roads, bridges, etc. These checks are made using test methods in the laboratory or directly on the field and will be briefly presented in the paper as classic methods used here in Romania, along with modern methods successfully applied in countries with highly developed industries.

2. Quality control of soils compaction in Romania

As known, soil compaction is defined as the increase of bulk density or decrease in porosity of soil due to externally or internally applied loads. Taking this aspect into account, at the compaction works of the soils it is necessary to know some characteristic parameters that are determined by different methods (static or dynamic), both in the laboratory, and in-situ, described below:
a) laboratory tests: oedometric test (STAS 8942/3-90 [2]), cyclic triaxial test (NP 125:2010, Annex B [3]), Proctor test (STAS 9850-89 [4]). On the basis of these laboratory geotechnical tests, the followings are determined: the time for complete compaction of the terrain (NE-008-97 point 2.14.), oedometric modulus of deformation, drawing the stress-strain curve and the time variation of the pore pressure, optimum compaction moisture and maximum dry weight or maximum dry density, compaction degree, Proctor curve;
b) in-situ tests: evaluation of the static modulus of linear deformation of soils (by calculation, based on the oedometric modulus according to STAS 3300/2-85 [5], point 3.4.5, or by direct measurement in-situ, by the plate loading test according to STAS 8942/3, evaluation of the settlement of soils under a single passing of the compactor (and by correlating with the values of the linear deformation modulus of the terrain, the experimental curves within figure 11 of NE-008-97 result), experimental evaluation of the layer thickness (according to NE-008-97 point 2.6 applying the procedure described in the NE-008-97, Annex 2.2., point 2).
Based on these results, the geotechnical parameters will be evaluated for adequate application of the technological solution, in order to obtain a higher compaction efficiency.

In addition, the main parameters evaluated in-situ tests, which enable the identification of the degree of field compaction, according with Romanian Regulations, are summarized in the Table 1.

Table 1: Romanian Regulations and methodologies for compaction quality control

Requirement	Application methodology	Romanian Regulations
Correlation of parameters associated with the vibratory roller-terrain system	Measuring the width of the contact area between the compactor roller and the ground and, then, by checking the values within the range for the ratio of measured width divided by roll diameter, depending on the degree of compaction resulting from the Proctor test	NE-008-97
Duration of soil compaction and the effective consolidation effort	Calculated on the basis of the specific settlement and the primary consolidation time obtained by the Casagrande semi-logarithmic representation method	NE-008-97 STAS 8942/1- 90
	In-situ, by measurements of pressure doses to determine the pressure transmitted in the layer	
Modulus of elasticity E_s, G_d and the damping ratio ζ of the terrain	Testing of loading with the plate equipment on the terrain to determine static modulus of linear deformation	NP125:2010 STAS 3300/1-85 Annex C, Table 9 NP 125:2010 - Annex D
	Cyclic triaxial testing for each loading cycle to determine dynamic deformation modulus	
	Hysteresis curve (axial stress-deformation, on each cycle) to determine the damping ratio	
	In-situ measurements to determine the logarithmic decrement of the vibrations due to the free fall of a weight	

Quality control and quality assurance (QA/QC) of the compaction process are indispensable for the long-term performance of roads or foundation works. The practical methods of on-site measurement, provided in our national standards, ensure the assessment and verification of compliance with the requirements of the technical project of the respective compaction work. However, these methods also have shortcomings and cannot provide complete information about the quality of compaction.
In the case of the topic addressed in this paper, in Romania there are intense concerns in the direction of the study and numerical simulation, on the one hand, of the functional behavior of vibratory compactors, and on the other hand, of the transmissibility and amplitude of vibrations felt in soils (filling, weakly cohesive, with consolidation, etc.) [6-13]. All these technological aspects have a great influence on the efficiency of the compaction process, facilitating the fulfillment of the proposed goal (by reaching the required compaction coefficient after a small number of passes, according to the regulations in the field of soil compaction).
With the technical progress in the field of automation and information processing, an intelligent technology has been implemented on the compaction machines, which has a great potential to solve some of the shortcomings of the classical standardized methods for evaluating the quality of the compaction process. Such intelligent systems for monitoring the parameters of the compaction process are made up of hardware and software components capable of providing information of this technological process in real time, but also their management through an efficient management system. A brief presentation of them, used more and more in developed countries, will be given below.

3. Best practice for quality control of soils compaction worldwide

The performance evaluation system of the vibration compaction process is carried out based on the scheme in Figure 1 based on the identification of some parameters that describe the behavior of the compacted material in terms of certain physical and mechanical properties. Certainly, two important compaction parameters namely the dry weight (γ_{kmax}) and optimum moisture content

(W_{opt}) values can be obtained by standard compaction test in laboratory. But, in order to estimate some other compaction parameters, many studies have been approaced by different researchers. These bring in attention that in-situ control of the compaction process requires the appropriate choice of the following parameters: compaction point spacing, vibration frequency, probe penetration and extraction, and duration of compaction. At the end of the compaction process, the soils fall into five types, from the point of view of their compaction efficiency, as follows: good, fine, ordinary, poor and bad. Each soil type corresponds to a wide range of specific parameters, such as those centralized in Table 2.

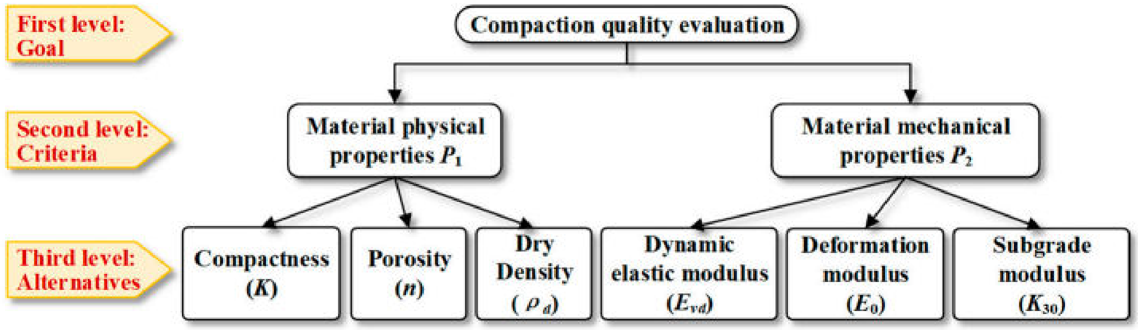

Fig. 1. Indicators for evaluating the quality of the compaction process

Table 2: The standard classification level for physical-mechanical indices in soil compaction

Quality level	I (good)	II (fine)	III (ordinary)	IV (poor)	V (bad)
D (%)	>99	98-99	95-98	90-95	<90
ρ_d (x10^3 kg/m^3)	>2.27	2.25-2.27	2.23-2.25	2.21-2.23	<2.21
E_{ud} (MPa)	>9.7	9.5-9.7	9.3-9.5	9.1-9.3	<9.1
E_0 (MPa)	>16.5	16-16.5	15.5-16	15-15.5	<15
k_{30} (MPa/m)	>29	27.5-29	26-27.5	24.5-26	<24.5
Dimensionless value	50	40	30	20	10

The parameters in Table 2 have the following significations: D is the degree of compaction; ρ_d – density of the material in the dry state; E_{vd} – the dynamic modulus of linear deformation; E_0 – static modulus of linear deformation; k_{30} - layer stiffness.
The test methods acceptable for use for quality assurance of pavement and subgrade materials that have the potential to reliably provide a direct measure of the strength or in-situ modulus value, and which offer significant time savings in turnaround time of test results, in Figure 2 are shown.

Fig. 2. Usual devices for in-situ measurements of the terrain properties with:
Light Weight Deflectometer, Dynamic Cone Penetrometer, Clegg Hammer, Plate Load Testing.

Nowadays, on an international level, various devices as multi-purpose units for acquiring, measuring and processing vibration signals are available, assimilated with mobile laboratories for in situ testing of the quality of the works performed (compaction, vibro-injection, etc.). Some such examples are illustrated in Figure 3.

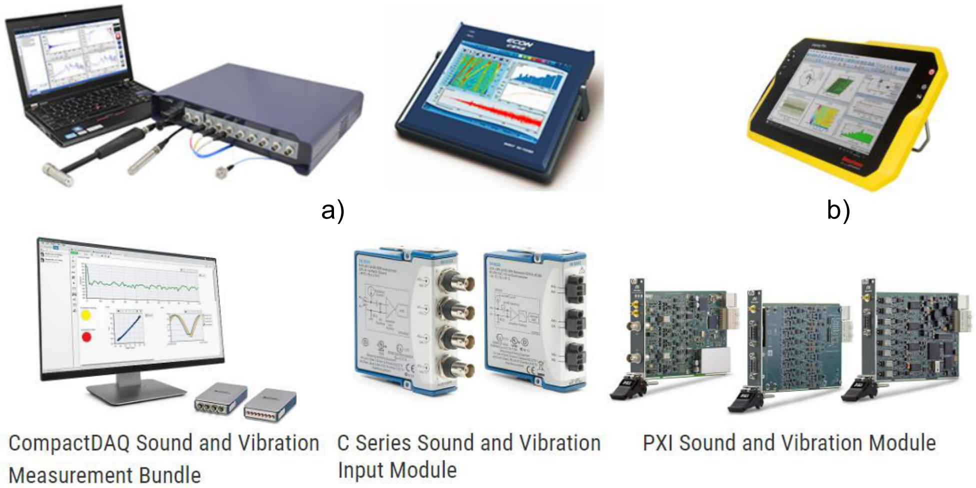

a) b) c)

Fig. 3. High-performance systems for acquisition, measurement and processing of vibration signals:
a) Econ MI generatio 7 / Dynamic Signal Analyzer Module [14];
b) Impaq Pro Portable Vibration Analyzer [15];
c) PC-Based Sound and Vibration Devices / PXI Sound and Vibration Module USB 4431 [16].

More than 30 years ago, the European Community initiated the implementation of continuous compaction measurement and control (CCC) methods, so that today modern vibratory compactors are equipped with continuous (in situ) monitoring and control systems of influencing parameters major impact on the performance of the terrain vibration compaction process. Thus, three CCC systems are known worldwide, which will be briefly described below.
CCC – compactometer that monitors the variation of the ratio between the acceleration amplitudes according to the frequency, by evaluating the CMV or CCV parameters as:

$$\begin{cases} CMV = C_0 \cdot \dfrac{A_{2\omega}}{A_{\omega}} \\ CMV = \left(\dfrac{A_{0,5\omega} + A_{1,5\omega} + A_{2,5\omega} + A_{3\omega}}{A_{2,5\omega} + A_{3\omega}}\right) \cdot 100 \end{cases}, \qquad (1)$$

where: A_{Ω} and $A_{2\Omega}$ are the amplitudes of the acceleration signal monitored on the vibratory roller (Figure 4) at the fundamental frequency Ω and of the first harmonic component of the real-time acceleration response signal; $A_{0.5\Omega}$ represents the first subharmonic and $A_{1.5\Omega}$, $A_{2.5\Omega}$ and $A_{3\Omega}$ represent the corresponding higher order harmonics. C_0 is a calibration constant that has values in the range 250 - 350.

Fig. 4. CMV technology [17]

The studies carried out by different researchers showed that by knowing the spectral composition of the acceleration signal of the vibratory roller in its vertical movement, the condition of the layer over which the vibratory roller moves can be identified. In the analysis of the acceleration signal, only the existence of the fundamental harmonic is noticeable, in the case of loose terrains, in contrast to the presence of a wide spectrum of higher harmonics, with increasingly smaller amplitudes until zero, in the case of terrains with very high rigidity, which have reached the maximum degree of compaction (Figure 5).

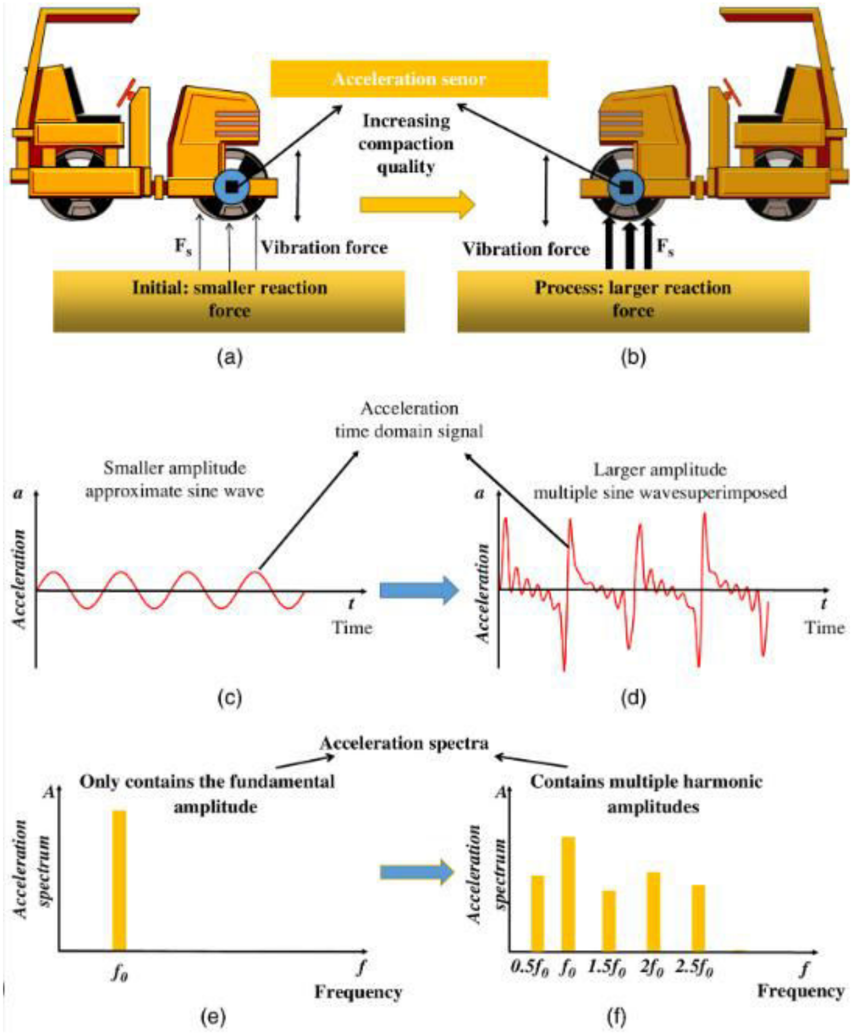

Fig. 5. The spectral composition of the vibration roller acceleration signal [18]

It is noted that the analysis of the response of the vibratory roller to the interaction with the ground provides important information (in situ) about the progress of the compaction process at any time, i.e. after each pass of the technological equipment over the layer. Taking into account the proportionality of the contact force between the roll and the ground, the law of variation of the measured acceleration signal provides information about the dynamic behavior of the roll upon impact with the ground. Through frequency spectral analysis of the contact force (with variation law determined on the basis of the measured acceleration) the nature of the vibrator roller-ground contact can be identified, which can be of three types: permanent, periodic and chaotic. Thus, Figure 6 shows how to know the state of compaction of the layer according to the spectrum of the harmonics of the monitored signal. In practice, however, during the technological process of compaction, the movement of the vibratory roller can be periodic or chaotic, which implies either a continuous contact between the vibratory roller and the ground, or periodic or chaotic loss of contact. In each individual work situation, the force of interaction between the vibratory roller and the ground has different dynamic behavior, being influenced by the stiffness of the material being compacted, as well as by the speed of the machine.

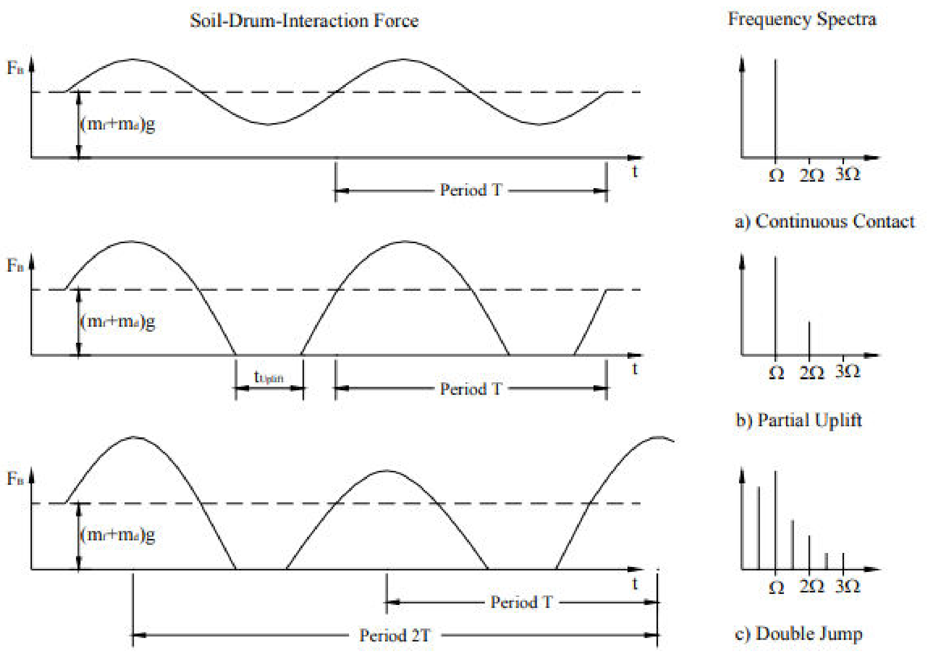

Fig. 6. Spectral analysis of the vertical acceleration of the vibratory roller – terrain in the 3 phases of contact [19]:
a) permanent contact; b) periodic contact; c) chaotic jump.

Based on the CMV parameter (which measures the stiffness of non-cohesive soils, with layer thickness between 1...1.2 m), in the specialized literature [20] there are references about the determination of others, which specifically contribute to the definition of the compaction states of the layers, such as: RMV (resonance meter value, see definition in eq. 2), OMV (oscillometer value) or CCV (continuous compaction value).

$$RMV = 100\,\frac{A_{0,5\omega}}{A_{\omega}} \tag{2}$$

CCC – terrameter is another system that is based on the monitoring of two compaction status indicators, as follows:

a) the variation of the energy transferred to the ground during the passes of the vibratory compactor, by evaluating the OMEGA parameter [Nm];

b) the variation of the dynamic modulus of elasticity of the land during the passage over the layers of the land, by monitoring the E_{vib} parameter [MN/m^2].

The working principle by which the E_{vib} parameter is evaluated is illustrated in Figure 7.

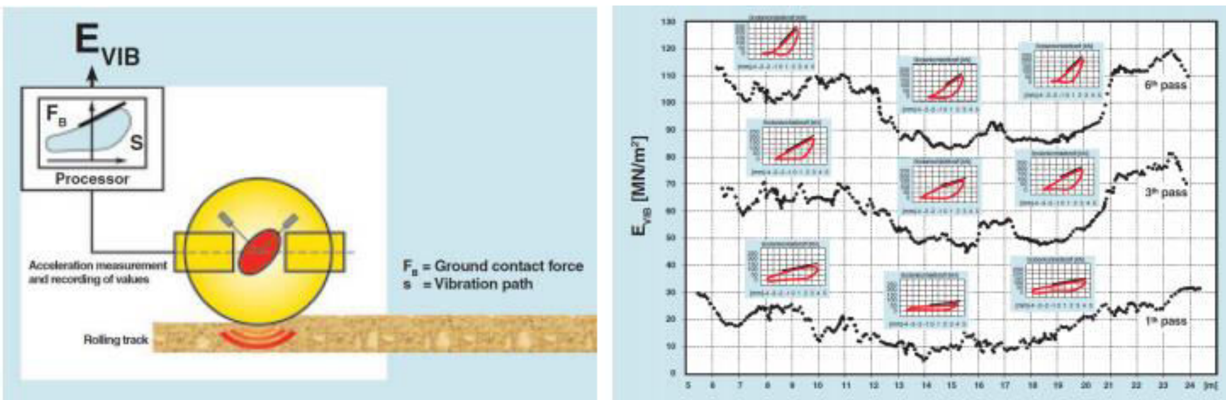

Fig. 7. Monitoring of the E_{vib} parameter [21,22]

When the stiffness of the compacted layer is continuously changed, a wide range of parameters that describe the working regime of the machine varies, such as: the energy required for the vibration process, the moment of the eccentric masses, their positioning, the amplitude and frequency of the vibrations (and implicitly the dynamic force transmitted to the terrain) etc. In the case of compactors of the new generation from the BOMAG company (Figure 8), they are equipped with systems called VarioRoller, later developed as VarioControl, which have the role of changing the direction of the disruptive force of the roller (Figure 9) according to the characteristics of the compacted layer, directly related to the stiffness obtained after each pass of the machine.

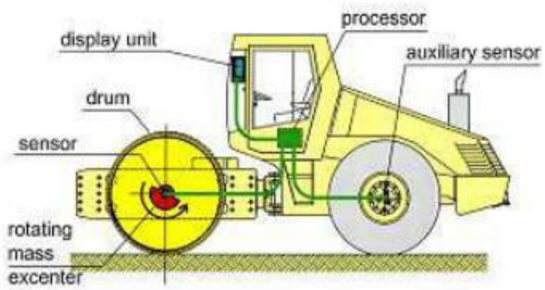

Fig. 8. Equipping with control systems for the compaction process [23]

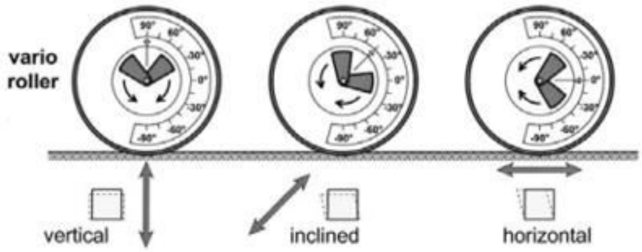

Fig. 9. Changing the direction of action of the exciting force of the vibratory drum [23]

CCC–ACE incorporates a new concept that monitors the variation of ground stiffness during the movement of the compactor on the ground subject to vibration compaction, by monitoring the parameter k_b [N/m]. The relationship for k_b evaluation is:

$$k_b = \omega^2 \left[(m + m_0) + \frac{(m_0 e k_{vario}) cos\varphi}{A_{(z)}} \right], \tag{3}$$

where: where $A_{(z)}$ is the amplitude of the displacement and φ is the it's angle of phase; m and m_0 represent the vibratory drum mass, and, respectively, eccentric masses. The dimensionless index k_{vario} is used for a reduction of the dynamic excitation.
MDP (Machine drive power) implemented a new technology for evaluating the degree of compaction of a layer, patented by CAT and implemented on Caterpillar B-Series compactors (Figure 10). The method consists in monitoring the driving power of the machine by measuring the rolling resistance during compaction, by continuously correlating the vibration parameters of the roller with the characteristics of the layer [24, 25].

Fig. 10. MDP technology [24]

Thus, this method directly measures the stiffness of the ground. Its application is recommended for evaluating the degree of compaction of all types of soil (cohesive and non-cohesive), measuring the stiffness of layers between 30-60 cm thickness.
SCV (Sound Compaction Value) is an evaluation index of the noise recorded during compaction, used mainly to evaluate the progress of the compaction of the base layers of the road infrastructure. The noise detection technique is based on two phases: recording and then analyzing the acquired signal. The principle of noise detection is described in Figure 11, on a compactor with a single vibrating roller.

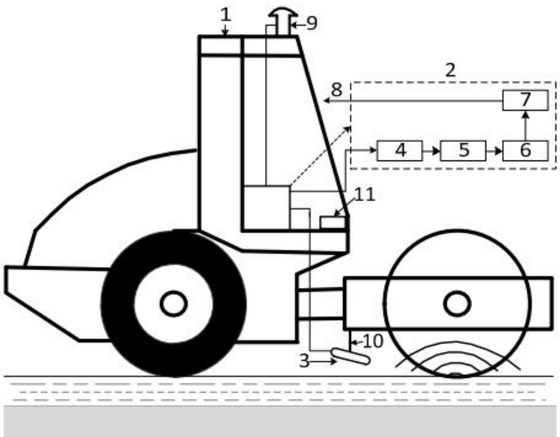

Fig. 11. Scheme of the method of detecting acoustic waves generated during the compaction of filling materials used in road infrastructure [26]:
1. vibrating compactor; 2. noise detection system; 3. microphone; 4. signal conditioning mode; 5. signal acquisition mode; 6. signal processing mode; 7. display; 8. the dashboard of the compactor; 9. GPS receiver; 10. the microphone holding system; 11. battery.

Depending on the change in the structure of the layer, its behavior also changes during the dynamic action of the vibrating roller, generating noise that has different acoustic pressure when the stiffness of the layer changes (Figure 12). The working principle of the evaluation of the SCV index is presented in Figure 13.
Finally, a classification can be made of all the methods applied to evaluate the degree of compaction of soils/asphalt mixtures according to the conformity of the results verified by other available methods (laboratory or "in situ" experimental tests).

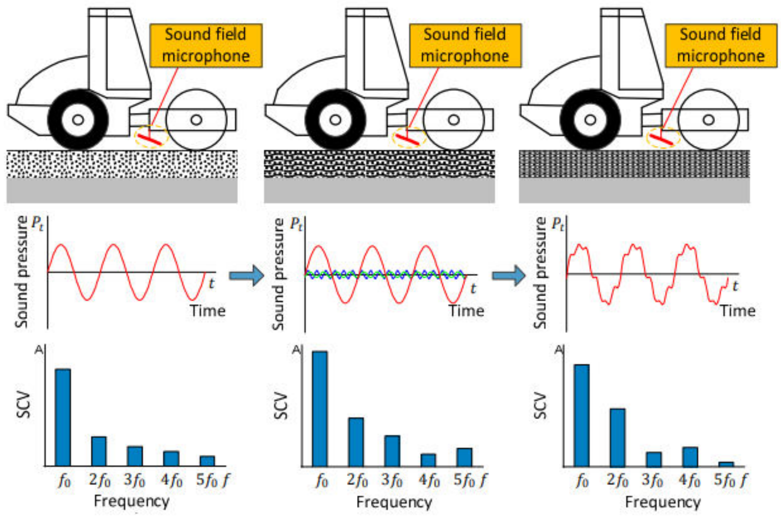

Fig. 12. Illustration of changes in sound pressure and SCV with increasing layer stiffness [26]

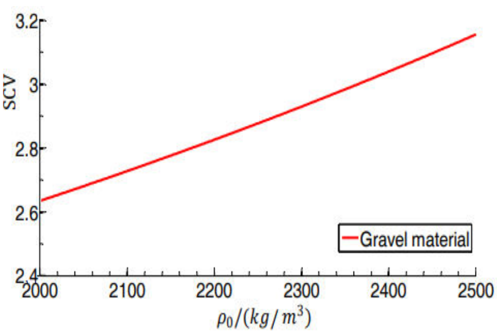

Fig. 13. SCV index vs. dry density of the compacted material [26]

Thus, five levels of acceptability are distinguished, used in the specialized literature [27] in the field of compaction identified according to the constitutive type of the calculation model adopted and the degree of precision of each of the measured, monitored and processed data (Table 3).

Table 3: The five levels and their degree of accuracy accepted for evaluation of the vibratory roller compaction process

<table>
<tr><th rowspan="2">No</th><th rowspan="2" colspan="2">Level description</th><th rowspan="2">Measured parameter</th><th colspan="2">Application</th><th rowspan="2">Accuracy</th><th rowspan="2">Model type</th></tr>
<tr><th>S</th><th>MA</th></tr>
<tr><td rowspan="2">1</td><td colspan="2">Empirical models based on frequency response of drum vibrations</td><td>Harmonics ratio (CMV, RMV, CCV)</td><td>X</td><td>X</td><td>Weak</td><td>N/A</td></tr>
<tr><td colspan="2">Empirical models based on frequency response of drum oscillations</td><td>Harmonics ratio (CCC)</td><td>-</td><td>X</td><td>Weak</td><td>N/A</td></tr>
<tr><td>2</td><td colspan="2">Energetic empirical models based on rolling resistance response of drum</td><td>Energy index (MDP)</td><td>X</td><td>-</td><td>Weak</td><td>Dynamic/ static</td></tr>
<tr><td rowspan="2">3</td><td rowspan="2">Simplified static mechanistic models</td><td>Layered half-space models</td><td rowspan="2">Stiffness, modulus, rolling force (E_{vib}, K_s)</td><td rowspan="2">X</td><td rowspan="2">X
X</td><td rowspan="2">Satisfac-tory</td><td rowspan="2">Dynamic</td></tr>
<tr><td>Discrete elements models: Kelvin-Voigt, Maxwell, Zener, Burgers etc.</td></tr>
<tr><td>4</td><td colspan="2">Dynamic models</td><td>Modulus, rolling force (VCV)</td><td>X</td><td>-</td><td>Good</td><td>Dynamic</td></tr>
<tr><td>5</td><td colspan="2">Dynamic models with artificial intelligence</td><td>Estimated modulus, estimated density (M_{NN}, r_{ODMS})</td><td>-
X</td><td>X
X</td><td>Excellent</td><td>Dynamic</td></tr>
</table>

Note: S – soil: MA – asphalt mixture.

4. Conclusions

In general, the prediction methods (implemented in control systems) are mainly based on linear and/or non-linear regression in order to predict the degree of compaction and compaction state of the soils or asphalt mixtures. Thus, a lot of papers shows results of good practice to use CCC/IC technology for prediction of the compaction of the filling materials and, by interpolation, compactness of the entire working area.
Summarizing the above presented, it can observe that the factors that affect the compaction effect of soils and asphalt mixtures are divided into internal and external factors. Thereby, the internal factors mainly include material characteristics and the strength of the underlying layer, then, the external factors consist of compaction parameters of working regime, compaction energy, constructive drum variant of machinery, compaction mode (static or dynamic), and compaction technology (taking account by machine velocity, number of passes etc.).

References

[1] NE-008-97: Regulation regarding the improvement of weak foundation land through mechanical procedures (Normativ privind îmbunătăţirea terenurilor de fundare slabe prin procedee mecanice).
[2] STAS 8942/3-90: Foundation land. Determination of the linear deformation modulus by field tests with the plate (Teren de fundare. Determinarea modulului de deformaţie liniară prin încercări pe teren cu placa).
[3] NP 125:2010: Regulations regarding the foundation of constructions on soils sensitive to wetting (Normativ privind fundarea construcţiilor pe pământuri sensibile la umezire).
[4] STAS 9850-89: Land improvement works. Checking the compaction of embankments (Lucrări de îmbunătăţiri funciare. Verificarea compactării terasamentelor).
[5] STAS 3300/2-85: Foundation land. Calculation of the foundation land for direct foundation (Teren de fundare. Calculul terenului de fundare în cazul fundării directe).
[6] Debeleac, C. "On the efficiency of compacting equipment." *The Annals of "Dunarea de Jos" University of Galati* 2, no. XVI, Fascicle XIV Mechanical Engineering (2010): 51-54.

[7] Dobrescu, C.F. “Analysis of the dynamic regime of forced vibrations in the dynamic compacting process with vibrating roller.” *Acta Technica Napocensis* 2, no. 1 (2021): 71 – 76.
[8] Debeleac, C., and S. Năstac. “On Non-linear Characteristics Evaluation of Vibratory Tool and Terrain Interaction for Embankment Works.” *Proceedings in Applied Mathematics and Mechanics - PAMM* 12, no. 1 (2012): 605–606.
[9] Bratu, P., and C. Debeleac. “The analysis of vibratory roller motion.” Paper presented at the VII International Triennial Conference Heavy Machinery – HM 2011, Vrnjačka Banja, Serbia, June 29–July 2, 2011.
[10] Debeleac, C., A. Buraga, and S. Năstac. “Nonlinear analysis of the terrain layers response at vibrating compaction process.” Paper presented at the 27rd International Congress on Sound & Vibration (ICSV27), Online, July 11-16, 2021.
[11] Leopa, A., C. Debeleac, and S. Nastac. “Simulation of Vibration Effects on Ground Produced by Technological Equipments.” paper presented at the 12th International Multidisciplinary Scientific GeoConference SGEM 2012, Albena, Bulgaria, June 17–23, 2012.
[12] Debeleac, C., S. Nastac, and A. Buraga. “On nonlinear dynamics of vibrating compaction process of construction materials.” Paper presented at the 26th International Congress on Sound and Vibration (ICSV26), Montreal, Canada, July 7-11, 2019.
[13] Debeleac, C., and S. Năstac. “Stochastic Approaches of Nonlinear Model-Based Simulations for Vibratory Compaction Process.” Paper presented at the 85th Annual Meeting of the International Association of Applied Mathematics and Mechanics (GAMM), Erlangen, Germany, March 10 - 14, 2014.
[14] ECON Technologies Co., Ltd. “Dynamic Signal Analyzer.” Accessed November 29, 2022. https://www.econ-group.com/en/productshow33.html.
[15] Benstone Instruments Inc. “Portable Sound & Vibration Analyzers. impaq Pro Portable Vibration Analyzer.” Accessed November 28, 2022. https://www.benstone.com/tm/?mode=product&mid=1&id=31&name=impaq-Pro-portable-vibration-analyzer.
[16] National Instruments. “Sound and Vibration.” Accessed November 29, 2022. https://www.ni.com/ro-ro/shop/hardware/sound-and-vibration-category.html#.
[17] Asphalt Pavement Association of Oregon. Accessed November 14, 2022. http://www.apao.org/presentations/past-asphalt-conferences/intelligent-compaction-technology-discussion.pdf.
[18] Ma, Yuan, Yang Zhang, Wei Zhao, Ximao Ding, Zhiwen Wang, and Tao Ma. “Assessment of Intelligent Compaction Quality Evaluation Index and Uniformity.” *Journal of Transportation Engineering, Part B: Pavements* 148, no. 2 (June 2022): 04022024.
[19] Anderegg, R. “ACE AMMANN Compaction Expert.” Technical Paper, Ammann. Verdichtung AG, Langenthal, Swiss.
[20] Vennapusa, P. K. R., D. J. White, and M. D. Morris. “Geostatistical analysis for spatially referenced roller-integrated compaction measurements.” *Journal of Geotechnical and Geoenvironmental Engineering* 136, no. 6 (2010): 813–822.
[21] Kelm, M. *Numerical simulation of the compaction of non-cohesive soils using vibratory rollers / Numerische Simulation der Verdichtung rolliger Böden mittels Vibrationswalzen*. Dissertation. Technische Universität Hamburg-Harburg (TUHH), 2004.
[22] Briaud, Jean-Louis, and Jeongbok Seo. “Intelligent Compaction: Overview and Research Needs.” December, 2003. Accessed November 15, 2022. https://intelligentconstruction.com/downloads/PapersReports/Texas_Briaud_IC%20Report_200409.pdf.
[23] Bekker, M.G. *Introduction to Terrain-Vehicle Systems*. Ann Arbor, Michigan, USA, University of Michigan Press, 1969.
[24] Chang, George. “Fundamentals of Intelligent Compaction.” May 3, 2012. Accessed November 16, 2022. https://es.slideshare.net/gkchang/fundamentals-of-intelligent-compaction/12.
[25] Lee, Soomin, Abubakar Sharafat, In Sup Kim, and Jongwon Seo. “Development and Assessment of an Intelligent Compaction System for Compaction Quality Monitoring, Assurance, and Management.” *Appllied Science* 12, no. 14 (2022): 6855.
[26] Zhang, Qinglong, Tianyun Liu, and Qingbin Li. “Roller-Integrated Acoustic Wave Detection Technique for Rockfill Materials.” *Applied Sciences* 7, no. 11 (2017): 1118.
[27] Donghai Liu, Youle Wang, Junjie Chen, and Yalin Zhang. “Intelligent compaction practice and development: A bibliometric analysis.” *Engineering*, *Construction and Architectural Management* 27, no. 5 (2020): 1213-1232.

ISSN 1453 – 7303 "HIDRAULICA" (No. 4/2022)
Magazine *of Hydraulics, Pneumatics, Tribology, Ecology, Sensorics, Mechatronics*

Aspects regarding the Use of Hydraulic Motors

Prof. PhD. math. **Alexandru BOBE**[1], PhD. Eng. **Tiberiu AXINTE**[2,*], PhD. Eng. **Cătălin NUȚU**[3], Dipl. Eng. **Cătălin FRĂȚILĂ**[2], Dipl. Eng. **Mihai DIACONU**[2]

[1] Ovidius University of Constanta, Romania

[2] Research and Innovation Center for Navy, Romania

[3] Constanta Maritime University, Romania

*tibi_axinte@yahoo.com

Abstract: *This article represents research regarding use of hydraulic motors. The role of hydraulic motors is to convert fluid pressure into rotary motion. The motor considered in this article is a hydraulic actuator. The hydraulic motor works only with a pump unit. A pump unit usually has a maxim pressure of $6 \cdot 10^5$ Pa. Hydraulic motors can be used for various applications, such as: excavators, shredders, drilling rigs, winches, crane drives, cooling fan drivers, feeder, roll mills, launch and recovery systems (LARS), etc. After introduction, the authors study two pneumatic circuits using hydraulic motors. The first one has only one device (hydraulic motor 1-1). The second one has two such devices (hydraulic motors 2-1 and 2-2). Afterwards, the two corresponding electro-hydraulic schemes are presented: a simple electro-hydraulic scheme that has only one hydraulic motor and the second electro-hydraulic scheme, which has a hydraulic motor and logic module. The hydraulic and electro-hydraulic schemes given in this paper are designed using FluidSim software from Festo.*

Keywords: *Actuator, hydraulic, shaft, valve, circuit*

1. Introduction

A hydraulic motor is a device that converts hydraulic pressure or flow into angular displacement (rotation) and torque. The first hydraulic motor was constructed by Arthur Rigg in 1885. However, over time, hydraulic motors have developed a lot from a constructive point of view.
Likewise, the hydraulic motors used in the research ship's installations are a mechanical actuator. This actuator converts hydraulic pressure and flow into angular displacement and torque.
At present, these hydraulic actuators can be used in many technical fields.
They are used especially in any application requiring rotational force (torque), [1].
In practice, there are various models of hydraulic motors: vane motors, gear motors, gerotor motors, radial piston motors, internal curved plunger motors and axial piston motors.
In terms of revolving speed, the hydraulic motors can be: low-speed and high-speed motors, [2].
The hydraulic motors have a compact structure and stability in movement, Fig. 1.

Fig. 1. Hydraulic motor

The main operating specifications to be considered for hydraulic motors:

- Operating temperature – the fluid temperature range the motor can accommodate;
- Operating torque – the torque motor is capable to deliver. Operating torque is directly proportional to the pressure of the working fluid delivered to the hydraulic motor;
- Operating speed – the rotation speed of the moving parts of the hydraulic motors. Operating speed is expressed in radian per second (1 rad/s), according to the International Systems of Units (SI);
- Operating pressure – the pressure of the working fluid delivered to the hydraulic motor. The working pressure directly affects operating torque, engine power, flow and speed, [3].

The power of the hydraulic motor depends on the flow rate and pressure of the fluid passing through actuator.
The hydraulic motor that is an actuator is represented by a specific standard symbol, Fig. 2.

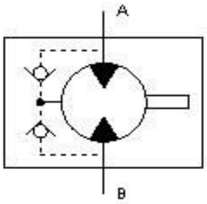

Fig. 2. Symbol of hydraulic motor

Pascal's law is defined as a changed pressure of a fluid in any of its point transmitted undiminished to all point in that fluid.
This principle is valid also for the hydraulic motor, [3].
The relation of the Pascal's principle is:

$$\Delta p = \Delta h \cdot g \cdot \rho \quad (1)$$

Where:

- Δp – the difference in pressure at two different points within a fluid column;
- Δh – the difference in elevation between the two points within the fluid column;
- g – the acceleration due to gravity;
- ρ – the fluid density.

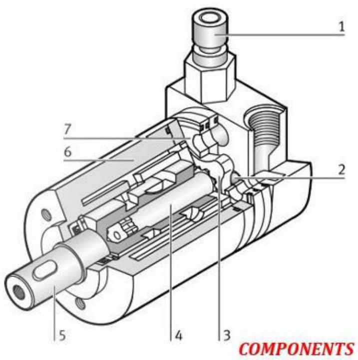

Fig. 3. Components of hydraulic motor

Main components of a hydraulic motor, Fig. 3:

1) Ports;
2) Shuttle valve;
3) Gear with external teeth;
4) Cardan shaft;
5) Working shaft with collector piece;
6) Housing with pilot ducts;
7) Stationary gear with internal gear teeth.

2. The hydraulic circuits

The pneumatic scheme with only one hydraulic motor has a very simple design.
A hydraulic motor using this pneumatic circuit is often used in areas of extreme temperatures due to safety of using air rather than electricity or hazardous chemicals. In fact, the installation with this hydraulic motor is an affordable option regarding costs, [4].
The following hydraulic circuit presented in this manuscript operates only when to 4/3 way fluid directional valve will be given a manual command.
First hydraulic scheme has only one hydraulic motor 1-1, Fig. 4.

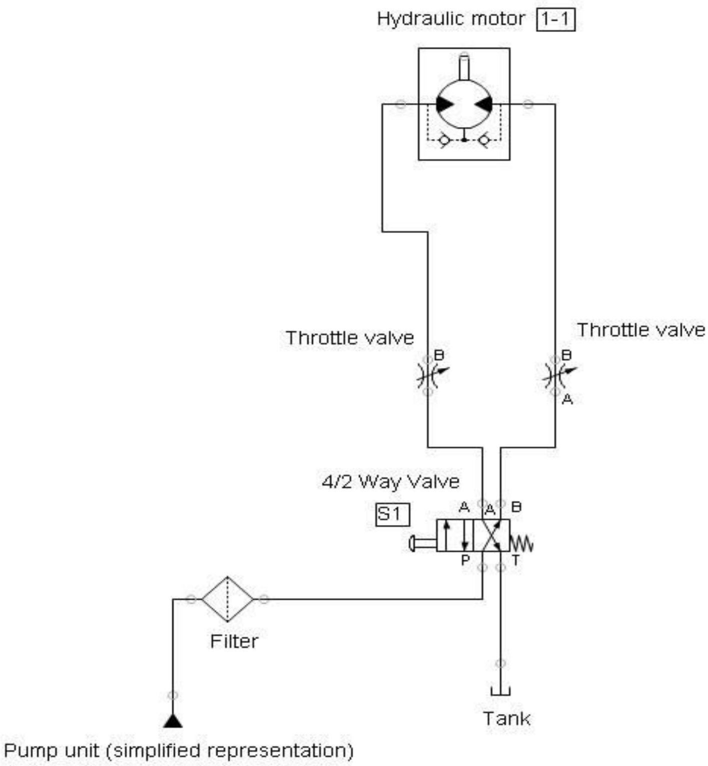

Fig. 4. First hydraulic circuit using one actuator

In the table below there are seven devices used in this first hydraulic scheme, Table 1.

Table 1: Devices in the first hydraulic scheme

Description	Number of components
Hydraulic motor 1-1	1
Throttle valve	2
4/2 way valve with spring	1
Filter	1
Pump unit (simplified representation)	1
Tank	1

This first hydraulic circuit operates if operator presses S1 button of the 4/2 way directional valve with spring. Then, the working shaft rotates clockwise. After that, the working shaft returns, because the 4/2 way directional valve has a spring causing this return, Fig. 5.

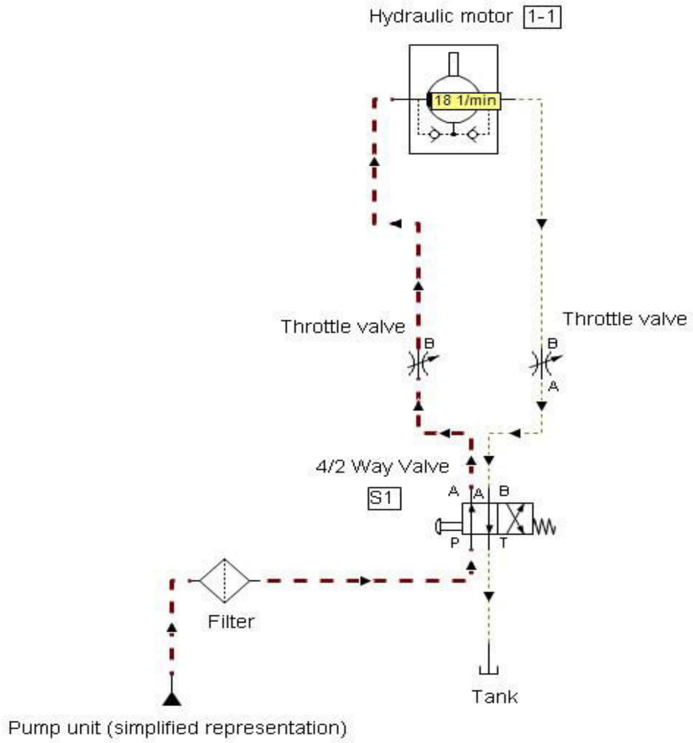

Fig. 5 First hydraulic circuit using one actuator

The diagrams given show variation of the following functional parameters of the hydraulic motor 1-1: revolution (rpm) and flow rate (q), Fig. 6.

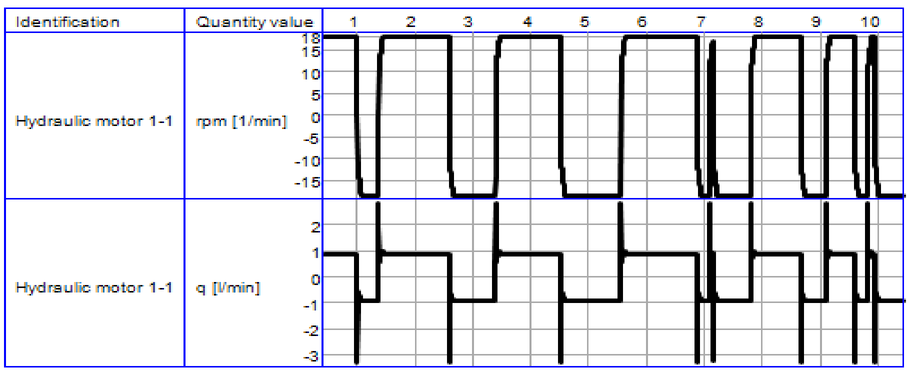

Fig. 6. Diagrams of functional parameters variations of the hydraulic motor

Besides the relation of flow rate for hydraulic motors is:

$$q = \frac{D \cdot n}{1000 \cdot \eta_v} r^2 \quad (2)$$

Where:

- q – flow rate;
- D – displacement;
- n – shaft speed;
- η_v – volumetric efficiency.

The second hydraulic scheme studied has two symmetric actuators: hydraulic motor 2-1 and hydraulic motor 2-2, Fig. 7.

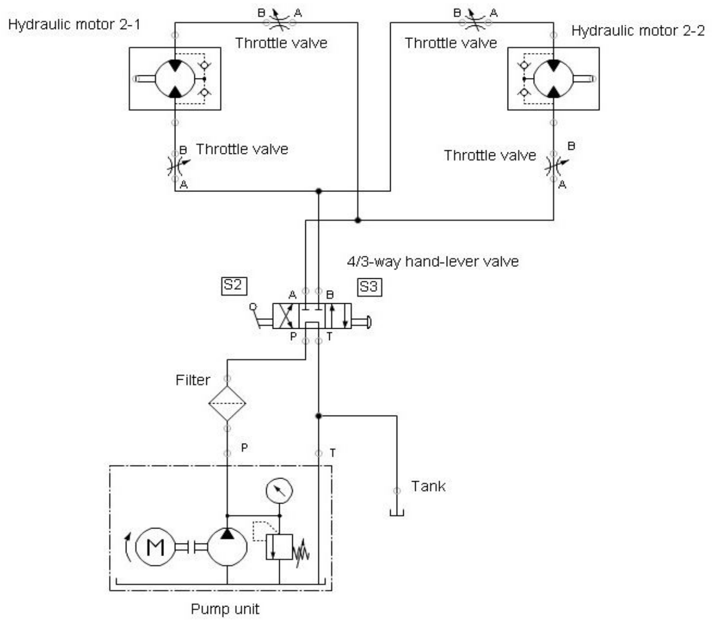

Fig. 7. Second hydraulic circuit using two actuators

In the table below there are ten devices used in the second hydraulic scheme, Table 2.

Table 2: Devices in the second hydraulic circuit

Description	Number of components
Hydraulic motor 2-1	1
Hydraulic motor 2-2	1
Throttle valve	4
4/3 way hand-level valve with button	1
Filter	1
Pump unit	1
Tank	1

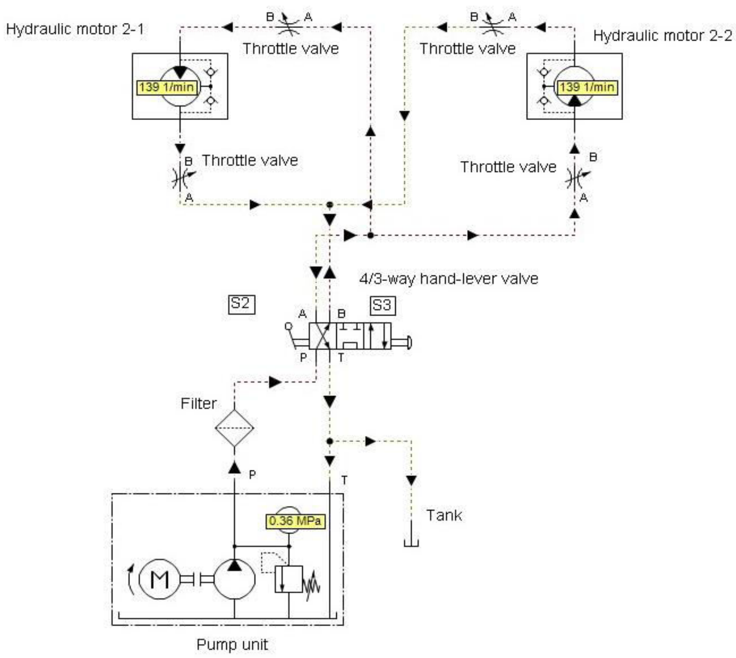

Fig. 8. Simulation of the second hydraulic circuit

In this case, the operator pushes the S2 lever to start the second hydraulic circuit. However, in order to close the same second hydraulic circuit, the S3 button has to be pressed, Fig. 8.

3. The electro-hydraulic circuits

Electro-hydraulic circuits using hydraulic motors are more complex than hydraulic circuits using the same actuators.
The main advantages of electro-hydraulic circuits using hydraulic motors are: easy motion control, excellent resistance to vibrations, high power density, simple thermal exchange management, capability of absorbing impulsive loads, [5].
First electro-circuit has only one hydraulic motor 3-1. The first electro-hydraulic scheme comprises a few basic hydraulic and electrical devices. It must be noted that the authors used a latched 4/3 – way solenoid valve, having "memory". This "memory" has an effect on commands given by the operator of this hydraulic installation, Fig. 9.

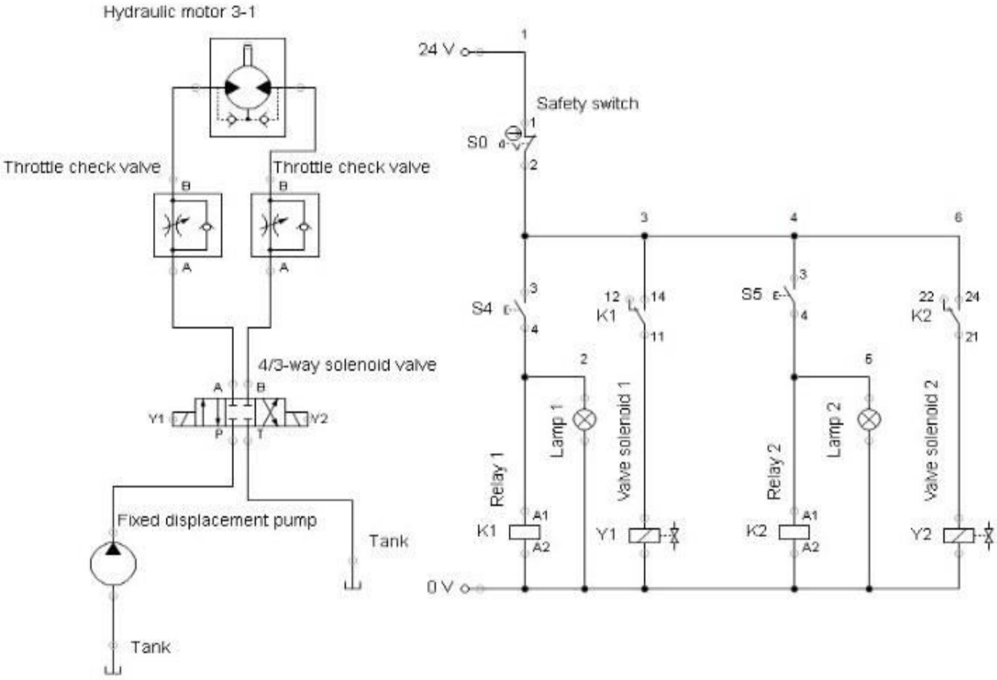

Fig. 9. First electro-hydraulic circuit

In the table below there are fourteen devices used in the first electro-hydraulic circuit, Table 3.

Table 3: Devices in the first electro-hydraulic circuit

Description	Number of components
Hydraulic motor 3-1	1
Throttle check valve	2
4/3 way solenoid valve	1
Fixed displacement pump	1
Tank	2
Safety switch	1
Relay	2
Valve solenoid	2
Lamp	2

In order to operate the electro-hydraulic circuit having one hydraulic motor 3-1, the operator has to press S4 button.

Then, the working shaft rotates clockwise and lamp 1 shows a yellow signal, Fig. 10.

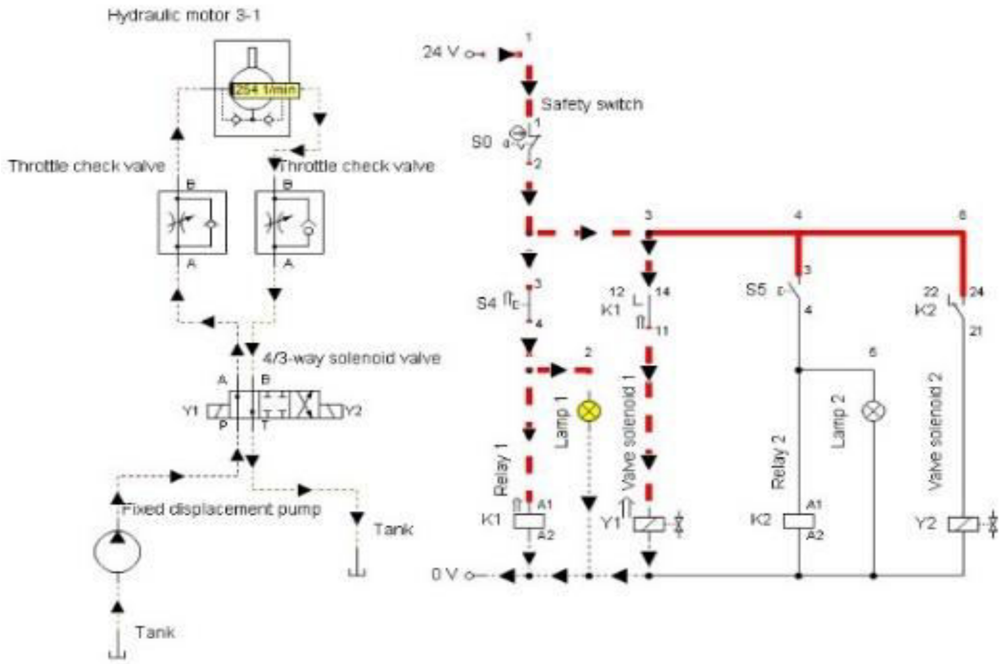

Fig. 10. Opening the first electro-hydraulic circuit. Simulation I

In order to close the first electro-hydraulic circuit, operator has to press the S5 button.
Then, working shaft rotates counterclockwise and lamp 2 shows a green signal, Fig. 11.

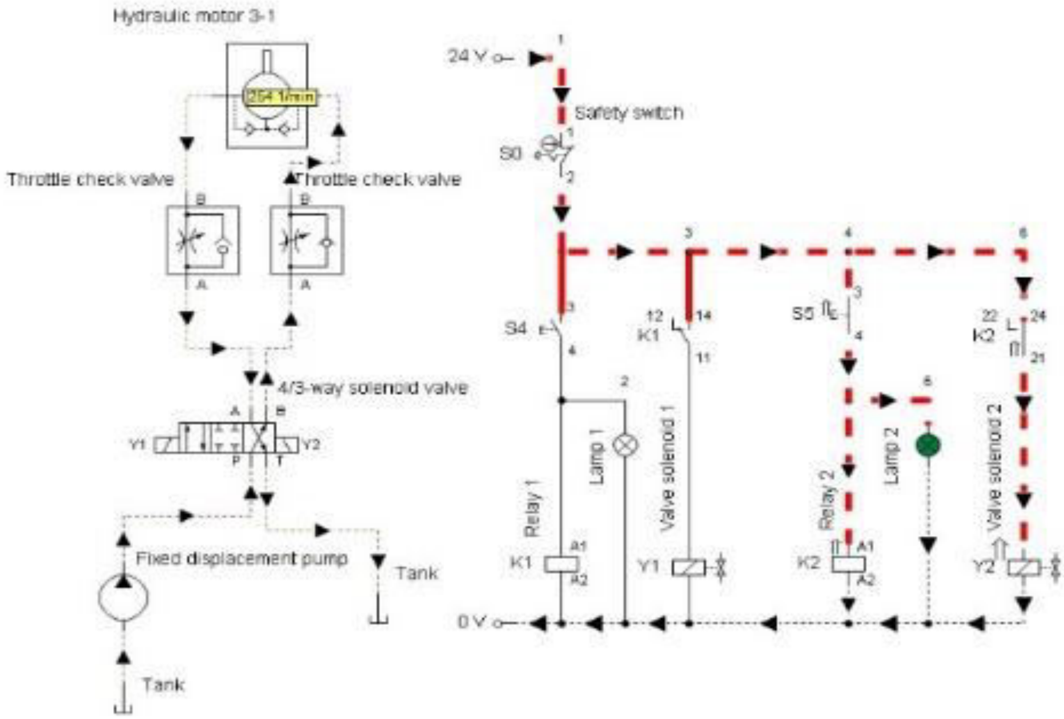

Fig. 11. Closing the first electro-hydraulic circuit. Simulation II

Another further improvement for the scheme presented above is to use a logic module.
Which also offers much more flexibility in controlling the hydraulic motor 4-1, using a variable displacement pump, Fig. 12.

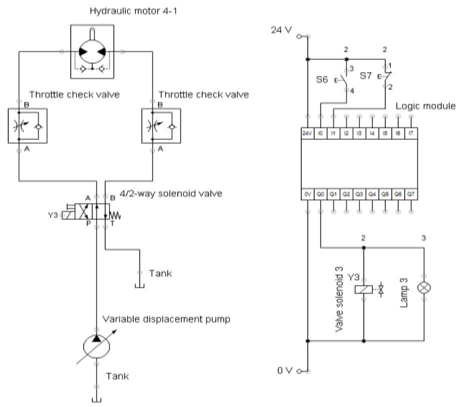

Fig. 12. Second electro-hydraulic circuit using digital module

In the table below there are eleven devices used in the second electro-hydraulic circuit, Table 4.

Table 4: Devices in the second electro-hydraulic scheme

Description	Number of components
Hydraulic motor 4-1	1
Throttle check valve	2
4/2 way solenoid valve	1
Variable displacement pump	1
Tank	2
Logic module	1
Valve solenoid	2
Lamp	1

The next two figures show the movement of the hydraulic motor 4-1, [6].
Thus, in order to open the second electro-hydraulic circuit, operator must press S6 button.
In this case, the working shaft of hydraulic motor 4-1 rotates counterclockwise and lamp shows a blue signal, Fig. 13.

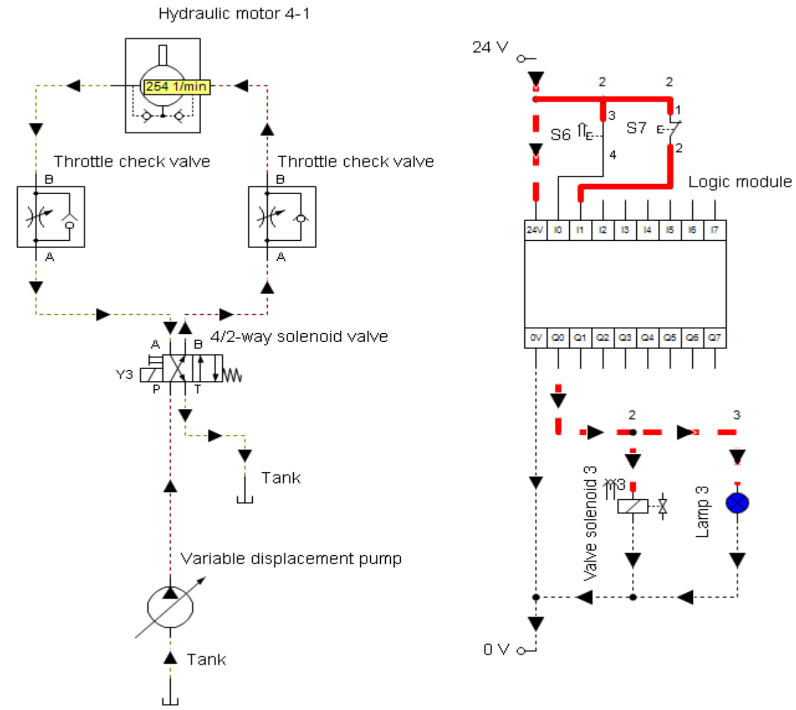

Fig. 13. Opening the second-hydraulic circuit using a logic module. Simulation I

However, in order to close the second electro-hydraulic circuit, operator should press S7 button. Now, the working shaft of hydraulic motor rotates clockwise, Fig. 14.

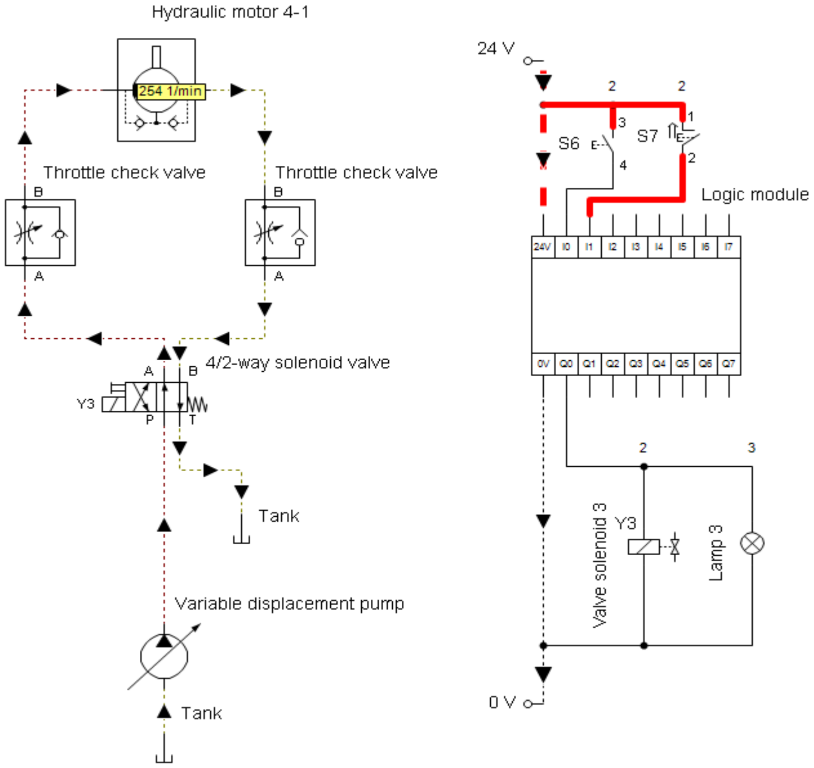

Fig. 14. Closing the second-hydraulic circuit using a logic module. Simulation II

4. Conclusions

Taking into consideration all what has been presented in this paper, the electro-hydraulic circuits using hydraulic motors offer some important advantages over traditional electro-hydraulic scheme using other devices (semi-rotary, single acting cylinder, double acting cylinder, etc.).
These advantages are:

- they run only when needed;
- installations using them are very smooth and quiet;
- self-containment and compactness;
- these installations do not leak;
- these installations use a DC power supply.

Given their superior strength, it seems hydraulic motors will replace in time, in some applications, the hydraulic cylinders from electro-hydraulics installations. Because each product development generates its own individual challenges, it would be however, a nonsense to claim that hydraulic motors could be a complete substitute for a hydraulic device from electro-hydraulic installations.
Depending on the particular installations and specific technical applications, other technical solutions replacing use of hydraulic motors are also possible. To make a correct economical and technical decision in this direction, all aspects involved, such as costs of acquisition, operational costs also including energy costs, strength and resistance to specific mechanical stresses, maintenance and reliability are to be taken into consideration.
Hydraulic actuators however offer some unique features, which are to be explored especially to winches and cranes from ships.
Researches and operators should be encouraged to take into account a hydraulic motor when searching for a suitable fluid movement device in electro-hydraulic installations.
A more sophisticated electro-hydraulic circuits with hydraulic motors and programmable logic controller (PLC) is to be developed in future article to be submitted.

References

[1] Surdu, G. "Sustainable development a challenge for research in the field military equipment and space." *Impact of Socio-economic and Technological Transformations at National, European and International Level (ISETT)* 7 (2015).

[2] Deleanu, D., and C. L. Dumitrache. "Numerical study of a container ship model for the uncoupled parametric rolling." *IOP Conference Series: Materials Science and Engineering* 591 (2019): 012106.

[3] Nastasescu, V., and L. Gavrila. "Controlled flow simulation using SPH method." Paper presented at the International Conference of Scientific Paper AFASES, Brasov, Romania, May 24-26, 2012.

[4] Hruzik, L., A. Burecek, L. Dvorak, K. Fojtasek, P. Monka, M. Vasina, and M. Bova. "Valve control of drive with rotary hydraulic motor." *MM Science Journal* (June 2019): 2902- 2909.

[5] Panaitescu, M., and F. V. Panaitescu. "Consideration on Hydraulic Modelling and Evaluation of Surface Waters with Environmental Risk." *Hidraulica Magazine*, no. 4 (December 2020): 59-71.

[6] Thiagarajan, D., and N. Manoharan. "Adapting concurrent engineering approach for design and development of a new rotary hydraulic motor for marine application." *ARPN Journal of Engineering and Applied Sciences* 10, no. 13 (July 2015): 5564- 5568.

ISSN 1453 – 7303 **“HIDRAULICA” (No. 4/2022)**
Magazine *of Hydraulics, Pneumatics, Tribology, Ecology, Sensorics, Mechatronics*

System for Velocity Adjustment and Control of a Closed-Circuit Secondary Adjustment Hydrostatic Transmission

PhD. Stud. Eng. **Alexandru-Polifron CHIRIȚĂ**[1*], PhD. Eng. **Radu Iulian RĂDOI**[1], MSc. Stud. Eng. **Bogdan Marian ȘERBAN**[1], Res. Assist. **Ana-Maria POPESCU**[1], MSc. Stud. Eng. **Andrei-Alexandru BENESCU**[1]

[1] National Institute of Research & Development for Optoelectronics / INOE 2000 – Subsidiary Hydraulics and Pneumatics Research Institute / IHP, Bucharest, Romania

* chirita.ihp@fluidas.ro

Abstract: *This article focuses on the design and testing of a close-circuit secondary adjustment hydrostatic transmission. The interface between the acquisition board and the computer is done by LabView programming environment. The process is regulated by a PID controller. The system uses the controller output value to push the process variable toward the setpoint value. Control schematics include a feedforward multiply loop for more precise response.*

Keywords: *Secondary adjustment, hydrostatic transmission, closed-circuit, feedforward, PID controller*

1. Introduction

Over the past few decades, stationary and mobile machinery has become more automated and productive thanks to fluid power and motion control systems. The high power density, quick reaction, good controllability of movements, and affordable, direct rotary actuation using hydraulic motors are some of the main benefits of hydraulic systems. Different well-known and tested system designs are available to hydraulic system designers: power and motion control might be based on proportional valves, servo-valve, direct pump, or secondary control [1].
In traditional hydraulic valve control systems, to vary the flow rate supplied by the pump, needle valves that shrink the flow section are used. A downside of those types of equipment is that they lead to an increase of pressure in the system that causes the relief valve to open, high-pressure flow rate enters the tank and causes futile power use. Reduced use of the relief valve can decrease power consumption and increase system performance. This can be obtained by using a variable displacement pump, motor or both, rather than a relief valve in response to load demands (higher or lower velocity or torque). This is where hydrostatic transmissions intervene, allowing hydraulic power to be transferred easily from one point to another in a controlled manner. With other types of drives, obtaining such high requiring demands is very difficult or even impossible. These performances have been made feasible by the control of hydrostatic drives utilizing analog and digital electronic equipment in closed open-loop control systems [2, 3].
The closed-circuit hydrostatic (HST) drives used in industrial equipment stand out for their high power density, improved controllability, and wide speed-torque range. To create its design principles and components, the HST drive needs a steady-state performance analysis based on operational characteristics. Without creating prototypes, the appropriate HST components (pumps and motors) can be chosen for investigation based on the projected performance of the drives [4].
An HST's performance qualities depend on how it is set up, including whether it has a fixed or variable displacement pump, motor, or both. These setups and their individual performance characteristics are summarized in Figure 1 and described below. Depending on its configuration, the HST can drive a load from full speed in one direction to full speed in the opposite direction, with infinite variation of speed between the two maximums—all with the prime mover operating at its optimum speed. A fixed-displacement pump drives a fixed-displacement motor in the most basic hydrostatic transmission (Fig. 1A). Although this transmission is cheap, it only has a few applications, mainly because more energy-efficient alternatives to it exist. The pump must be sized to operate the motor at a set speed under full load since pump displacement is fixed. Fluid from the pump output flows over the relief valve when running at full torque is not necessary and heat is wasted as a result.

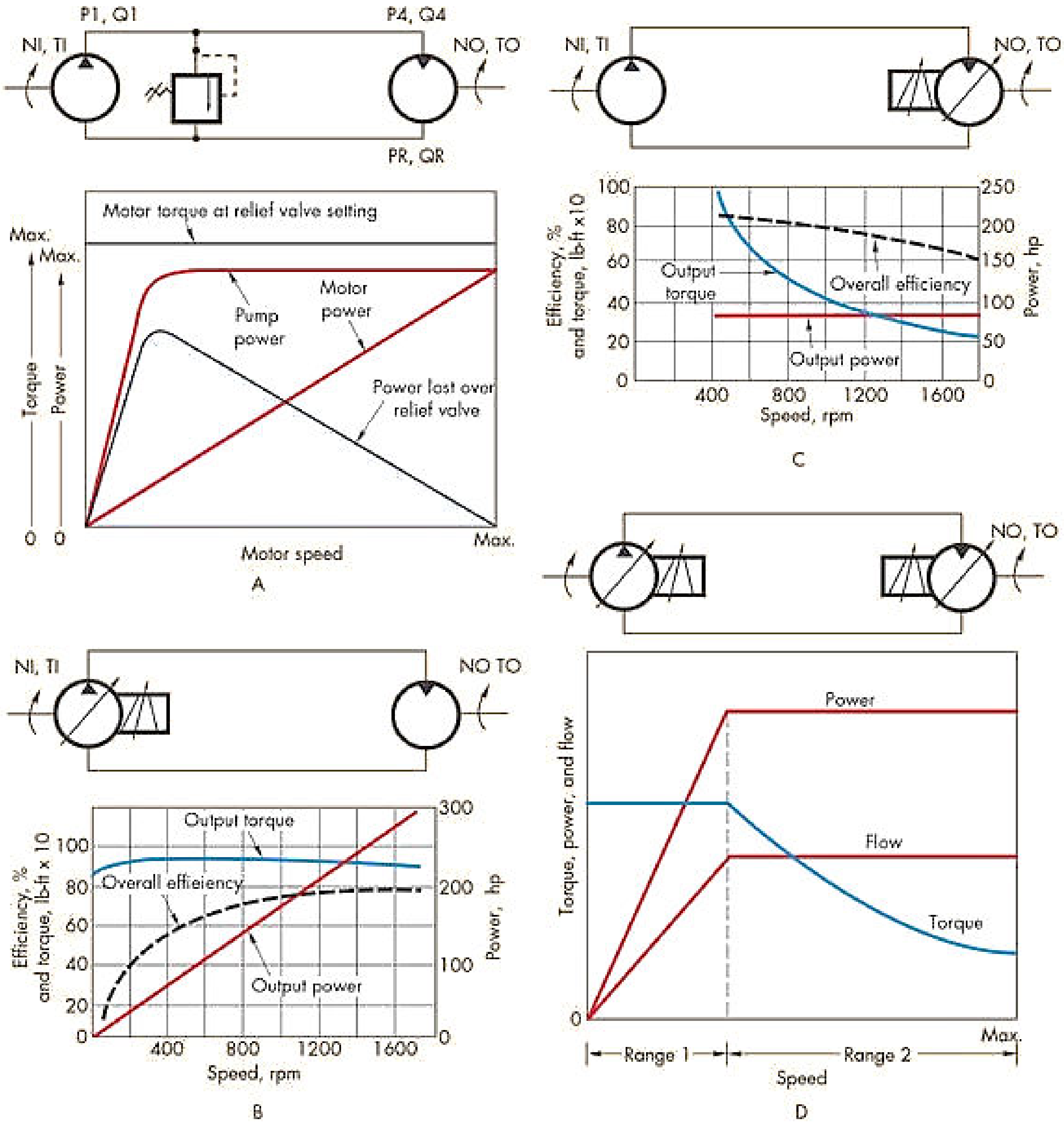

Fig. 1. Types of adjustment in closed hydrostatic transmissions – adapted from [4]

Primary adjustment hydrostatic transmission (PAHT): A constant torque transmission is produced by switching from a fixed displacement pump to one with a variable displacement (Fig. 1B). Because torque is solely dependent on fluid pressure and motor displacement, torque output is constant at any speed. Motor speed rises or falls as pump displacement increases or decreases, although torque is largely constant. As a result, power rises as pump displacement does.
Secondary adjustment hydrostatic transmission (SAHT): Transmissions that give constant power are made by combining a fixed-displacement pump and a variable-displacement motor (Fig. 1 C). Power delivered remains constant if flow rate to the motor is constant and motor displacement is changed to keep the ratio of speed to torque constant. Motor displacement reduction raises motor speed while lowering torque, which together maintains constant power.
Mixt adjustment hydrostatic transmission (MAHT): Figure D depicts a variable-displacement pump and motor [5].
Two ranges of adjustment are shown by the curves in Fig. 1D. Pump displacement reaches from zero to maximum while the motor displacement remains constant at its peak in "Range 1". Pump

displacement growth does not affect torque; however, it does affect power and speed. The second "Range" starts as soon as the pump achieves its maximum displacement and continues as the motor's displacement falls. While speed rises across this range, power stays constant. Torque declines. (Theoretically, the motor speed might be endlessly raised, but, in practice, dynamics would be the limit).
The secondary adjustment principle, which works in a regime of quasi-constant pressure, assumes the existence of a SAHT capability, which, when operating at a nominal pressure, seeks the appropriate volumetric capacity to maintain a constant rotation speed [6]. A fast-acting electro-hydraulic servomechanism is used to vary the displacement of the axial piston motor and is controlled by a command unit. The command unit automatically calculates the torque necessary - in just a few milliseconds - to ensure that the rotation speed is kept to the set point.

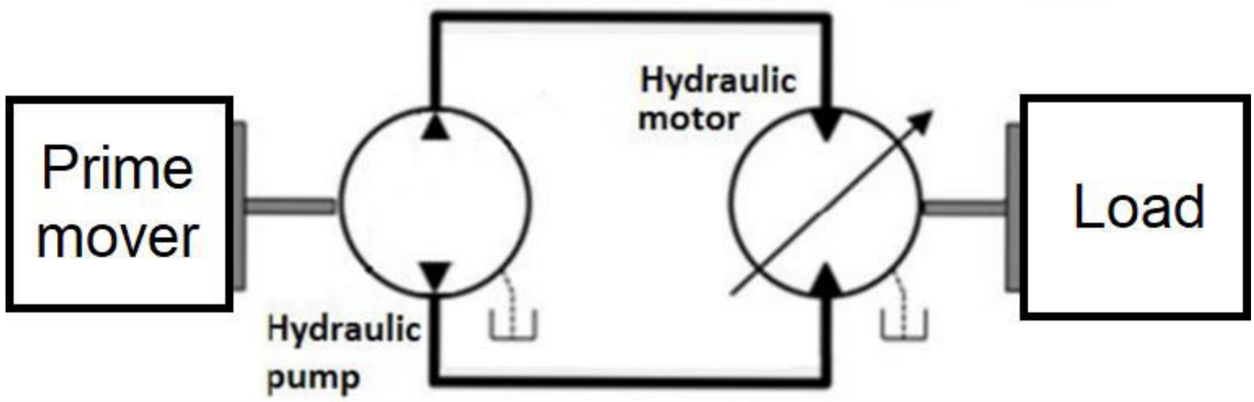

Fig. 2. Simplified schematic of hydrostatic drives with control of the secondary unit – adapted from [7]

Secondary-control drives avoid the need to throttle down the flow rate, as is the case in typical open systems, even when several utilizing units with different loads are connected to the system. By adjusting the machine's volume displacement to the loading situation, the power drain or energy return to the supply network is managed to match needs.

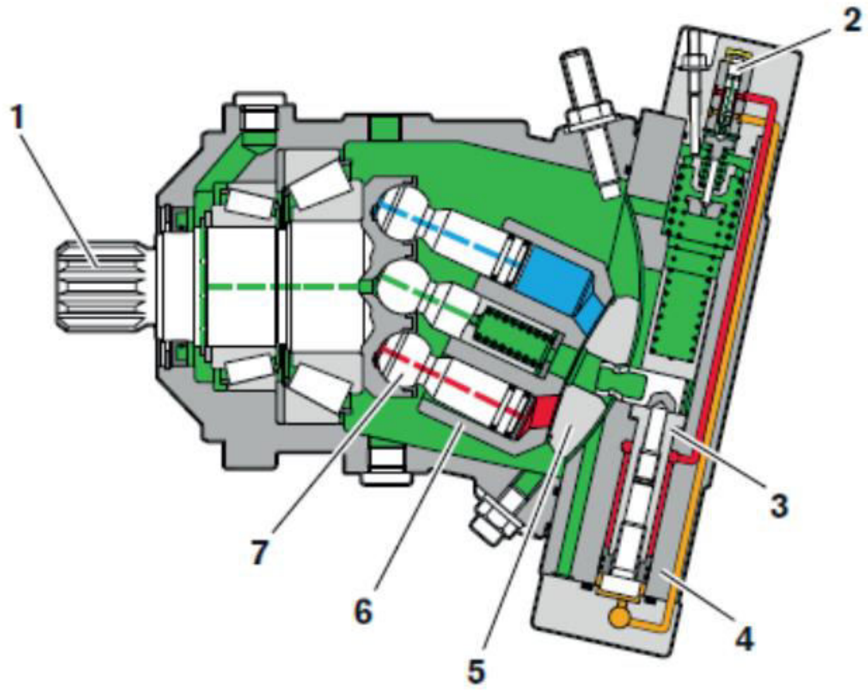

Fig. 3. Cross-section of the A6VM variable displacement axial piston hydraulic motor by Bosch Rexroth
1 – driving shaft, 2 – control piston, 3 –piston stroke control unit, 4 – casing in which the control piston is placed, 5 – lens plate, 6 – cylider block, 7 – piston [9]

This explains why the number of units acting as pumps or motors can be linked in parallel without affecting the system's energy balance, even in open systems.
The performance of secondary-control drives is unaffected by even extensive distances between secondary and primary units that must be traversed utilizing lengthy hydraulic lines [8]. A major advantage of using hydrostatic transmissions is the ability to vary the speed and torque output with a great degree of accuracy, even when load requirements are changing quickly.
The chosen hydrostatic motor for this system is A6VM Bosch Rexroth axial piston motor, depicted in Fig. 7. The hydraulic motor's inflow and outflow spaces are connected to the pistons 7 inside the cylinder block 6, which are rotating and together with the cylinders constitute the working chamber, through holes in the cylinder block 6's face space. The working volume expands as the plunger moves to the left, joining with the inflow (pressure) area to get filled with liquid. When the pistons moves to the right, the working volume shrinks and the liquid is supplied into the outflow area.
While the motor is running, a portion of its chambers is filled with the working fluid, while fluid from the remaining chambers is discharged into the outflow conduit. The spherical lens plate 5, with spaces connected to the channels in the motor casing and the input and outflow holes, was attached to the motor. Leaks from the high-pressure area into the low-pressure area occur in the motor, particularly in the lens plate 5. In this instance, the directional valve 2 spool position that enables the displacement of the motor to vary is determined by a PID controller.
Regarding the largest speed fluctuations per second as a function of power, figure 3 compares hydrostatic machines with secondary adjustment to machines that are electric and electric machines that are adjustable. The comparative standards were derived from the data in manufacturer leaflets. The B/B1 field in the graphic depicts the secondary regulation's present state (double logarithmic scale).

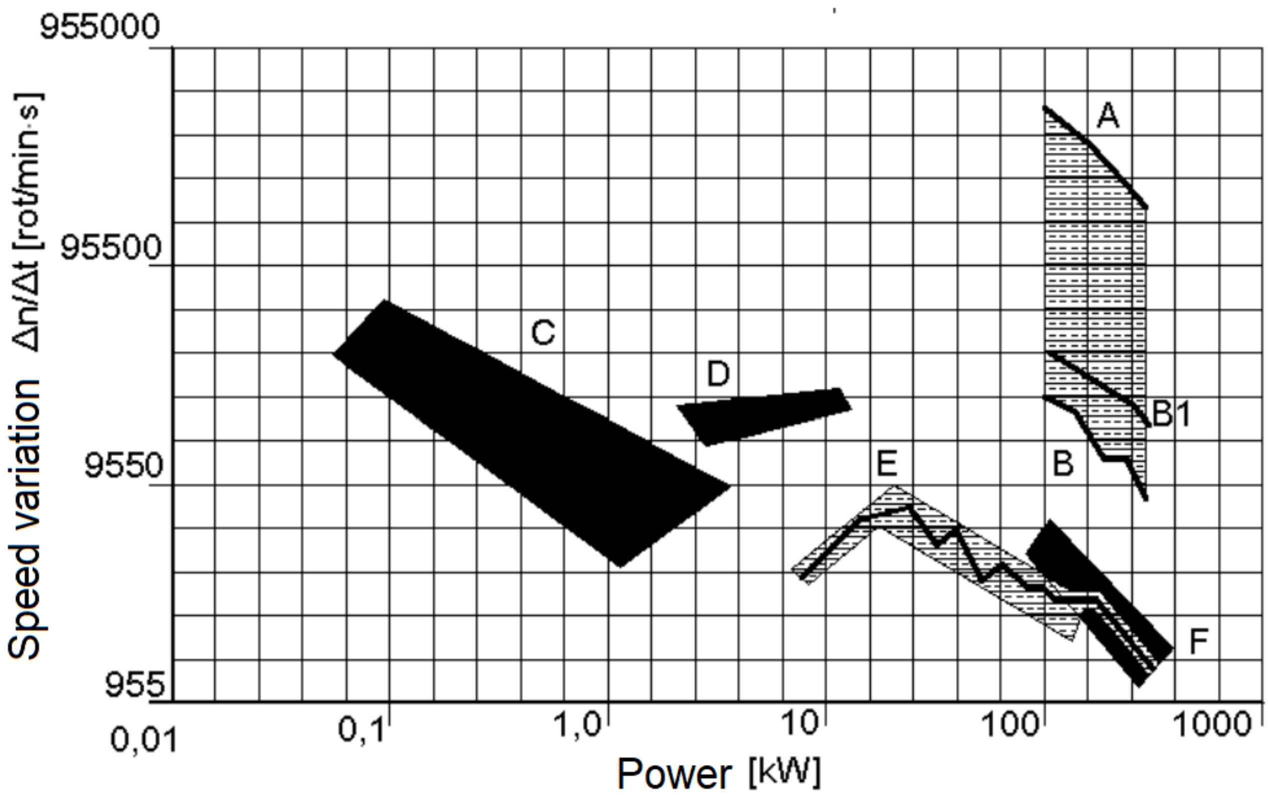

Fig. 4. Speed variations (max.) for various engines as a function of power
A - hydraulic engine (theoretical possible value); B - hydraulic motor (speed adjustment - secondary adjustment A4 VEL); B1 - hydraulic motor (speed adjustment - secondary adjustment A4 VEL); B1 - hydraulic motor (speed adjustment - secondary adjustment A4 VEL). hydraulic motor (speed regulation - secondary regulation A4VS); C - DC servo motor; D - hydraulic motor (speed regulation - secondary regulation A4VS) three-phase servomotors; E - three-phase motor (with frequency regulation); F - three-phase motor (with air venting external ventilation) [3]

2. Material and Method

This chapter is composed of two parts, the mathematical model of the static control characteristics of the hydraulic motor rotary and Hydraulic transmissions with a secondary adjustment experimental system.

2.1 Mathematical model of the static control characteristics of the hydraulic motor rotary

Usually, rotary hydraulic machines can function as a pump as well as a motor. Hydraulic rotary motors are available with fixed or adjustable capacity for a variety of speed and torque ranges, with fast, semi-fast, or slow operation.
Rotary motors, which are used as drive elements, have unique structural and functional characteristics, and some are even special machines. Because a relatively wide range of motors is used in practice, each with its own set of constructional and functional principles, as well as energy and dynamic performances, the most accurate knowledge of the following sizes, as well as the corresponding control methods, is required.
Given its position and role in a hydrostatic transmission, the hydraulic motor can be thought of as an energy converter that accepts energy from a positive displacement pump and converts it into mechanical energy applied to a load, as shown in Figure 5.

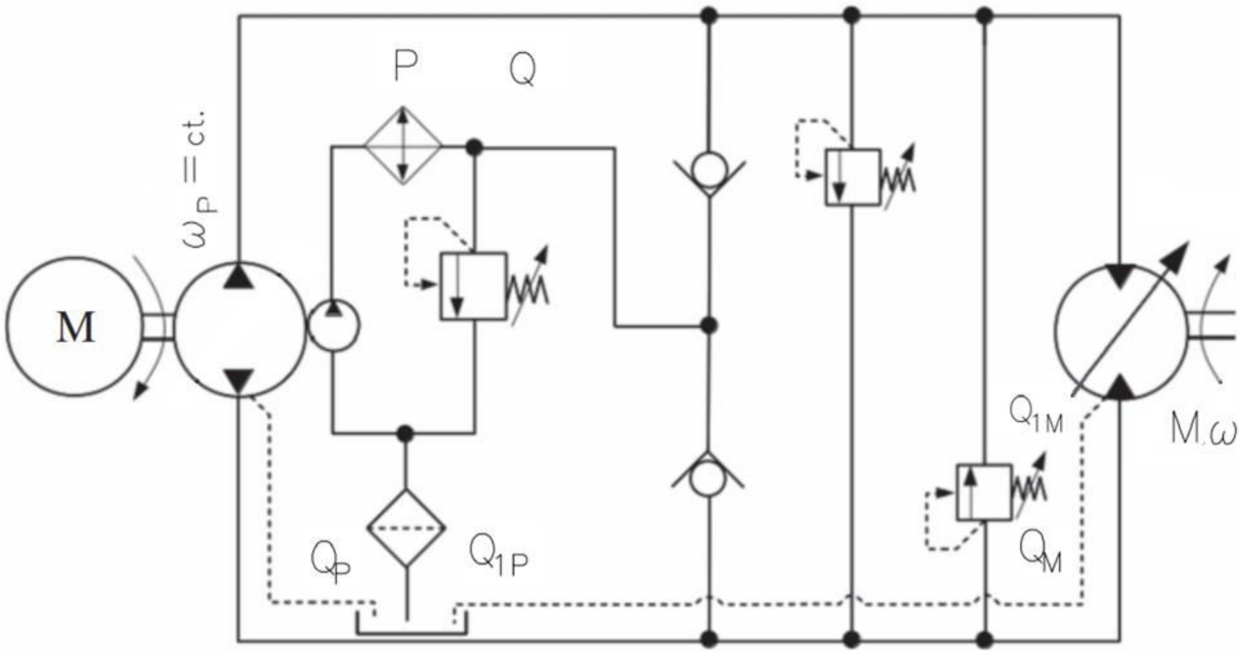

Fig. 5. Schematic diagram of hydraulic transmission with secondary adjustment – adapted from [10]

We will disregard the compressibility of the working fluid and consider flow losses if the system runs only as far as the pressure relief valve in the system may be opened. The equations characterizing stable equilibrium under these circumstances are:

$$Q = \boldsymbol{\omega}_p \cdot \boldsymbol{q}_p - \boldsymbol{\alpha}_p \cdot p = \boldsymbol{\omega}_M \cdot q_M + \boldsymbol{\alpha}_M \cdot p \quad (1)$$

$$M_M = \eta_{mM} \cdot q_M \cdot p \quad (2)$$

These equations lead to the following generic equation for the mechanical characteristic of the engine:

$$\boldsymbol{\omega}_m = \boldsymbol{\omega}_p \cdot \frac{q_p}{q_M} - \frac{\boldsymbol{\alpha}_p + \boldsymbol{\alpha}_M}{q_M^2 \cdot \boldsymbol{\eta}_{mM}} \cdot M_M \quad (3)$$

Where:

$$q_p = q_{p\,max} = constant$$

$$\omega_p = q_{p\,nominal} = constant$$

As the engine flow rate increases drops, hydraulic motor capacity command (q_M) results in mechanical characteristics that are linear but with an increasing slope. The mechanical properties no longer rely on torque and become straight parallel to the torque axis if flow losses in the system are ignored.

By lowering the particular engine flow q_M from $q_M = q_{M\,max}$ to the value $q_M = q_{M\,min}$ corresponding to the maximum speed M_{max}, without going above the maximum mechanical power, the secondary adjustment enables the achievement of greater speeds than the.

The examination of the relationship demonstrates that the dependence of the mechanical feature on the engine specific flow rate is highly non-linear (3), therefore, linearization of the mechanical properties around a static operating point is required for the implementation of a system for controlling the rotational speed of a load utilizing hydraulic motor capacity control.

The linearization of mechanical characteristics is obtained by applying the relation:

$$\boldsymbol{\Delta\omega}_M = \left(\frac{\boldsymbol{\partial\omega}_M}{\boldsymbol{\partial} q_M}\right)_{\mathbf{0}} \cdot \boldsymbol{\Delta} q_M + \left(\frac{\boldsymbol{\partial\omega}_M}{\boldsymbol{\partial} M_M}\right)_{\mathbf{0}} \cdot \boldsymbol{\Delta} M_M \tag{4}$$

After calculating the derivatives from (4) we obtain:

$$\boldsymbol{\Delta\omega}_M = -\left(\frac{\boldsymbol{\omega}_p \cdot q_p}{q_{M0}^2} - \frac{\mathbf{2} \cdot \boldsymbol{\alpha} \cdot M_{M0}}{\boldsymbol{\eta}_{mM} \cdot q_{M0}^3}\right) \cdot \boldsymbol{\Delta} q_M - \frac{\boldsymbol{\alpha}}{\boldsymbol{\eta}_{mM} \cdot q_{M0}^2} \cdot \boldsymbol{\Delta} M_M \tag{5}$$

Where:

$\alpha = \alpha_p + \alpha_M$ –total flow rate loss of the system

Using the notation:

$$K_1 = \frac{\boldsymbol{\omega}_p \cdot q_p}{q_{M0}^2} - \frac{\mathbf{2} \cdot \boldsymbol{\alpha} \cdot M_{M0}}{\boldsymbol{\eta}_{mM} \cdot q_{M0}^3} \tag{6}$$

And

$$K_{\mathbf{2}} = \frac{\boldsymbol{\alpha}}{\boldsymbol{\eta}_{mM} \cdot q_{M0}^2} \tag{7}$$

The linearized mechanical characteristic of the engine can be written in the form:

$$\boldsymbol{\Delta\omega}_M = \frac{\boldsymbol{\omega}_p \cdot q_p}{q_M^2} - K_{\mathbf{2}} \cdot \boldsymbol{\Delta} M_M \tag{8}$$

It is essential to understand the fluctuation of the amplification factor K1 as a function of the variable independent q_M, or the graph of the function, in order to assess the dynamic stability of the speed control system.

$$K_{\mathbf{1}}(q_M) = \frac{\mathbf{Q}_{tp}}{q_M^2} - \frac{\mathbf{2} \cdot \boldsymbol{\alpha} \cdot M_M}{\boldsymbol{\eta}_{mM} \cdot q_M^3} \tag{9}$$

The derivative's equation gives rise to the following mode of variation for this parameter:

$$\frac{dK_1}{dq_M} = -\frac{\mathbf{2} \cdot \mathbf{Q}_{tp}}{q_M^3} + \frac{\mathbf{6} \cdot \boldsymbol{\alpha} \cdot M_M}{\boldsymbol{\eta}_{mM}} \cdot \frac{\mathbf{1}}{q_M^4} \tag{10}$$

Considering the torque in the M_M expressed as a function of pressure, the following results are obtained:

$$\frac{dK_1}{dq_M} = -\frac{\mathbf{2}}{q_M^3}(\mathbf{Q}_{tp} \cdot \mathbf{3} \cdot \boldsymbol{\alpha}\mathbf{p}) \tag{11}$$

Where:

$$\alpha p_{max} \leq 0.02 \cdot Q_{tp}$$

Results:

$$Q_{tp} - 3 \cdot \alpha p > 0$$

Implies:

$\frac{dK_1}{dq_M} < 0$ in any point of the system.

Therefore, the amplification factor K_1 decreases continuously with increasing specific flow rate q_M of the hydraulic motor, as shown in figure 5.

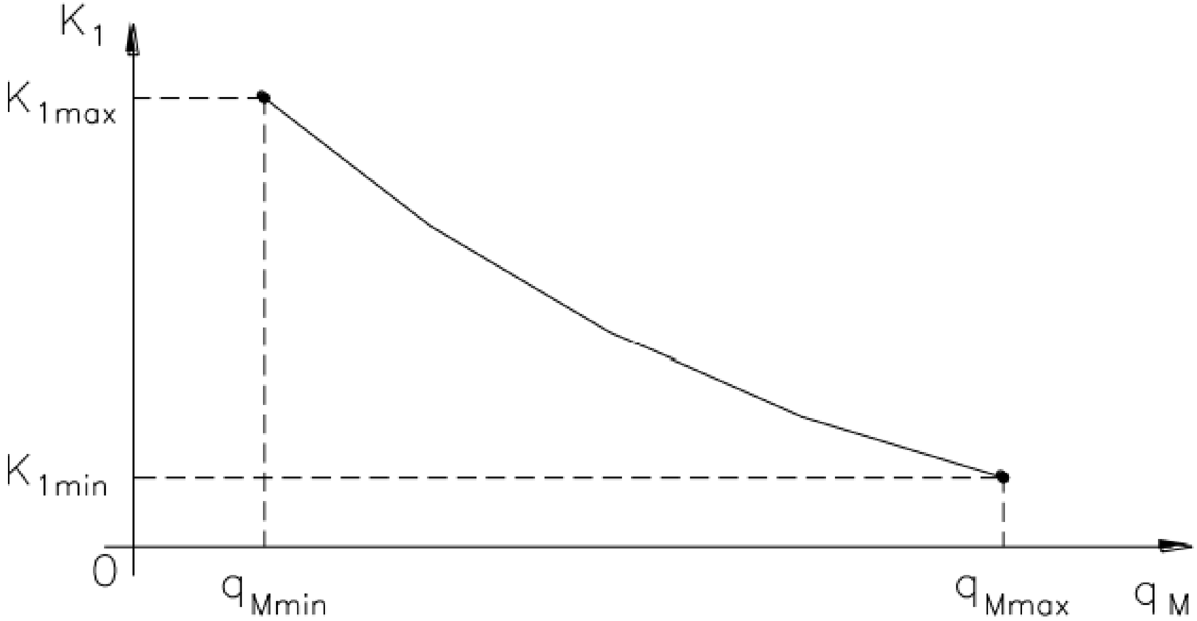

Fig. 6. Variation of amplification factor versus flow rate specific hydraulic motor

The linear displacement x of a moving component, which alters the particular flow rate in accordance with the relation: An electrohydraulic servomechanism for regulating the specific flow to the motor contains this output variable.

$$q_M = q_{M\,max} - K_{qx} \cdot \boldsymbol{x} \tag{12}$$

Where:

K_q – $transfer\ factor\ determined\ by\ kinematic\ elements\ and\ of\ the\ driven\ mechanism$

2.2 Hydraulic transmissions with secondary adjustment experimental system

In figure 7 is presented system on which the experimental results have been produced.
The rotation speed of the motor is controlled such that it is reached at the network pressure, regardless of the load pressure. To that end, the displacement of the motor must be changed until a balance is created between the motor torque and the load, and the desired rotation speed is reached at the same time.

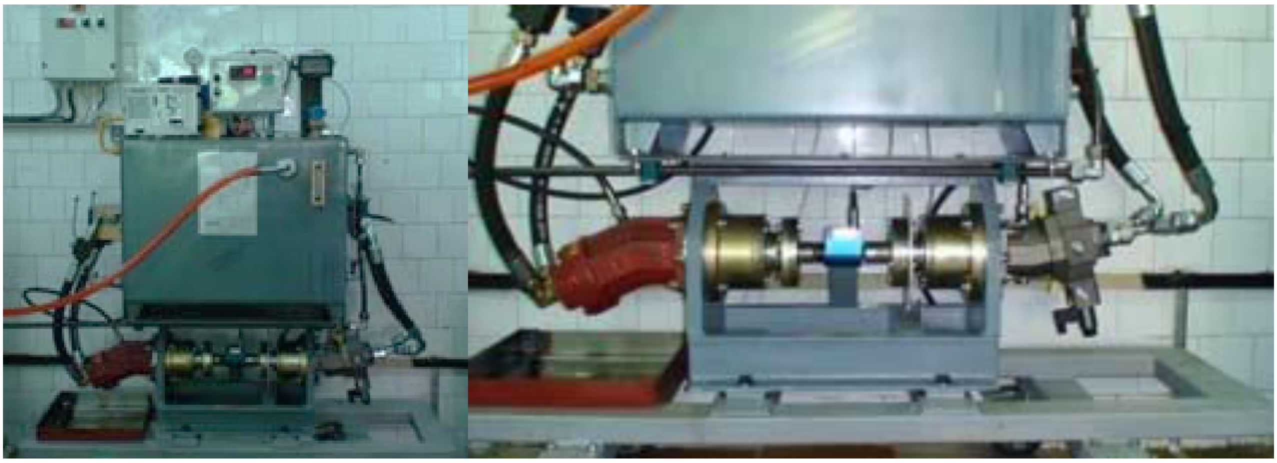

Fig. 7. Experimental stand for the study of the closed-loop transmission with secondary adjustment

The system is composed of two main hydraulic lines that run from the pump to the motor (Branch "A") and back to the pump (Branch "B") as shown in figure 8. Each component either supplies fluid to both hydraulic lines or drain it. Mechanical work is generated by the triphasic electric motor E_M that is transmitted to the hydrostatic primary pump P_P through an elastic coupling, which is further connected to a compensation pump C_P that prevents the apparition of cavitation in the primary pump. Primary pump PP generates a flow rate that is directed to the hydrostatic variable displacement motor H_M. By varying the bent axis angle of the axial pistons of the HM, a larger angle of the pistons produces an increase in velocity, while a smaller angle leads to an increase in the pressure of the system and a drop in power. The displacement of the H_M is accomplished using a hydraulic linear motor, which positions is controlled using a 3/2-way proportional directional valve. The hydraulic linear motor is connected to H_M lens plate, which shifting in position leads to a change in the capacity of the motor.
To prevent pressure bursts that could lead to potential damage in the system, relief safety valves have been used, preventing the main branches to develop pressures bigger than 350 bars, case in which the oil is discharged to the tank.
The hydrostatic variable displacement motor H_M is further linked to the load pump L_P, in between the two is placed a velocity sensor that sends feedback to the acquisition board DAQ NI 6211. The L_P output is connected to a proportional relief valve that shrinks proportionally the flow rate section, which leads to a boost in the pressure and respectively in torque in L_P. The increase of L_P torque is transferred to the H_M, were pressure rise in "A" branch.
For precise measurement, 2 pressure sensor are mounted on both branches of the system and a flow rate sensor is mounted on branch "A". The values registered by the sensor are gathered by the DAQ NI 6211 acquisition board that also communicates with the PC. From the acquisition board, control signal is sent to the REXROTH VT11724 analog amplifier module that actuates the H_M displacement control susbystem's proportional valve.
The software used to interface the DAQ NI 6211 acquisition board with the PC is LabView. The PID controller used to control the proportional electromagnet of the hydrostatic motor displacement sub-system is emulated by the LabVIEW programming environment, shown in figure 9, and the system then uses the controller output value to push the process variable toward the setpoint value. The PID controller parameters are generated based on an input/output signal. The control schematics include a feedforward multiply loop for a more precise response. In the context of a PID controller, the term "feedforward" refers to a measurement of the projected future error based on the current error and the system's known behaviour. Feed-forward control is a process to minimise the influence of interference in control circuits. The correcting variable is subjected to a disturbance variable which compensates for interference present in the controlled subsystem by estimating the disturbance variable with an observer and connecting it inversely to the feedback controller. The feedforward is multiplied by the proportional, integral, and derivative gains in this instance to determine the output of the controller, which is then used to adjust the system in order to decrease the error and bring it closer to the desired setpoint and provide a more precise and

prompt response to changes in the system, which can help improve the overall performance of the control system.

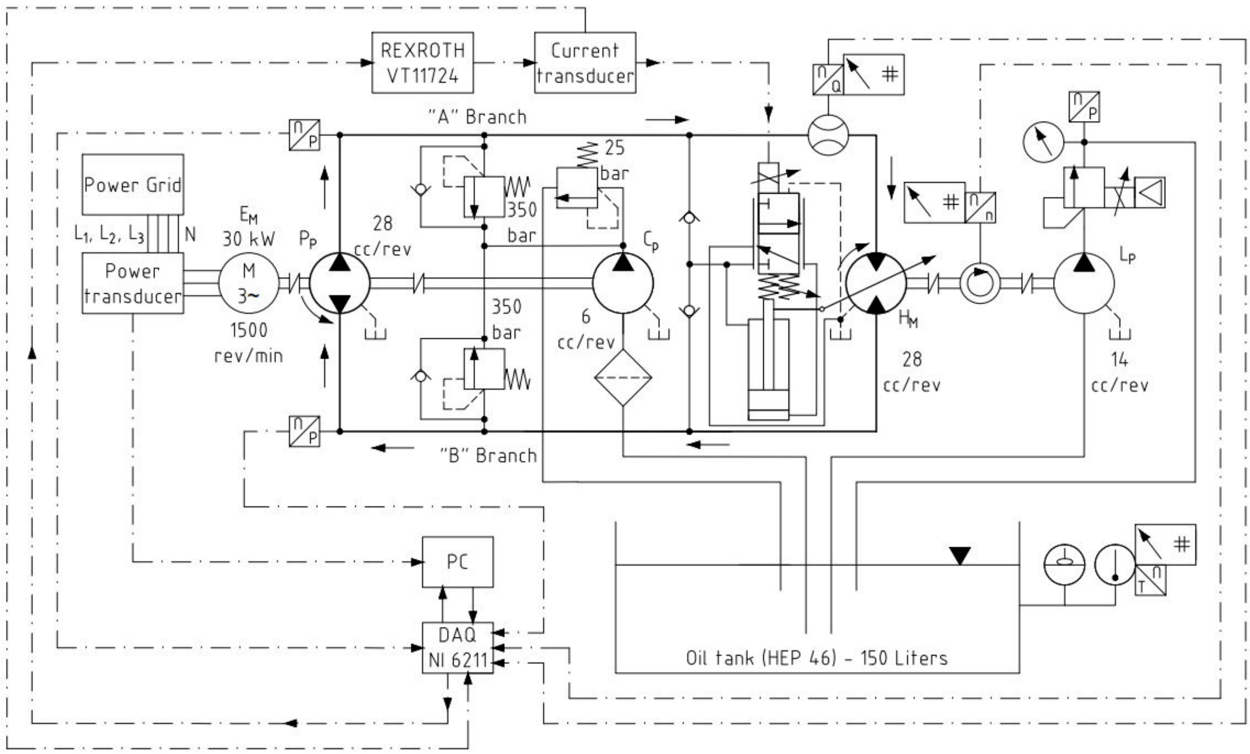

Fig. 8. Hydraulic scheme of the experimental stand for the study of the closed-loop transmission with secondary adjustment and of the servo-mechanism for regulating the motor displacement

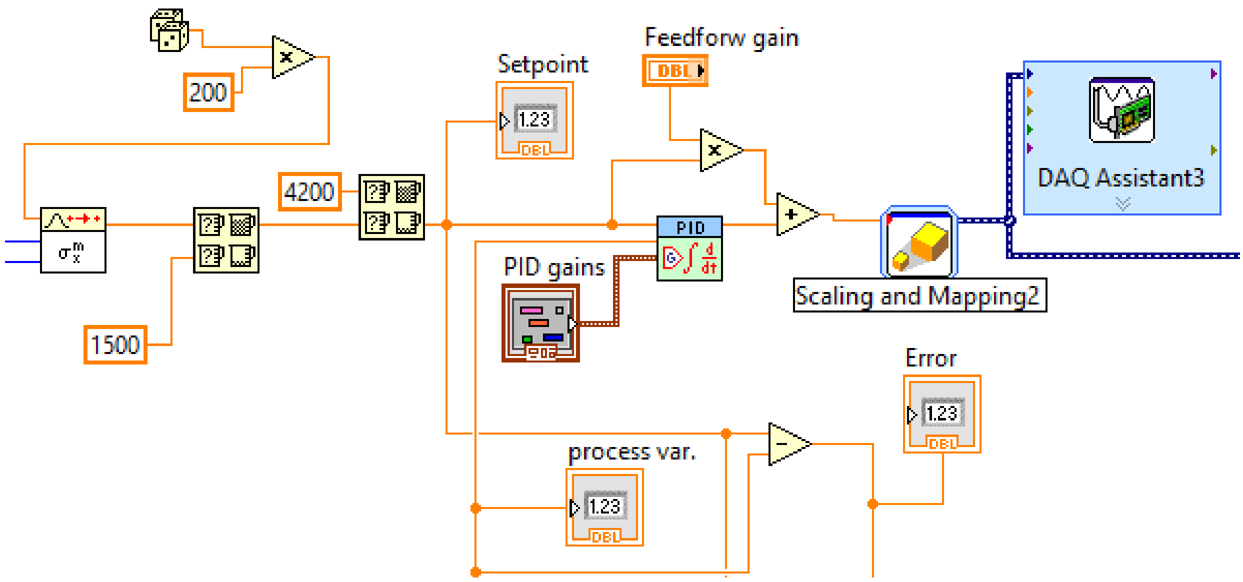

Fig. 9. LabVIEW graphical programming environment network for PID controller with feedforward

3. Experimental results

This chapter presents the results of the experimental testing of the system as described in the chapter 2.2. To vary the load, respectively the torque of the hydrostatic motor H_M, on the load pump L_P circuit, the proportional relief valve vary the flow cross-section. As a result the torque obtained between H_M and L_P is inverse proportional to the opening of the proportional relief valve.

To highlight the performances of the system and the fast response of the control part, the graph presented are over a small time period (25 seconds).
As one can see in the figure 10, the rise time period took 0.75 seconds, after the overshot peak at 1.5 seconds, at 2.5 seconds until the end of the shown period of time, the achieved velocity remained in the interval of the steady-state error within the tolerance band.

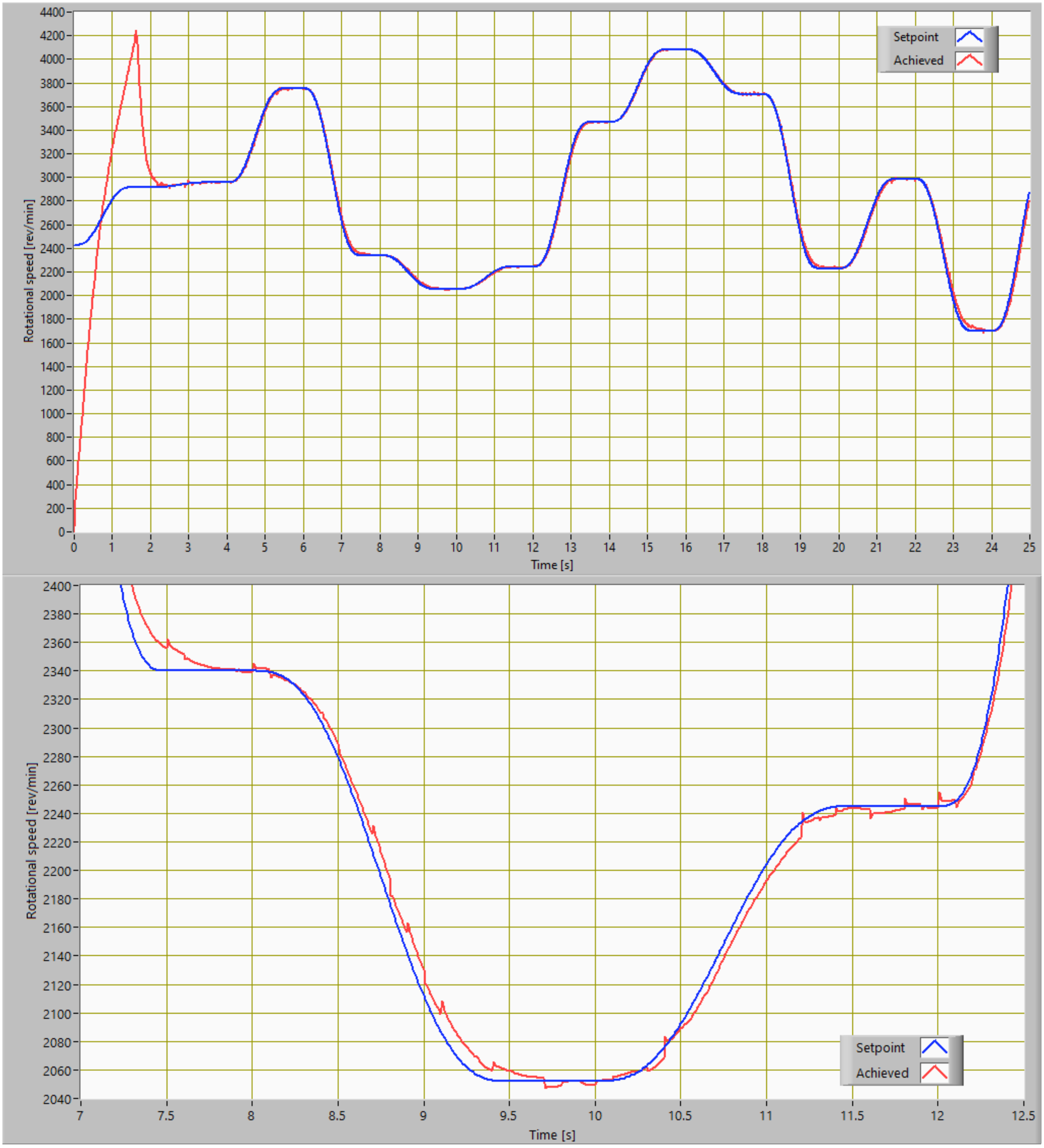

Fig. 10. The setpoint compared to the achieved speed over time

Figure 11 presents the torque produced by the load pump L_P used to mimic the torque variation in an industry application of the SAHT (for example automotive industry). As one can see, the torque varies between 4 and 19 [Nm] values determined by the flow section of the proportional relief valve.

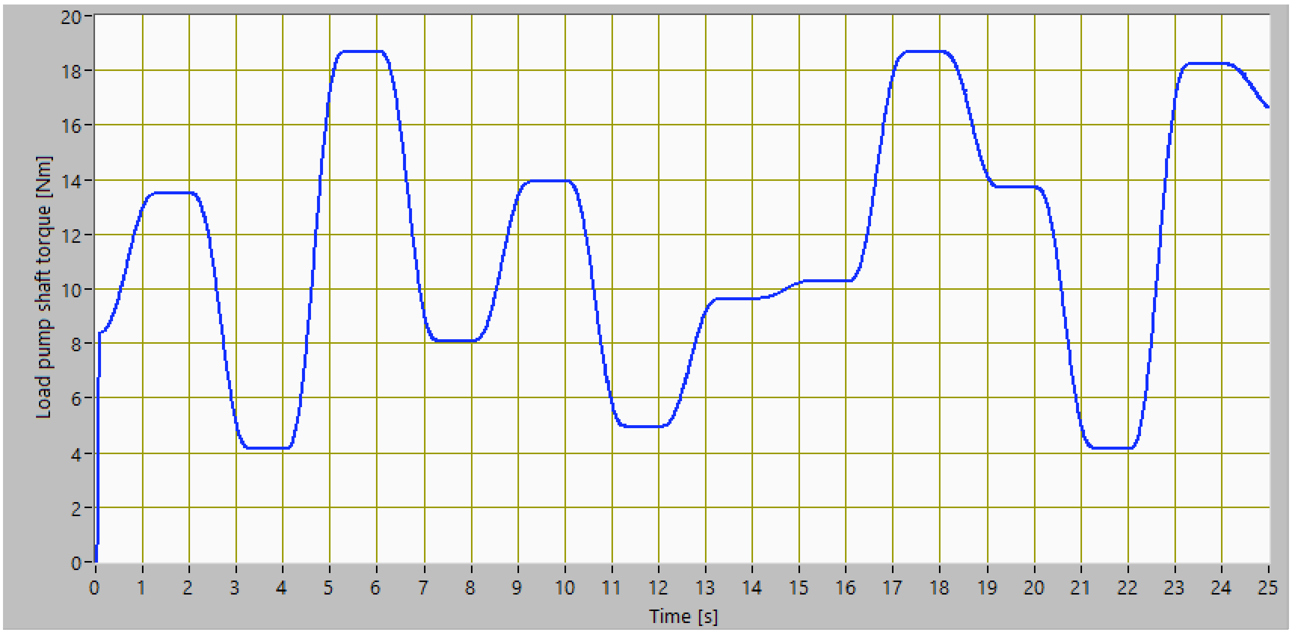

Fig. 11. The load pump shaft torque over time

Figure 12 shows the differential pressure in closed circuit over time (pressure in branch "A" excluding pressure in the branch "B"). This characteristic underlines the direct effect of pressure rises and drops in the load pump L_P to the two main branches of the hydrostatic closed-circuit and shows that smaller pressure in the L_P system (respectively lesser torque) leads to bigger pressure drops in the hydrostatic system. As the pressure in L_P circuit rises, so does the pressure drop in the hydrostatic closed-circuit.

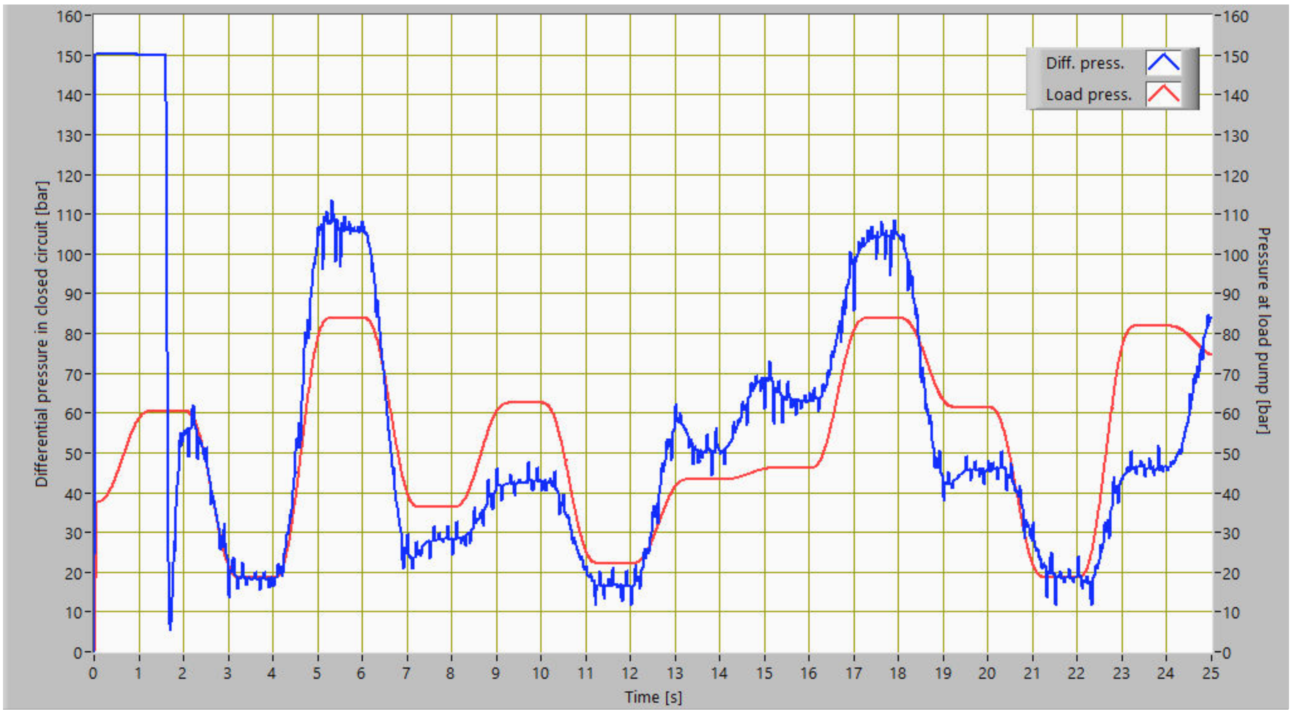

Fig. 12. The load pump shaft torque over time

Figure 13 presents the instantaneous control error and a detail of it. Here the credit of the feedforward multiply loop combined with the PID controller are seen, as the error is almost linear. Compared with the velocity from figure 10, the instantaneous error band is less than ±5%, beside the error generated by the overshot, and also a very fast system response to error.

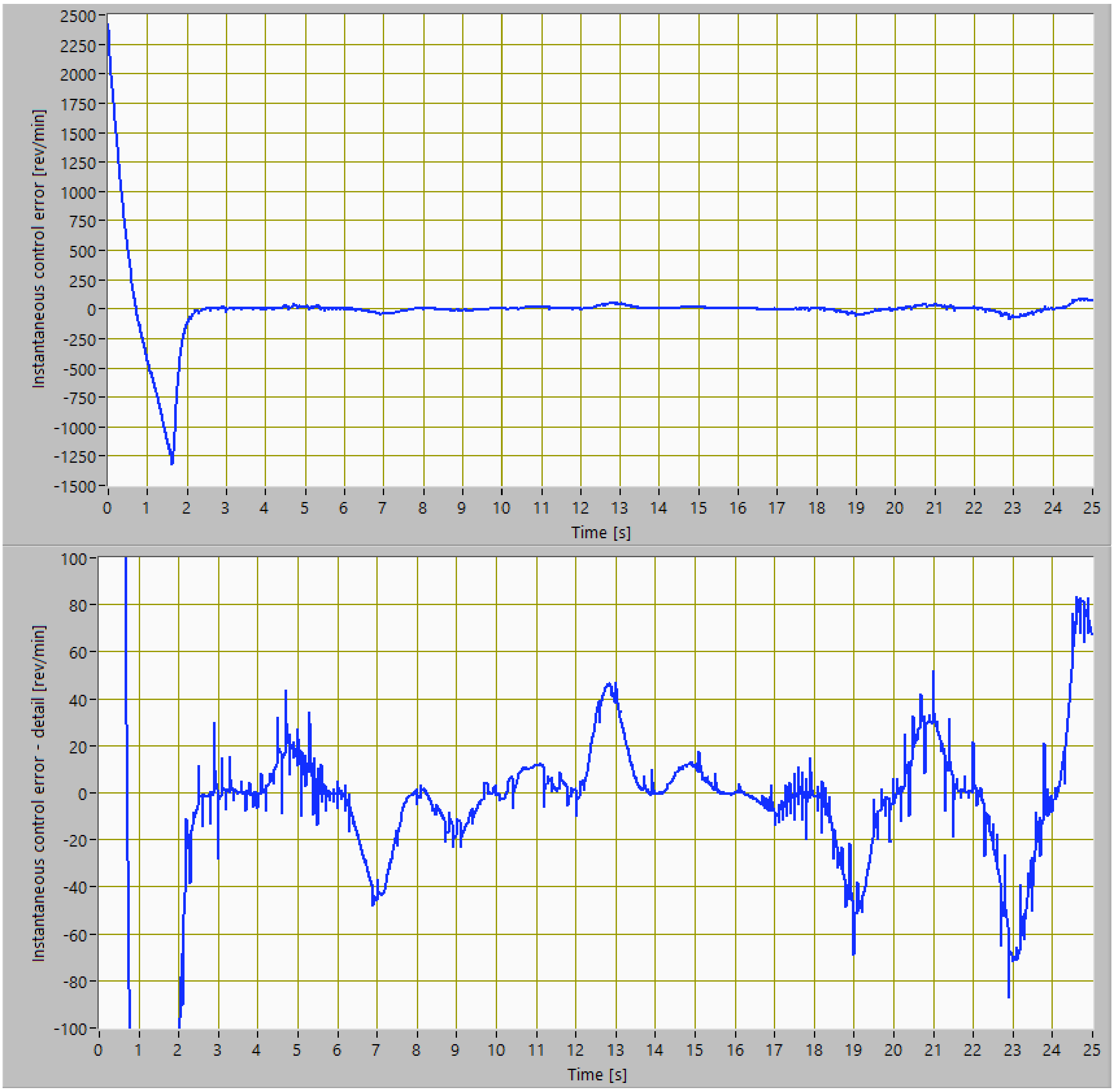

Fig. 13. The instantaneous control error over time

4. Conclusions

This paper developed both a theoretical and experimental system that have been used to emphasise the performances that closed-circuit secondary adjustment hydrostatic transmission can achieve, using the programming environment LabView as an interface between the computer and the acquisition board DAQ NI 6211, that also contain the core components of the control system: the PID controller and the feedforward multiply loop. It has been proven that, using these two together helped lower the control error and the systems response, allowing the velocity of the hydrostatic motor H_M to follow the desired value allows for precise and accurate control of the mechanical device being powered by the motor. This is particularly important in applications where precise and consistent movement is required, such as in manufacturing or other industrial settings. By carefully controlling the velocity of the hydrostatic motor, it is possible to ensure that the mechanical device moves in a consistent and predictable manner, allowing for more efficient and effective operation.

Acknowledgments

This paper has been funded by the Romanian Ministry of Research and Innovation under NUCLEU Programme, Financial Agreement no. 18N/2019, Ad 16/2022, Project code PN 19-18.01.01, Project acronym: OPTRONICA VI, Phase no. 12 titled "Research on the development of intelligent hydraulic control, adjustment and automation methods using standard electronic blocks and specific computer applications". Financial support has also been granted under a project funded by the Ministry of Research, Innovation and Digitalization through Programme 1- Development of the national research & development system, Sub-programme 1.2 - Institutional performance - Projects financing the R&D&I excellence, Financial Agreement no. 18PFE/30.12.2021.

References

[1] Helduser, S. "Electric-Hydrostatic Drive—an Innovative Energy-Saving Power and Motion Control System." *Proceedings of the Institution of Mechanical Engineers, Part I: Journal of Systems and Control Engineering* 213, no. 5 (August 1999): 427–37. https://doi.org/10.1243/0959651991540250.

[2] Hasan, Md. Ehtesham, K. Dasgupta, and Sanjoy Ghoshal. "Comparison of the Efficiency of the High Speed Low Torque Hydrostatic Drives Using Bent Axis Motor: An Experimental Study." *Proceedings of the Institution of Mechanical Engineers, Part E: Journal of Process Mechanical Engineering* 231, no. 4 (December 2015): 650–66. https://doi.org/10.1177/0954408915622413.

[3] INOE 2000-IHP Bucuresti. "Conceptual definition study of secondary control of hydraulic drive systems / Studiu de definire conceptuală a reglajului secundar al sistemelor de acţionare hidraulice." *Project no. 21060/18.09.2007 - "Research on increasing the energy efficiency of hydraulic drive systems, by applying secondary control techniques - EESAHRS." / Proiect nr. 21060/18.09.2007 – "Cercetări privind creşterea eficienţei energetice a sistemelor de acţionare hidraulice, prin aplicarea tehnicilor reglajului secundar – EESAHRS."* Accessed November 10, 2022. https://ihp.ro/program4/2007/EESAHRS/etape_realizate/etapa_I.pdf.

[4] Pandey, Ajit Kumar, Alok Vardhan, and K. Dasgupta. "Theoretical and Experimental Studies of the Steady-State Performance of a Primary and Secondary-Controlled Closed-Circuit Hydrostatic Drive." *Proceedings of the Institution of Mechanical Engineers, Part E: Journal of Process Mechanical Engineering* 233, no. 5 (January 2019): 1024–35. https://doi.org/10.1177/0954408918821779.

[5] ***. "Engineering Essentials: Hydrostatic Transmissions." July 9, 2016. *Power & Motion*. Accessed November 21, 2022. https://www.powermotiontech.com/hydraulics/hydraulic-pumps-motors/article/21882804/engineering-essentials-hydrostatic-transmissions.

[6] Kordak, Rolf. *Hydrostatic drives with control of the secondary unit – The Hydraulic Trainer, Volume 6*. Second edition. Lohr Am Main, Mannesmann Rexroth GmbH, 1996.

[7] Ionescu, Clara M., Michiel Haemers, Anca Maxim, Cosmin Copot, Stijn Derammelaere, and Kurt Stockman. "Automatic Tuning of Predictive Control in a Hydrostatic Drive Train System in Nominal Operation." Paper presented at the 23rd International Conference on System Theory, Control and Computing (ICSTCC 2019), Sinaia, Romania, October 9-11, 2019.

[8] Bosch Rexroth AG. "Secondary Controlled Drives: Dynamic, Efficient, Precise and Versatile." March 2014. Accessed November 16, 2022. https://www.boschrexroth.com/en/xc/trends-and-topics/know-how/secondary-controlled-drives-dynamic-efficient-precise-and-versatile.

[9] Maczyszyn, A. "Method of Sum of Power Losses as a Way for Determining the Ki Coefficients of Energy Losses in Hydraulic Motor." *Polish Maritime Research* 23, no. 2 (April 2016): 57–63. https://doi.org/10.1515/pomr-2016-0021.

[10] Costa, Gustavo, and Nariman Sepehri. *Hydrostatic Transmissions and Actuators. Operation, Modelling and Applications*. Wiley, 2015.

Reliability Analysis and Automation of the Equipment for Pressing Axial Bearings in the Gearboxes

MSc. Eng. **Roxana-Luiza IFRIM**[1], Lect. PhD Eng. **Ioan-Lucian MARCU**[1,2,*], Lect. PhD Eng. **Daniel-Vasile BANYAI**[1,2]

[1] Technical University of Cluj-Napoca, Faculty of Road Vehicles, Mechatronics and Mechanics, Alba Iulia University Extension

[2] Technical University of Cluj-Napoca, Faculty of Road Vehicles, Mechatronics and Mechanics

* Lucian.Marcu@termo.utcluj.ro

Abstract: *This paper aims to highlight the development of industrial modernization of a simple process: the pressing of axial bearings in the gearboxes, which is a crucial step in the assembly process, as it ensures that the bearings are securely fitted and able to withstand the forces that will be applied to them. In the past, this task was performed manually, which was time-consuming and prone to errors. However, with the development of industrial modernization, new methods and technologies have been introduced that make the pressing process more reliable and efficient.*

Keywords: *Axial bearing, gearbox, mechanization, electronic drives*

1. Introduction

Press-fit is an operation whereby a shaft-type part and a bore-type part are brought into the physical state where clamping forces occur between them, to cause the assembly to lock together. Bearings are used to restrain parts that perform rotating or oscillating motions. The following steps must be considered when fitting them:

1. Select the bearings and the other components of the assembly according to the size and the force applied to the assembly.
2. Check the symbolization (radial and/or end shields).
3. Check cracks and bearing.
4. Ensure that the elements to be assembled are correctly positioned.
5. Actual mounting of bearings.
6. Check the clearance, insertion of the shaft into the bearing housing and fitting of the covers.

Manual assembly of an axial bearing inside a gearbox is carried out by an operator or worker and consists of carrying out the assembly operation by hand, without the need for tools. Usually, the parts to be assembled in this way have clips in their construction so that they can be easily pressed or the assembly between the bore and the shaft does not require great pressing forces. Even if it implies low process costs, it comes at the price of low reliability and low process repeatability, and even assembly errors [1-5].
The mechanization of the assembly process aims to replace manual labour with machines, apparatus, stations, tools and mechanisms, etc., to be able to carry out some operations, with the worker being responsible only for adjusting and controlling the action of the machines.
In assembly work, simple mechanization is carried out using tools, devices, and stations, which make work easier or even replace it. It has the advantage of ensuring high productivity and better-quality work carried out. Complex mechanization consists of the introduction of assembly lines on which actual assembly work but also preparatory, auxiliary or finishing work is carried out.
The automation of a process is defined as the installation of devices to ensure that assembly operations are carried out without operator intervention. As the degree of automation increases, so does the need for sensors and actuators (Various types of local networks have been created to communicate between them). To have high-speed connections, closed local systems have been implemented in some facilities, which work for real-time signal processing without delays [4-7].

The operator must be sufficiently and timely informed without errors to make the right decisions. The control panel must be easily accessible and intuitive for easier understanding [8].
Following the results of the research on the state of the art, it has been found that automated operation is the most reliable and improves the pressing process.

Fig. 1. Mechanised vs automated (pneumatic) bearing pressing station

As safety methods, compliance with all rules is an important condition for creating safe machines and systems [9].

2. Material and methods

The most reliable solution analysed was the fully automated one, using a fully autonomous system and with exceptional results provided by Kistler.
It consists of a servo motor assembly with an electric motor connected to a precision ball screw. Inside the assembly, there are a piezoelectric force sensor and a distance sensor.

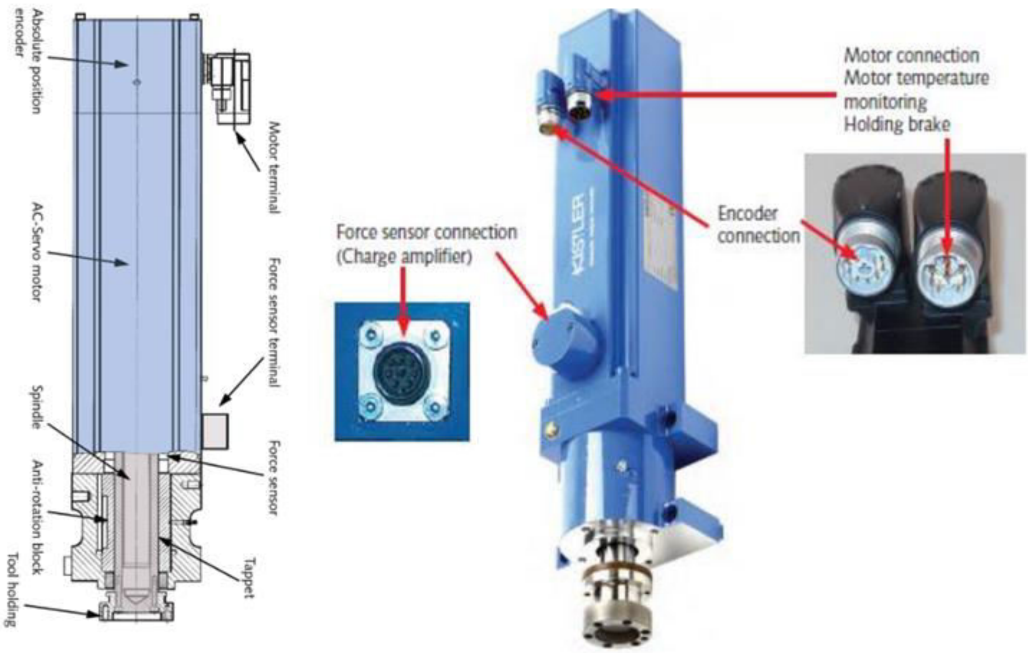

Fig. 2. Kistler pressing system

User communication is via the maXYmos communication interface, which is a PC unit that links the PLC of the station with the control drive of the servo press.

The signals received from the force and distance sensors are interpreted by the interface, and by using user-created pressing windows the system decides whether the pressing process has been performed under the conditions imposed by the user.

Fig. 3. maXYmos communication system

The drive is based on the tubular shaft motor principle. The extremely compact design means that the screw drive passes through both the force sensor and the drive motor.
A specially designed servo motor with high dynamics drives the ball screw, so that the rotation is converted into a forward motion through the integrated ball groove.
The force sensor can absorb compression and tension forces; thus, joining processes with subsequent tensile testing are possible.

3. Results

The pressing process will be determined by the operator (positions, displacement speed rates ...). With integrated process control in the maXYmos NC (fig.3) monitoring and evaluation system, the pressing process is controlled according to the machine and the PLC of the plant.
For this purpose, the pressing sequences (e.g. movement of the press into working position, speed rates, etc.) are parameterized for the pressing process in the maXYmos NC type 5847A monitoring and evaluation system.

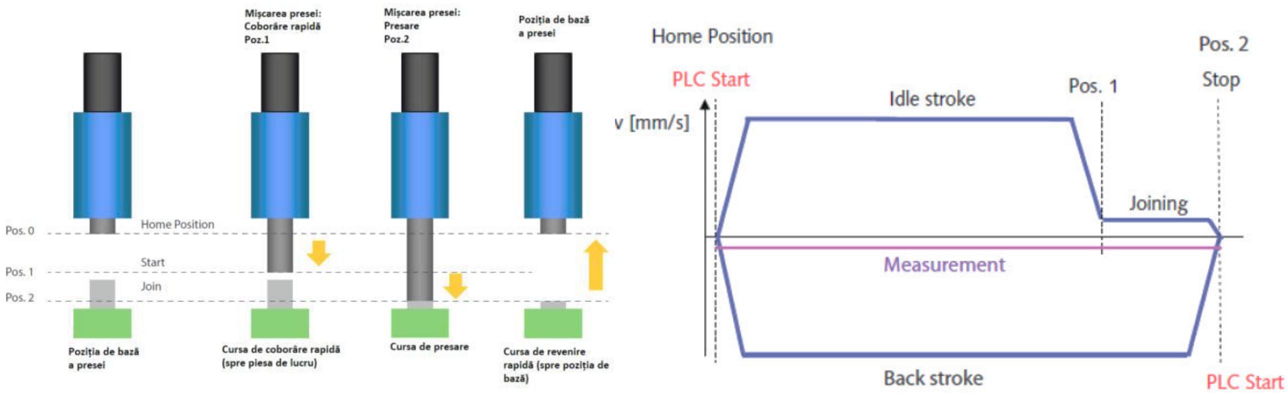

Fig. 4. Diagram of the pressing process

The PLC starts the sequence in "sequence" operating mode. The required speed reduction to the end of the pressing stroke is performed by triggering an error and is reported by the monitor. Now the PLC can start the return stroke to ‘home position’.
Position 0 represents the place of the press that is located at 0 mm, i.e. the press is in the ‘home position’. This position is not editable in automatic operation but is editable only following a repair; the servo press encoder must be taught-in with its mechanical position.
Position 1 represents the distance to which the press descends at full speed (up to 76mm) and from here the pressing process starts at a slower speed until it reaches position 2 (80 mm - maximum pressing point). The measurement process follows and the data is sent to the maXYmos

(maximum pressing force and distance) PLC, and following the pre-set graphs, the measured data are compared; they must correspond to the pressing process data (figure 5). At this point, the maXYmos PLC sends a response to the PLC of the station whether the pressing process has been completed successfully or the part resulting from the process is scrap.

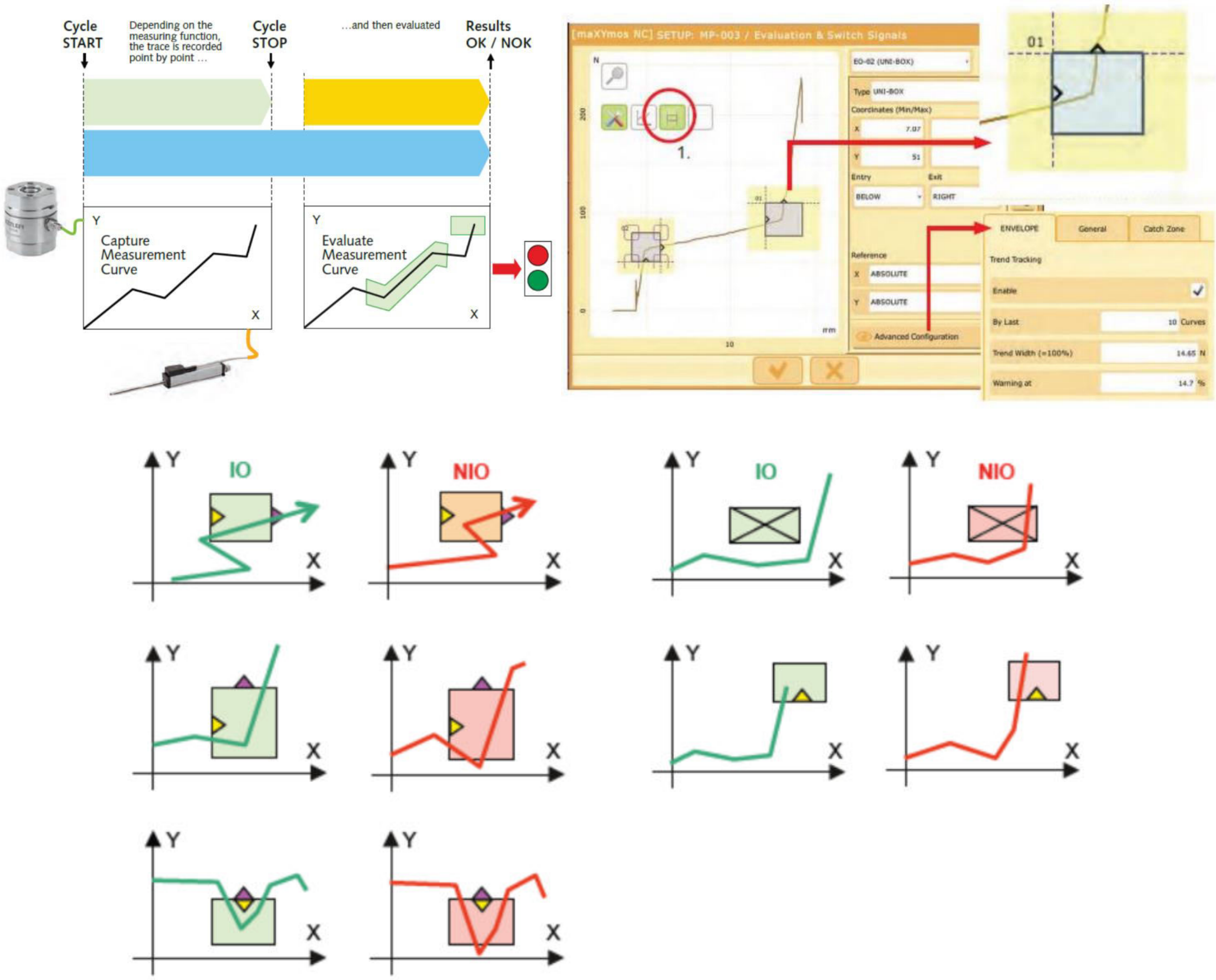

Fig. 5. Scheme of the pressing process evaluation

In the graph on the left, one can see the pressing force and distance, and in the graph on the right, the results are interpolated over the reference values of pressing. If the results of the pressing do not fall between the set limit values of the reference graph, the pressing result is NOK (NOT OK), and the pressing was not performed properly.
Catch zones are positioned around a particular EO (programs) in different ways, depending on the specified input and output configuration. When the EO configuration is complete, tap the "Show catch zone" button (see figure 5). The catch zones now appear on the graph as yellow areas.
ENTRY and EXIT process values are caught when they intersect BOX lines defined as the input and output sides and from there along their extensions (marked with broken lines) to the boundary of the catch zone.
The process values for the vertical reference lines will be Y values, and for the horizontal lines will be X values.
The measurement curve shall enter once through the specified input side and exit once through the specified output side. Any part can be specified as an input or output part.
The first point at which the curve crosses the boundary of a box is the input event, and the next to intersect a box boundary is the exit event.

How UNI-BOX process values are delivered depends on the configuration used. The best way to view them for a particular EO is by selecting Process View, Value table. These process values can either be subsequently displayed in the PROCESS value table or transferred via the Fieldbus.

INPUT - Process value

This is caught at the point where the curve intersects the first box line designated as the INPUT side and from there to the boundary of the catch zone (the extended input line). A value will only be generated if an input side has been defined.

EXIT - Process value

This is caught at the point where the curve intersects the first box line designated as the EXIT side and from there to the boundary of the catch zone (the extended exit line). A value will only be generated if an exit side has been defined.

Fig. 6. Pressing station after modification/ Port bearing piece/ Starting and ending of the pressing process

4. Conclusions

- The new pressing concept has meant major changes in terms of station reliability, quality and safety of the pressing process. Analysis results prove that the process has been improved.
- From the point of view of plant maintenance, the maintenance of the equipment is very easy to carry out, as the system is a simple construction.
- Preventive maintenance (checking visual, greasing and functional checks) can only be carried out by maintenance staff with the help of instructions and maintenance plans from the equipment supplier.
- While automation may require a higher initial investment, it can save money in the long run by reducing the need for labour and increasing the output of the assembly line. Automated systems are also flexible and can be easily adjusted to handle different types of parts or assembly tasks.
- In summary, the use of automation in the assembly process can improve the reliability, repeatability, and quality of the final product, while increasing productivity and efficiency. While it may require a higher initial investment, the long-term benefits of automation make it a worthwhile consideration for any company looking to improve its assembly process.

References

[1] ***. "Technological Assembly Processes in Machine Building." / "Procese Tehnologice de Montaj in Constructia de Masini." *Scribd*. Accessed November 15, 2022. https://ro.scribd.com/doc/266894717/Procese-Tehnologice-de-Montaj-in-Constructia-de-Masini.

[2] ***. "General Concepts of Automation, Cybernetization and Robotization of Technological Processes. 4.1 Automation of Technological Processes." / "Noţiuni generale de automatizare, cibernetizarea şi

robotizarea proceselor tehnologice. 4.1 Automatizarea Proceselor Tehnologice." Accessed November 14, 2022. https://www.academia.edu/33538514/NO%C5%A2IUNI_GENERALE_DE_AUTOMATIZARE_CIBERNETIZAREA_%C5%9EI_ROBOTIZAREA_PROCESELOR_TEHNOLOGICE_4_1_Automatizarea_proceselor_tehnologice.
[3] ***. "Bearings. Mounting with bearings." / "Rulmenti. Montaje cu rulmenti." *Scribd*. Accessed November 14, 2022. https://ro.scribd.com/doc/27203049/6-Rulmen%C5%A2i-Montaje-Cu-Rulmen%C5%A2i.
[4] ***. "Bearings. General Info." / "Rulmenti. Informatii generale." Accessed November 15, 2022. http://urb-s.ro/products/docs/Rulmenti_info_general.pdf.
[5] Jula, Aurel, and Mihai Lateş. *Machine Parts* / *Organe de maşini*. "Chapter 6. Rolling bearing cases." / "Capitolul 6. Lagăre cu rulmenți." Braşov, Transilvania University Publishing House, 2004.
[6] NTN-SNR Rulmenti - Romania. "Bearing Mounting." / "Montarea Rulmenților." Accessed November 15, 2022. https://www.ntn-snr.com/ro/montarea-rulmentilor.
[7] ***. "Mechanisation and Automation of Assembly Work." / "Mecanizarea si automatizarea lucrarilor de asamblare." *ePedia*. Accessed November 15, 2022. https://epedia.ro/2012/02/16/mecanizarea-si-automatizarea-lucrarilor-de-asamblare/.
[8] ***. "Industrial Automation." / "Automatizare Industrială." *Wikipedia*. Last modified October 29, 2022. Accessed November 15, 2022. https://ro.wikipedia.org/wiki/Automatizare_industrial%C4%83.
[9] Kistler Group. "Servo presses." Accessed November 15, 2022. https://www.kistler.com/INT/en/servo-presses/C00000153.

Some Pressure Drops Characteristics for Pressure Valves Operation within the Hydraulic Circuit

Associate Professor **Fănel Dorel ȘCHEAUA**[1,*]

[1] "Dunărea de Jos" University of Galați, Romania

* fanel.scheaua@ugal.ro

Abstract: *At present time, most machines and equipment in the industry use hydraulic actuation to ensure the fulfilment of the required work process. It represents a force system that successfully copes with the demands that the actuation of any working organ implies, but which must be well dimensioned and protected against overloads by means of protective equipment. The pressure valves represent protection elements of the hydraulic circuit against pressure peaks formed on the network as a result of some unpredictable external factors. Being offered in different constructive variants, the valves ensure several functions in addition to the protection function of the hydraulic circuit, such as pressure reduction, sequential, unloading or balancing. Constructive models can be normally closed or normally open, as is the case with pressure reduction valves. Some constructive solutions of valves, directly operated and pilot operated, are presented as well as some specific characteristics of these devices presented in terms of flow rate and pressure drops that usually occurs when they are installed in the circuit function of pressure stages registered during the installation operation.*

Keywords: *Hydraulic actuation, pressure valve, flow rate, pressure drop*

1. Introduction

The hydraulic actuation system has proven its efficiency in most applications in all industrial branches so far, being used mainly where force is needed to perform various tasks that are difficult to achieve by means of other drive types.
But this actuation type, based mainly on the working fluid circulation in terms of volumetric flow rate at high pressure values represents an assembly that must be very well dimensioned and made up according to the requirements for which it is intended to meet, because all component elements of the force circuit are strongly stressed by the hydrostatic forces that are inevitably formed because of high-pressure values within the system.
In this sense, in addition to the prior dimensioning of the circuit elements, the working pressure values at which the system is designed to operate must also be conditioned, so that any pressure peaks beyond of these values to be discharged to the tank in such a way as to protect the constituent elements of the network. This objective is ensured by means of pressure valves, which are primarily circuit protection devices in addition to the main function of regulating pressure values.
Devices for regulating pressure values are present in all hydraulic actuation systems, thus having the possibility to perform a wide variety of functions such as ensuring an imposed limited pressure value, up to ensuring a certain pressure value on a certain portion of the circuit that is required to operate a circuit component.
The main groups of pressure valves are represented by safety valves, pressure relief valves, sequence valves, discharge valves, connecting or disconnecting from the circuit of an apparatus, or balancing valves. Regarding the functional model, pressure valves are differentiated as normally open or normally closed versions.
Like any device that is added to the hydraulic circuit, pressure valves can induce a pressure drop in the system, which is usually presented for the pressure groups at which the valve operates, and by the volumetric flow rates of the circulating working fluid. These specific characteristics are presented in this paper for four groups of working pressures to highlight the dissipative aspect when introducing these pressure regulators into the hydraulic network.

2. Constructive solutions for pressure valves

Since the operation of the hydraulic drive circuit involves a continuous operation of the pump, the pressure value of the working fluid may exceed certain values that would endanger the integrity of the system at some moment in time if the working body encounter a resistance in operation for example that can lead to the hydraulic motor stop. This aspect is remedied by using pressure valves which, by adding to the hydraulic circuit, have the possibility to protect the hydraulic circuit from pressure peaks.
This is the reason why the design engineers of the hydraulic installation consider the inclusion of protective elements on the circuit that have the role of adjusting the pressure values of the working agent in order to avoid hydraulic system damage.
The use of pressure valves ensures a direct control of applied force at the circuit working body obtained at a reasonable level of working pressure. Other benefits of using pressure valves are represented by ensuring the sequential operation of the hydraulic actuators, limiting the pressure values to a safety level in operation, reducing the pressure values in the main circuit to ensure the operation of an auxiliary circuit, adjusting the pressure on certain portions of the circuit and discharge of pressure peaks at a given time.
A pressure relief valve direct operated is schematically presented in figure 1. The closing element is kept in position by means of a spring, while the valve opening can be done based on the hydrostatic pressure forces values that are formed on the front surface of the closing element, when the system pressure is able to overcome the elastic force in the spring. It represents a normal closed constructive pressure valve model.

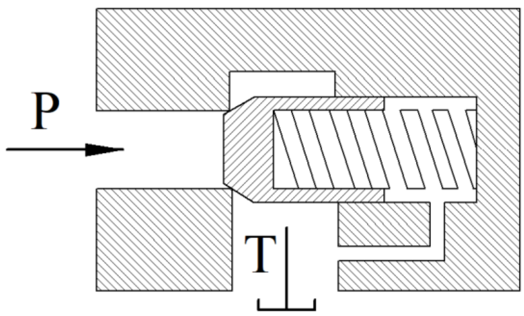

Fig. 1. Pre-set direct operated pressure relief valve

The constructive models of pressure relief valves have the possibility of limiting the ceiling pressure in a hydraulic circuit by creating an alternate path for fluid flow when a certain regulated pressure level is reached. It protects the system from having excess pressure as what is required in all fixed-volume pump circuits. Relief valves are important when actuators stall with the still-in-shifted-position directional valves.
The counterbalance valve protects the hydraulic system from line failure, pressure shocks, enabling the free fluid flow on a certain direction.
Being used for adjusting the pressure values within hydraulic circuit parts, the pressure-reducing valves are actuated by the pressure flowing downstream that tends to close as it reaches valve setting. They are usually used with a check valve that also enables the reversal fluid flow.
The unloading valve is used to send the excess fluid to the tank, at low pressure values.
These constructive variants are used mainly within high-low pump circuits, where there are two pumps that move an actuator at low pressure and high speed. So, the circuit can be positioned on a single pump, giving off high pressure to do the work.
The unloading pressure valves ensure the excess fluid circulation to the tank, especially for the situations of cylinder rod retraction.
The construction model corresponding to a pressure valve device is constituted by a body with inward orifices necessary for the circulation of the working fluid between the active plant branches and a valve closing/opening element maintained in the closed state by means of a compression

spring which ensures the blocking of the circulation fluid flow to the tank if the pressure value is within the parameters for which the system is operating safely.
When the pressure value rises above the value set on the valve (spring elastic force value), the locking piece is moved from the initial locking position by means of the action of hydrostatic forces, at which point the working fluid can circulate behind the enclosure being directed to the system tank, reducing the momentary pressure value in the system to the initial value.
Once the pressure value has been lowered, the closure element is again moved to the initial position, ensuring the closure of the fluid drainage orifices, which is maintained until a further increase in the system pressure value when the recovery cycle is achieved.
The constructive principle of a pressure relief valve direct operated with the possibility to adjust the pressure level is presented in figure 2.

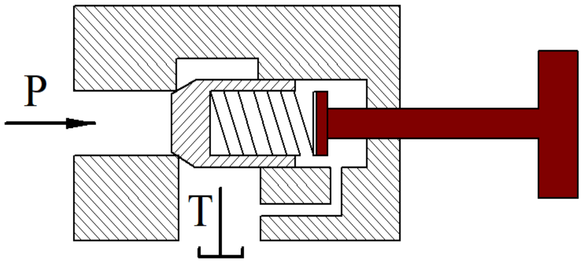

Fig. 2. Pressure relief valve direct operated with the possibility to adjust the pressure level

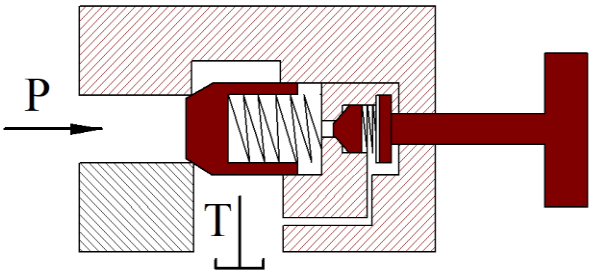

Fig. 3. Pilot operated relief valve

For the pilot operated pressure valve version, it is considered a higher circulating fluid flow rate, higher pressure values and is adopted for a stable operation that does not induce vibrations and wear of the valve closing member. It thus presents a more complex construction (figure 3), consisting in principle of two distinct components: a directly controlled valve called a pilot and an execution valve or the main valve, while the connections between the two assembly components being made in the overall body of the two devices.
During the operation of the pressure valve inside the hydraulic circuit the hydrostatic pressure forces are considered (F_h), which acts directly on the blocking element part determining a displacement and the discharge opening surface (*A*), enabling the working fluid return to the tank.
The necessary mechanical work (L_h) for the closure element movement inside the pressure valve is force and displacement dependent, for which a hydraulic fluid volume (*V*) is circulated, which also enters in calculating the required energy amount raised at the momentary pressure value. 000

$$F_h = p \cdot A \tag{1}$$

$$L_h = p \cdot A \cdot s_a \tag{2}$$

$$V = A \cdot s_a \tag{3}$$

$$E = V \cdot p \tag{4}$$

The movement resistances at the closure element are constituted by the compression spring elastic force which is acting directly on the pressure valve locking element to maintain the pressed position.
The spring elastic force (F_a) can be described as compression spring constant (c_a) combined with displacement value (s_a) which is achieved when the spring is compressed due to the hydrostatic forces action: 0

$$F_a = s_a \cdot c_a \tag{5}$$

$$F_a = \frac{G \cdot d_w^4 \cdot s_a}{8 \cdot D_a \cdot n} \tag{6}$$

$$s_a = \frac{8 \cdot D^3 \cdot F_a \cdot n}{d^4 \cdot G} \tag{7}$$

where:
D_a - spring average diameter;
d_w - spring wire diameter;
G – shear modulus;
n - spiral number.

The functioning stages for the pressure valves are acquired according with the involved forces values. Thus, when the hydrostatic pressure forces are lower than the spring force value the pressure valve remains closed and when this value exceeds the spring elastic force value, the valve opens and sends the working fluid excess direct to the tank, while the momentary pressure peak value of the system is discharged.

$$\begin{cases} F_h < F_a & -\mathrm{Pr}\,essure\ Valve\ Closed \\ F_h > F_a & -\mathrm{Pr}\,essure\ Valve\ Open \end{cases}$$

In general, the pressure valve models are normally closed, being activated only when the system high pressure values arise. If the hydraulic circuit would not have such a protective component mounted, the pressure would increase up to the energy limit of the pumping group and ultimately produce damage to one of the system components (breakdown of the hydraulic ducts, destruction of the distributor, etc.). 0

3. Pressure drop characteristics

For the pressure valves used within the working hydraulic circuit, the information is mainly provided regarding the main parameters that must be considered for the adoption and use of the constructive model in the respective installation. These parameters relate to set pressure values and pressure drop.
Adjusting the pressure level by means of a certain valve is achieved by lamination of the working fluid as it passes through a device section. This process is always accompanied by energy losses due to the decrease in the pressure value when the working fluid circulates between the pressure source and the pressure signal receiver.
The pressure valves characteristics are thus presented by means of specific diagrams for each constructive valve size that define the specific values of pressure drop and volumetric flow rate for different working pressure steps (figure 4).

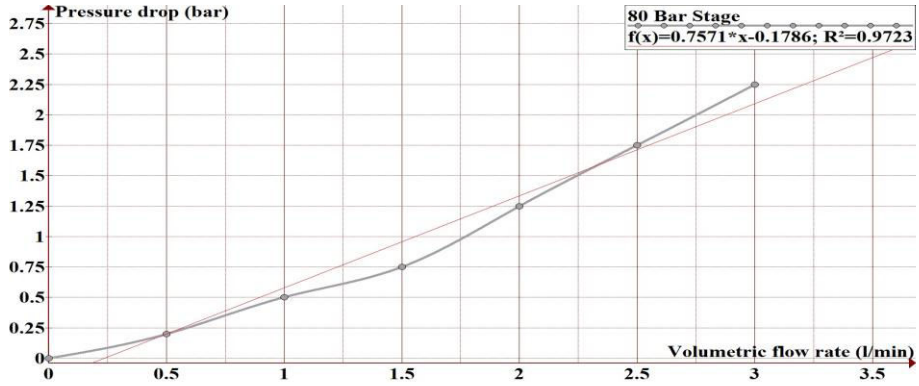

a) Pressure drop characteristic for 80 bar stage

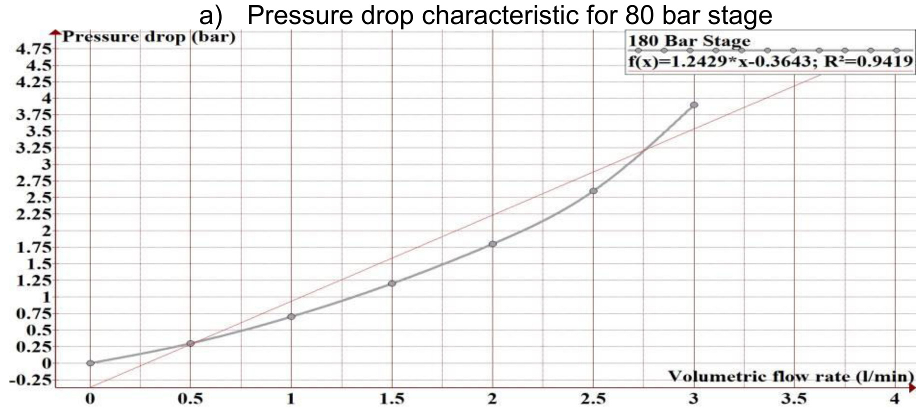

b) Pressure drop characteristic for 180 bar stage

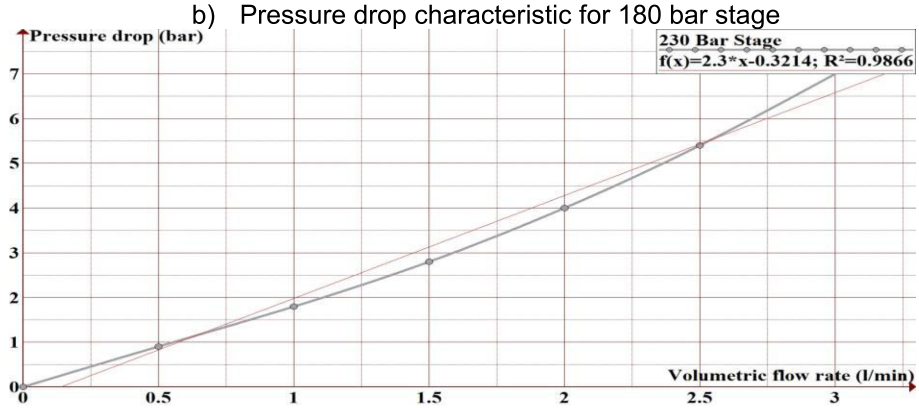

c) Pressure drop characteristic for 230 bar stage

Fig. 4. Pressure valve characteristics for three pressure stages

The pressure signal that can perform the displacement of the locking element, initially being in a closed position, is taken from the main circuit powered by the pump. It is the compression spring constant that determines the adjusted value of the pressure required to open the pressure valve. Also, such pressure valves models benefit from the adjusting system, needed to pre-set the pressure value at which the valve can be opened and for higher circulation fluid flow rates, for which case constructive models with pilot are used.

The pressure valves are used in circuits at pressure values in the range of 315-630 bar and fluid flow rates of 80-330 l/min, but pilot operated construction variants are capable to circulate higher flow rates values of up to 650 l/min.

4. Conclusions

The operation of a working hydraulic circuit involves a continuous flow rate of working fluid agent transported due to the pump action at certain values of the working pressure.

In order to protect the circuit from overload, to disconnect or connect a certain component to the network, valves specially designed to perform these operations in the circuit are needed.

The principle solutions of the directly operated and pilot operated pressure valves are presented, highlighting the efforts to which they are subjected for operation.
Also, some functional characteristics of the pressure valves have been presented in this paper to highlight the pressure drops that are recorded when such a component is added to the network or the working hydraulic circuit.
The presented characteristics are for three groups of working pressures at which the installation can work, being exemplified steps of low, medium and higher pressure values, being shown the pressure drops according to the volumetric flow rate transported.
It is thus possible to identify the dissipative character of these devices when working in the network, given the fact that there is an energy consumption for using these devices in the network, which increases exponentially with the volumetric flow rate, and the values can be identified on the three pressure steps that are shown.
It can be said that these devices are constituted as a resistance that appears in the way of the flow of the working fluid in the hydraulic circuit, being quantified to the total of the resistances that appear in operation that must be defeated by the system pump, which provides the nominal flow rate of the network at the nominal pressure.
Given the fact that the pump works continuously, the surplus fluid flow rate that contributes to the rise of the pressure values at a given moment is discharged to the tank by means of the discharge valves, or if it is about the connection valves they can come into operation and feed a circuit branch when the pre-set pressure value is reached. The same situation happens for the case of disconnection of a network element.
The role of the pressure valves is a special one within the operation of the hydraulic actuation circuit precisely through the multiple possibilities that ensure the functionality and reliability of the system once they are well established and sized for certain applications with specific usage requirements.

References

[1] Axinti, S., and F. D. Scheaua. *Introduction to industrial hydraulics* / *Introducere în hidraulica industrială*. Galati, Galati University Press, 2015.
[2] Axinti, G., and A. S. Axinti. *Hydraulic and pneumatic drives* / *Acţionări hidraulice şi pneumatice*. Vol I-V. Chişinău, Tehnica-Info Publishing House, 2008-2012.
[3] Scheaua, F. D. "Functional description of a hydraulic throttle valve operating inside a hydraulic circuit." *Hidraulica Magazine*, no. 1 (March 2016): 47-50.
[4] Scheaua, F. D. "Theoretical aspects regarding the pressure safety valves operation within a hydraulic circuit." *Hidraulica Magazine*, no. 1 (March 2018): 65-70.
[5] HENNLICH S.R.L. "Compression springs." / "Arcuri de compresiune." Accessed November 14, 2022. https://www.hennlich.ro/fileadmin/_migrated/ro_arc_compresiune.pdf.
[6] ***. "Engineering Essentials: Pressure-Control Valves." *Power & Motion*. January 1, 2012. Accessed November 14, 2022. https://www.powermotiontech.com/hydraulics/hydraulic-valves/article/21884995/engineering-essentials-pressurecontrol-valves.
[7] Master Mac 2000 Pty. Ltd. "The Role of Pressure Control Valves in Hydraulic Systems." Accessed November 15, 2022. https://mastermac2000.com.au/role-pressure-control-valves-hydraulic-systems/.

An Overview of the Linear Drive with Solenoid Coupling

Prof. PhD. Eng. **Viorel PANAITESCU**[1], PhD. Eng. **Tiberiu AXINTE**[2,*],
Dipl. eng. **Victor BĂDĂNĂU**[2], Dipl. eng. **Camelia PASCU**[2]

[1] Constanta Maritime University, Romania

[2] Research and Innovation Center for Navy, Romania

* tibi_axinte@yahoo.com

Abstract: *The paper presents an overview of the economic efficiency for linear drive with solenoid coupling. Moreover, the linear drive with solenoid coupling is also a pneumatic device. Thereby in this article, we are studying two pneumatic and one electro-pneumatic installation, which contains the linear drive with solenoid coupling. The first pneumatic circuit contains the following devices: compressed air supply, start-up valve with filter control valve, 4/2-way valve with spring, throttle valves, linear drive with solenoid coupling (LD 1-1). The second pneumatic circuit contains the following components: linear drives, throttle valves, 5/2-way valve, air service unit, compressed air supply. The last circuit which is actually an electro-hydraulic circuit contains the following components: compressed air supply, 5/2-way solenoid valve with spring, linear drive with solenoid coupling (LD 3-1), relays, valves solenoid and magnetic proximity switch.*

Keywords: *Linear, drive, solenoid, coupling, magnetic*

1. Introduction

The linear drive with solenoid coupling is an actuator that creates motion in a straight line. At the linear drive with solenoid coupling, the loads can be directly mounted on the slide.

Fig. 1. Linear drive with solenoid coupling

Adjustable parameters and symbol of multiple position cylinder are shown in the table below and in Fig. 2.

Table 1: Adjustable parameters of linear drive

Designation	Range	Value	Unit
Piston diameter	$10^{-3}...1$	$4\cdot10^{-2}$	m
Piston rod diameter	$10^{-3}...1$	$6\cdot10^{-3}$	m
Total stroke	$10^{-3}...2$	$2\cdot10^{-1}$	m
Piston position	$10^{-3}...5$	0	m
Damping length	$10^{-3}...10^{-1}$	0	m

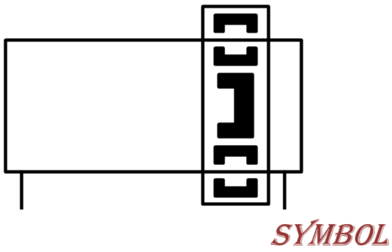

Fig. 2. Linear drive with solenoid coupling - Symbol

In the design of pneumatic or electro-pneumatic installations, the linear drive with solenoid coupling is represented by a specific symbol [1].
For linear drives with solenoid coupling three types of depreciation are available:
- elastic cushioning;
- pneumatic cushioning;
- hydraulic cushioning.

However, in this manuscript we only study actuators that contain pneumatic cushioning.

2. The linear drive with solenoid coupling in circuits

As an actuator, the linear drive with solenoid coupling can be easily monted according to needs in various pneumatic and electro-pneumatic installations [2].
The first pneumatic circuit made in this paper is designed as a simple pneumatic scheme which contains the linear drive with solenoid coupling, Fig. 3.

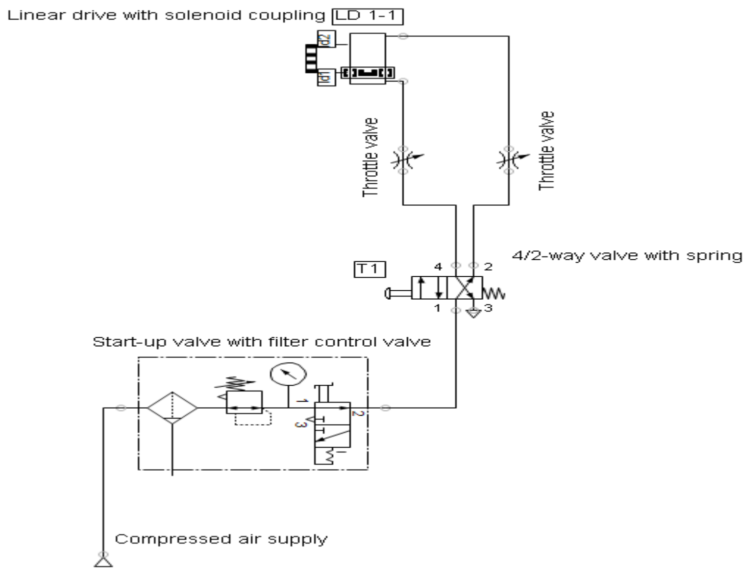

Fig. 3. Pneumatic scheme with linear drive (LD 1-1)

In the table below there are given six devices used in the pneumatic scheme, [3].

Table 2: The devices of first pneumatic circuit

Description	Number of components
Compressed air supply	1
Start-up valve with filter control valve	1
4/2-way valve with spring	1
Thtrottle valve	2
Linear drive with solenoid coupling (LD 1-1)	1

The 4/2 – way directional control valve with spring makes the connection between start-up valve with filter control valve and throttle valves, Fig. 4.
If the operator presses T1 button; this button belongs to the 4/2 - way solenoid valve with spring, [4].
Then, piston rod moves from point Id1 to point Id2. After that, those both piston rods returns from point Id2 to point Id1, because the 5/2 way valve has a spring, Fig. 4.

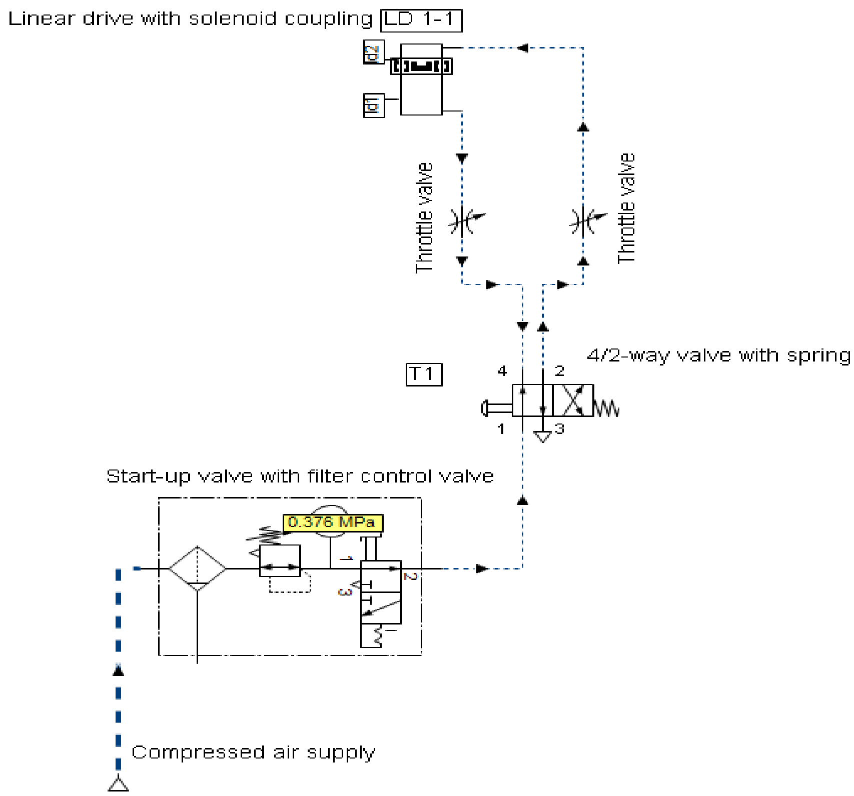

Fig. 4. Pneumatic scheme with linear drive (LD 1-1)

The parameters of linear drive with solenoid coupling (LD 1-1) are: position (x), velocity (v) and acceleration, Fig. 5.

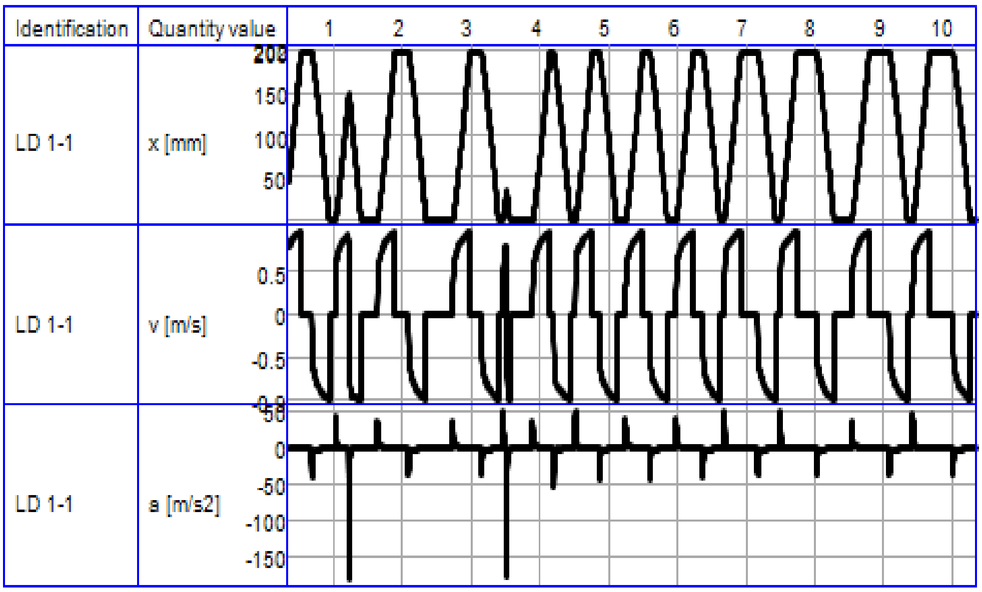

Fig. 5. The diagrams of linear drive with solenoid coupling (LD 1-1)

The second pneumatic installation holds two linear drives (LD 2-1 and 2-2), Fig. 6.
The 5/2 – way directional control valve with spring makes the connection between start-up valve with filter control valve and throttle valves, Fig. 6.

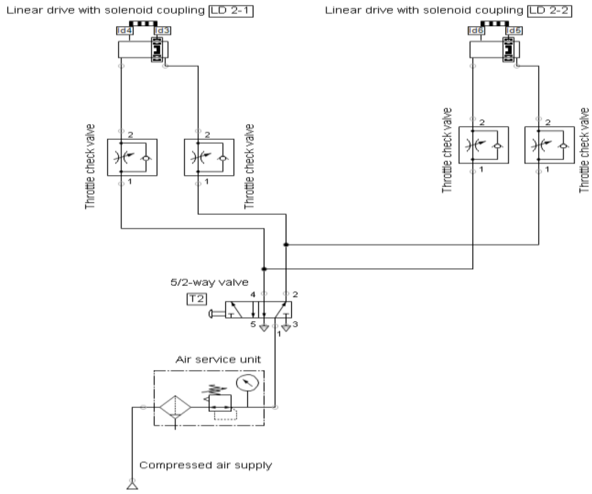

Fig. 6. Pneumatic circuit with a two linear drives

The simple pneumatic system with two linear actuators (LD 2-1 and LD 2-2) have the following eleven devices listed in the table below, [5].

Table 3: The devices of the second pneumatic circuit

Description	Number of components
Linear drives	2
Throttle valves	4
5/2-way valve	1
Air service unit	1
Compressed air supply	1

The second pneumatic circuit with linear drives opens if the operator presses T2 button from 5/2-way valve, Fig. 7.

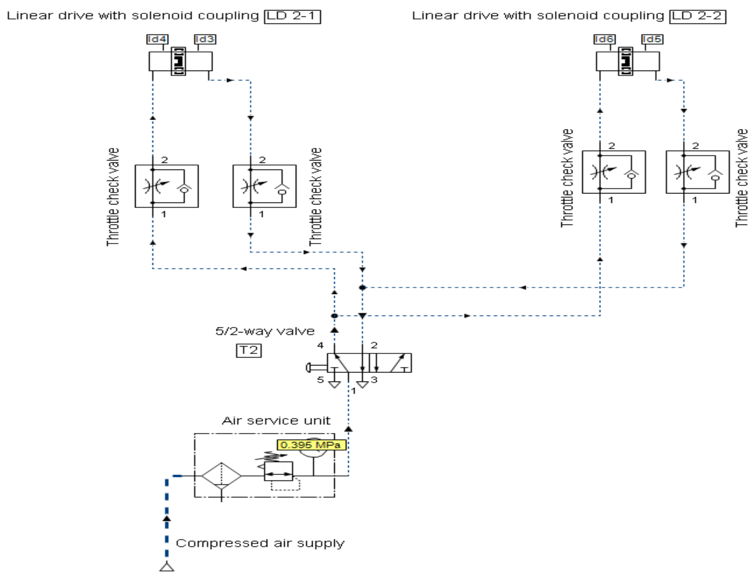

Fig. 7. Pneumatic circuit with two linear drives. Simulation I

Therefore, the piston rod of the linear drive (LD 2-1) moves from point Id3 to point Id4. After three seconds, the piston rod of the linear drive (LD 2-2) moves from point Id5 to point Id6, Fig. 8.

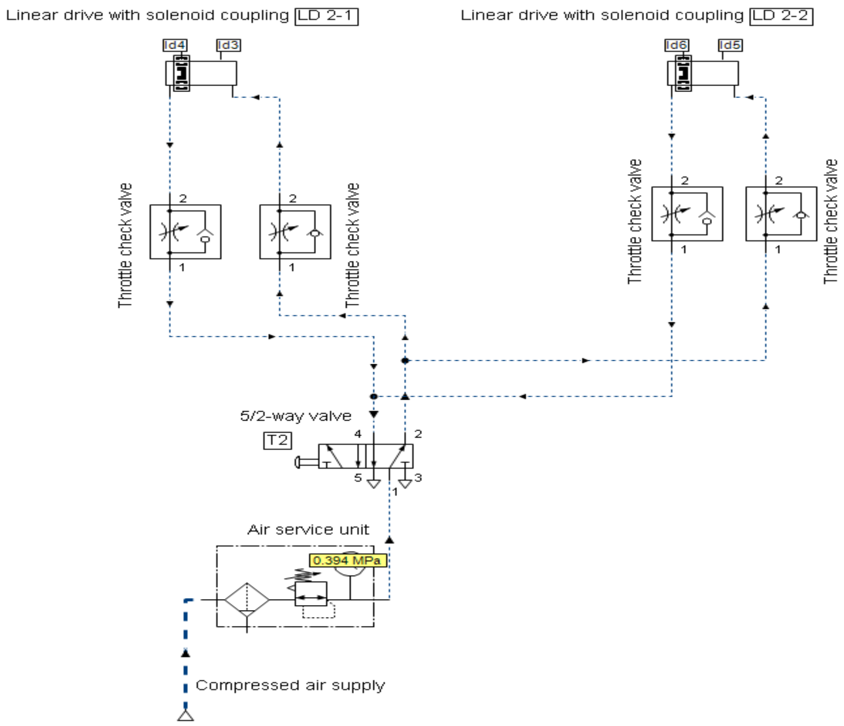

Fig. 8. Pneumatic circuit with two linear drives. Simulation II

If the operator presses T2 button again, the piston rod of the linear drive (LD 2-1) moves from point id4 to point Id3, [6].
Also, the piston rod of the linear drive (LD 2-2) moves from point Id6 to point Id5. With electro-pneumatic circuit with linear drive, the pneumatic components are controlled by electrical components, Fig. 9.

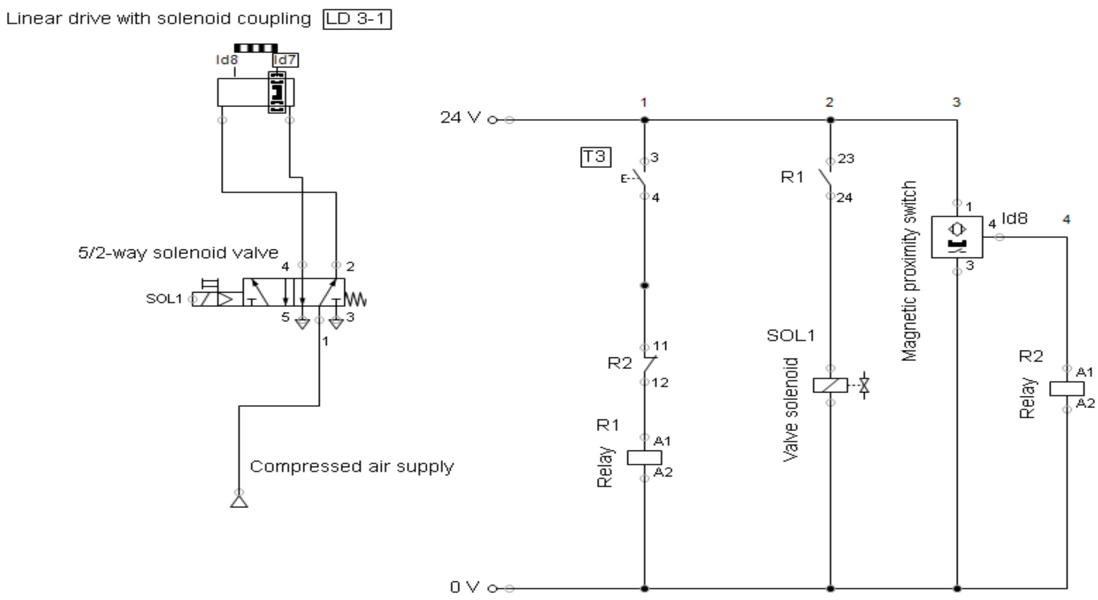

Fig. 9. Electro-pneumatic circuit with linear drive (LD 3-1)

An electro-pneumatic scheme consists especially of: a pneumatic scheme, a control circuit and a power circuit, [7].
The table below shows ten devices used in the electro-pneumatic scheme.

Table 4: The devices of the electro-pneumatic circuit

Description	Number of components
Compressed air supply	1
5/2-way solenoid valve with spring	1
Linear drive with solenoid coupling (LD 3-1)	1
Relays	2
Valves solenoid	2
Magnetic proximity switch	1

If the operator pushes T3 button, the piston rod must move from Id7 point to Id8 point. But, after six seconds, the piston rod of the linear drive with solenoid coupling (LD 3-1) should return, because this is done with magnetic proximity switch, [8].

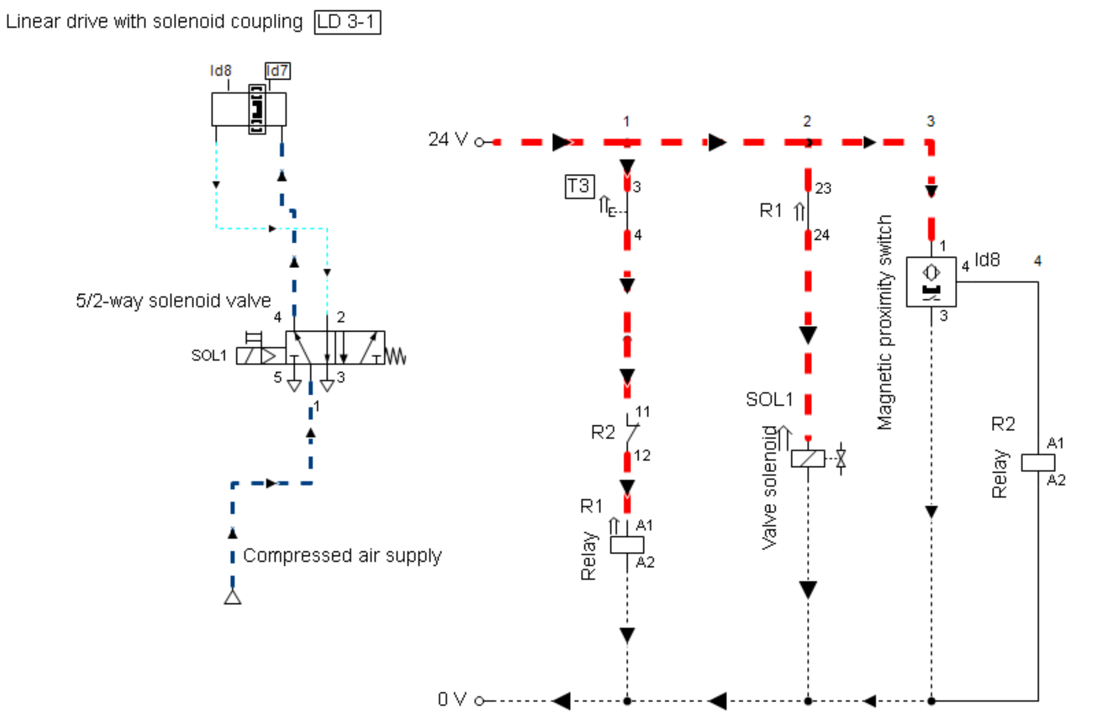

Fig. 10. Electro-pneumatic circuit with linear drive (LD 3-1). Simulation

3. Conclusions

The linear drives with solenoid coupling are actuators which are the most utilised on the penumatic instalations and also on the electro-pneumatic ones. Besides, these actuators have the following economic advantages:

- Low cost of compression.
- Silence.
- High accuracy.
- Easy handling.
- Reduced installation complexity.

In the future, we have planned to develop electro-hydraulic installations that use linear driving with cushioning in education and research.

References

[1] Memet, F., D. Mitu, and M. Panaitescu. "A point of view on effiency and innovation in refrigeration." Paper presented at the 4th International Conference on Development, Energy, Environment, Economics (DEEE'13) Recent advances in energy, environment, economics and technological innovation, Paris, France, October 29-31, 2013.

[2] Deleanu, D. "Concerning a new iterative method to solve nonlinear partial differential." *Constanta Maritime University Annals / Analele Universitatii Maritime Constanta* 10, no. 12 (2009): 375 – 380.

[3] Surdu, G. "Sustainable development a challenge for research in the field military equipment and space." *Impact of Socio-economic and Technological Transformations at National, European and International Level (ISETT)* 7 (2015).

[4] www.festo.com.

[5] Dumitrache, C., I. Călimenescu, and C. Comandar. "Naval Centrifugal Compressor Design using CAD solutions." *Applied Mechanics and Materials* 658 (2014): pp.59-64.

[6] Maloș, G., I. E. Sandu, and V. Năstăsescu. *Defense Systems Engineering / Ingineria sistemelor pentru apărare*. Bucharest, Military Technical Academy Publishing House, 2002.

[7] Bobe, A., A. Nicola, and C. Popa. "Weaker hypotheses for the general projection algorithm with corrections." *Annals of the Ovidius University Constanta - Mathematics Series / Analele Universității Ovidius – Seria Matematica* 23, no. 3 (2015): 9-16.

[8] Nutu, C. S. "Early Economic Systems." *Environmetal, Climate and Resource Issues on Earth. Governing Dynamics in Complex Systems*. B P International, 2022: 3-11.

UNIUNEA EUROPEANĂ

Instrumente Structurale 2014-2020

Proiect cofinanțat din Fondul European de Dezvoltare Regională prin Programul Operațional Competitivitate 2014-2020

Comunicat de presă

București, 16.12.2022

FINALIZARE PROIECT POC - Axa G

INSTITUTUL NAŢIONAL DE CERCETARE-DEZVOLTARE PENTRU OPTOELECTRONICĂ INOE 2000, cu sediul în localitatea Măgurele, Bucuresti-Ilfov, str. Atomiştilor, C.P. 077125 nr. 409, judeţul Ilfov, România, telefon 0214574522, fax 0314056397, anunță finalizarea, la data de 24.12.2022, a implementării proiectului ***"ELABORAREA DE TEHNOLOGII EFICIENTE ENERGETIC ÎN APLICAŢIILE DE NIŞĂ ALE FABRICAŢIEI SUBANSAMBLELOR MECANOHIDRAULICE LA CERERE ŞI MENTENANŢEI ECHIPAMENTELOR HIDRAULICE MOBILE"*, cod P_40_415, cod SMIS 2014+ 119809,** cofinanţat prin **Fondul European de Dezvoltare Regională,** în baza contractului de finanţare nr. 6 /25.06.2018 încheiat între **MCI** în calitate de **Organism Intermediar (OI)** pentru Programul Operaţional Competitivitate (POC), în numele şi pentru **Ministerul Fondurilor Europene (MFE)** în calitate de **Autoritate de Management (AM)** pentru Programul Operaţional Competitivitate (POC) și **INSTITUTUL NAȚIONAL DE CERCETARE-DEZVOLTARE PENTRU OPTOELECTRONICĂ INOE 2000.**

Valoarea totală a proiectului este de 8.301.282 lei, din care asistenţa financiară nerambursabilă este de 6.348.984 lei.

Proiectul s-a implementat de către beneficiarul INOE 2000 prin filiala Institutul de Cercetări pentru Hidraulică și Pneumatică (INOE 2000 Filiala IHP).

Obiectivul general al proiectului a constat în dezvoltarea interacţiunii INOE 2000 cu IMM-urile specializate în producţia şi mentenanţa de echipamente hidraulice pentru **transferul de cunoştinţe** în subdomeniul aplicaţiilor de nişă privind tehnologiile destinate producţiei de subansamble mecanohidraulice şi sisteme pentru utilaje complexe la cerere, şi al mentenanţei echipamentelor şi instalaţiilor hidraulice (întreţinere, reparaţii, verificări şi control).

Beneficiar proiect: INOE 2000

Beneficiari ai rezultatelor proiectului au fost firmele producătoare de subansambluri mecano-hidraulice la cerere (netipizate sau cu destinații speciale), firmele producătoare sau care se ocupă cu repararea de aparatură, echipamente și instalații hidraulice, firme care se ocupă de vânzarea, montarea, întreținerea și exploatarea unor astfel de produse.

Durata contractului: 54 de luni de la semnarea contractului între INOE 2000 şi Autoritatea Contractantă.

Rezultate prevăzute şi realizate: cursuri de instruire, acces la facilităţile institutului, studii de soluții, proiecte, realizare de modele experimentale şi prototipuri pentru diverse echipamente /instalații, metodologii de testare şi tehnologii de mentenanţă, articole etc.

Date de contact:
INOE 2000 Filiala IHP, București, sector 4, str. Cuțitul de Argint nr. 14, cod postal: 040558
Tel.: 0213363991, Fax: 0213373040, E-mail: dumitrescu.ihp@fluidas.ro
www.ihp.ro

FLUIDAS

NATIONAL PROFESSIONAL ASSOCIATION OF HYDRAULICS AND PNEUMATICS IN ROMANIA

fluidas@fluidas.ro